Colorado School of Mines
Department of Geophysics

2D and 3D High Accuracy Simulations of Resistivity Logging Measurements Using a Self-Adaptive Goal-Oriented hp Finite Element Method

D. Pardo, C. Torres-Verdín, L. Demkowicz, C. Michler

Collaborators: M. Paszynski, J. Kurtz

May 5, 2006

Department of Petroleum and Geosystems Engineering

THE UNIVERSITY OF TEXAS AT AUSTIN

OVERVIEW

1. Motivation: Simulation of Resistivity Logging Instruments.
2. Methodology:
   - The hp-Finite Element Method (FEM) - Exponential Convergence - .
   - Automatic Goal-Oriented Refinements - in the Quantity of Interest -.
3. 2D Numerical Results:
   - Verification of the Software.
   - Simulation of Resistivity Logging Instruments with Mandrel.
   - Simulation of Resistivity Logging Instruments with Casing.
   - Simulation of Cross-Well Measurements with One Cased Well.
   - Perfectly Matched Layers (PML).
4. 3D Numerical Results.
5. Conclusions and Future Work (Multi-physics).

RESISTIVITY LOGGING INSTRUMENTS

Logging Instruments: Definition

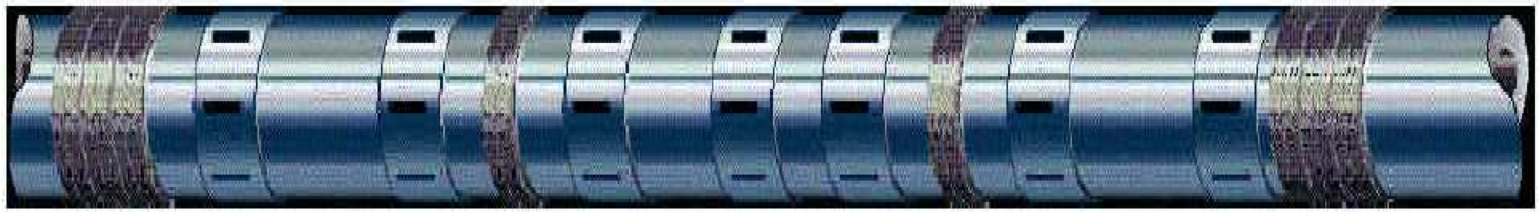

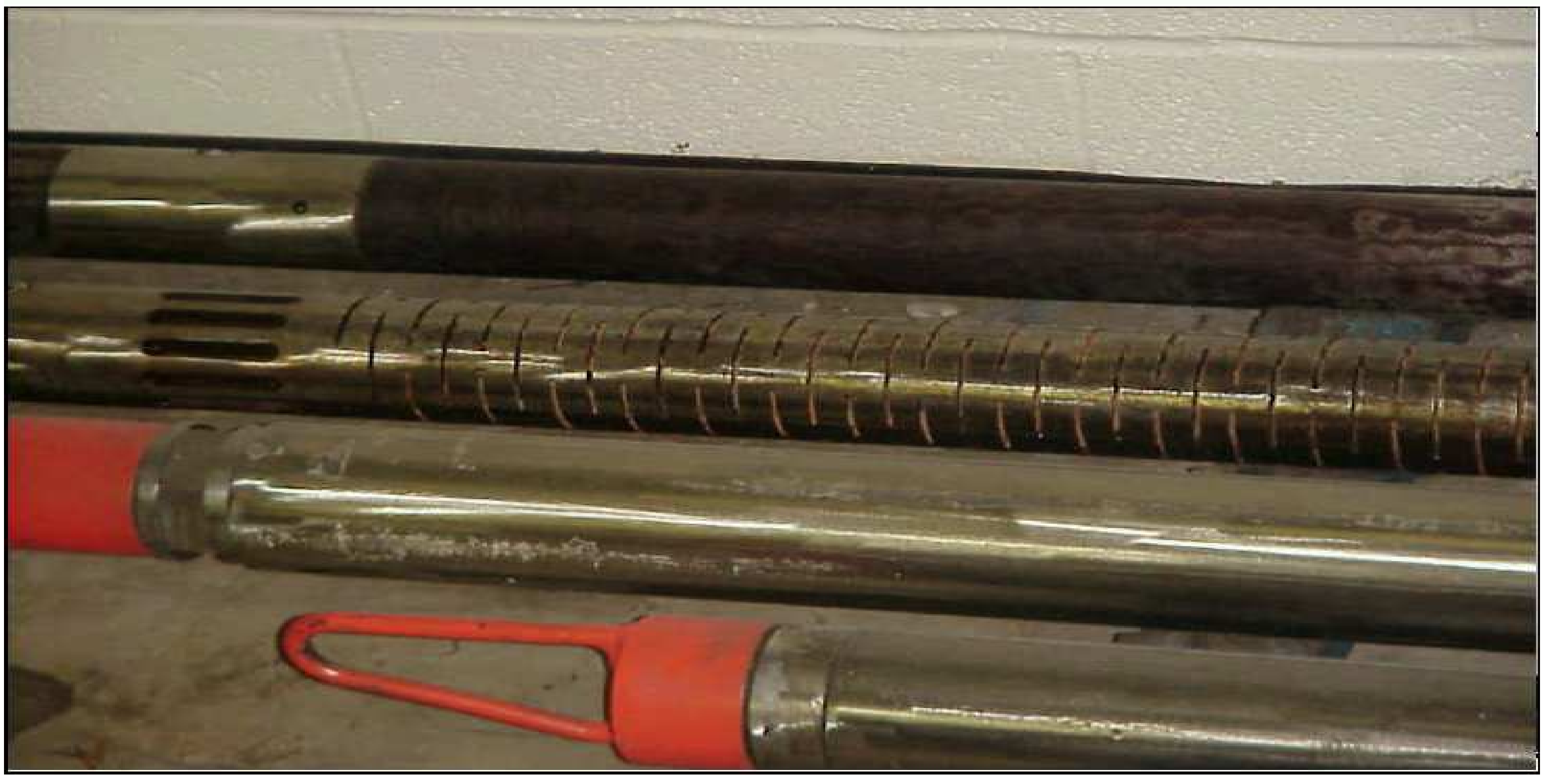

RESISTIVITY LOGGING INSTRUMENTS

Utility of Logging Instruments

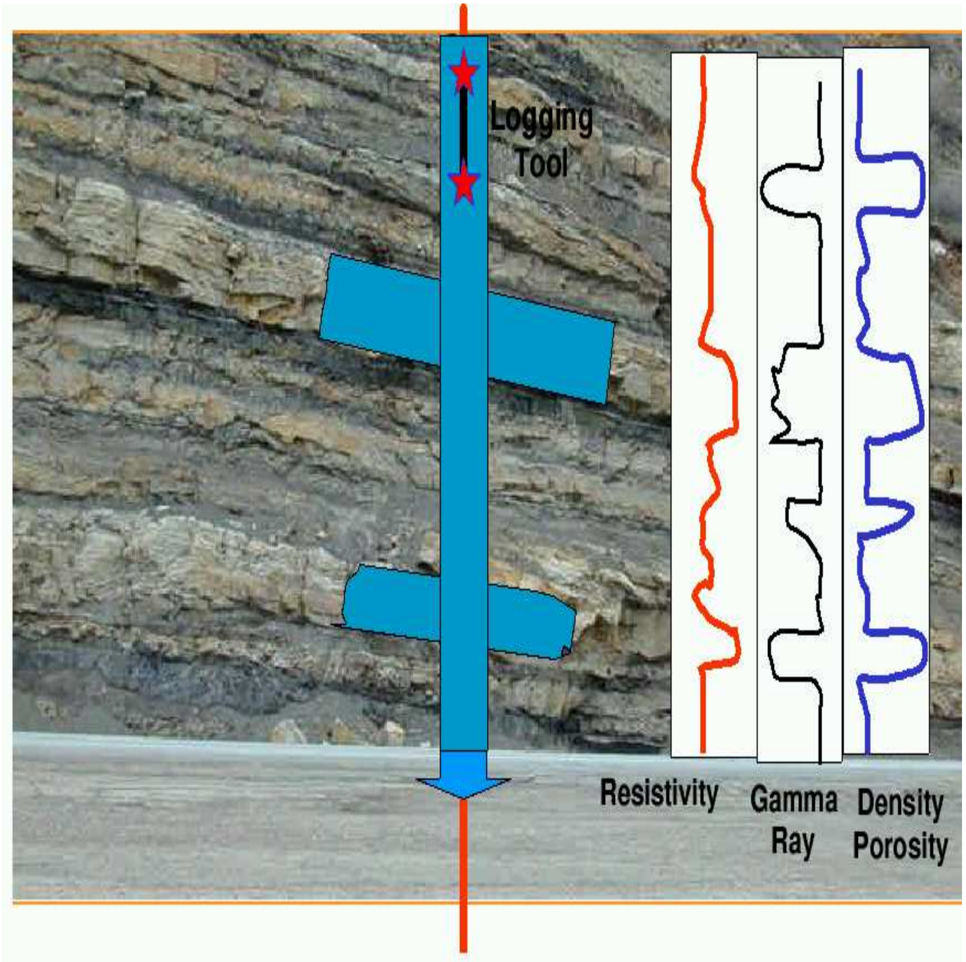

OBJECTIVES: To determine

- **Payzones (oil and gas).**
- **Amount of oil/gas.**
- **Ability to extract oil/gas.**

$

RESISTIVITY LOGGING INSTRUMENTS

Main Objective: To Solve an Inverse Problem

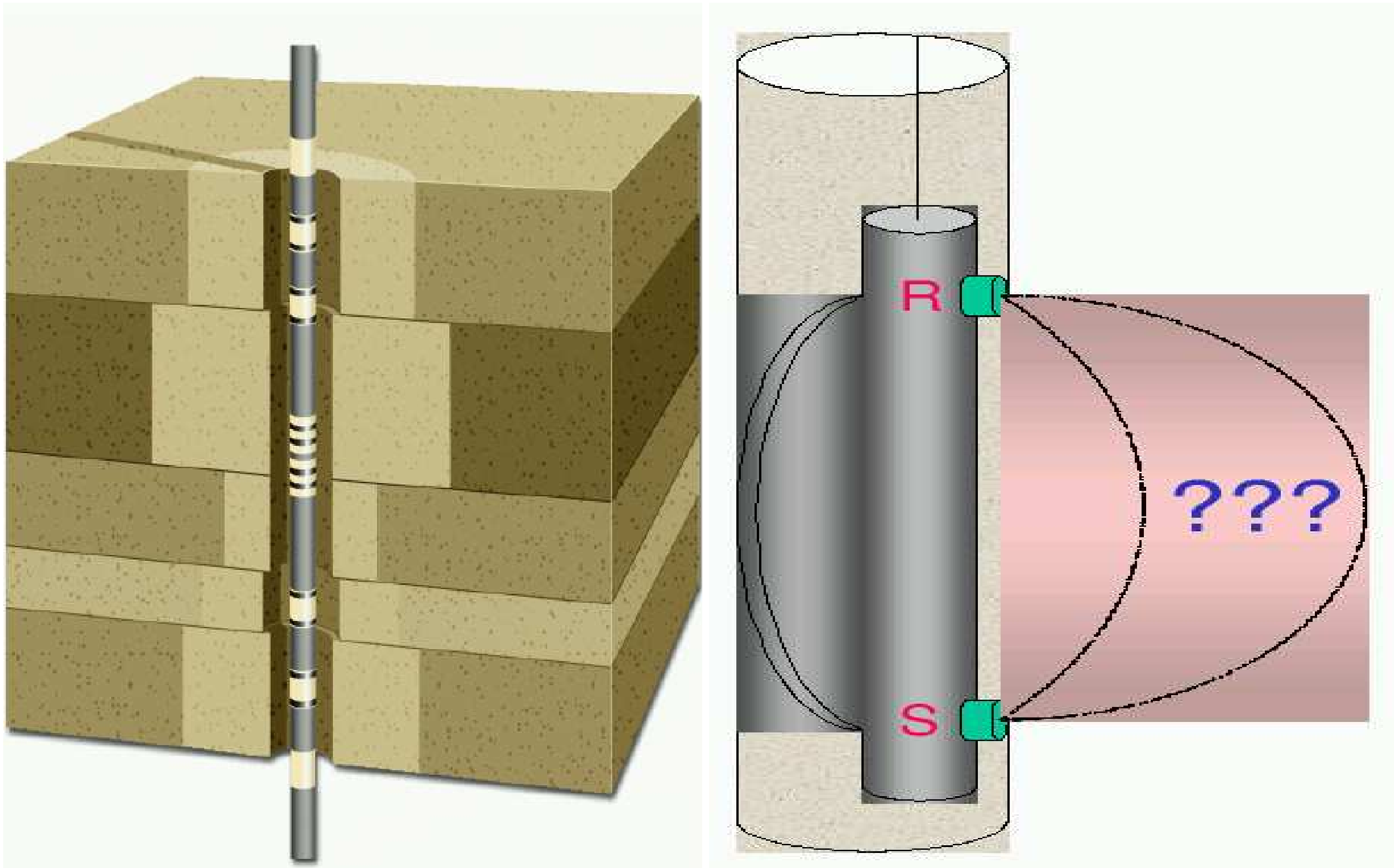

A software for solving the DIRECT problem is essential in order to solve the INVERSE problem

RESISTIVITY LOGGING INSTRUMENTS

Resistivity Logging Instruments

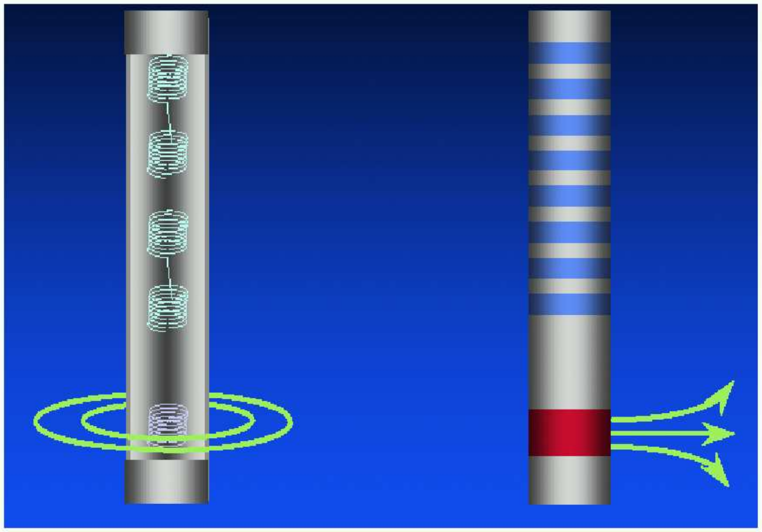

MAXWELL'S EQUATIONS

3D Variational Formulation

Time-Harmonic Maxwell's Equations

$\nabla \times \mathrm{H} = (\bar{\bar{\sigma}} + j\omega\bar{\bar{\epsilon}})\mathrm{E} + \mathrm{J}^{imp}$	**Ampere's law**
$\nabla \times \mathrm{E} = -j\omega\bar{\bar{\mu}}\mathrm{H} - \mathrm{M}^{imp}$	**Faraday's law**
$\nabla \cdot (\bar{\bar{\epsilon}}\mathrm{E}) = \rho$	**Gauss' law of Electricity**
$\nabla \cdot (\bar{\bar{\mu}}\mathrm{H}) = 0$	**Gauss' law of Magnetism**

E-VARIATIONAL FORMULATION:

$$\left\{ \begin{array}{l} \text{Find } \mathrm{E} \in \mathrm{E}_D + H_D(\mathrm{curl};\Omega) \text{ such that:} \\ \displaystyle\int_\Omega (\bar{\bar{\mu}}^{-1}\nabla \times \mathrm{E}) \cdot (\nabla \times \bar{\mathrm{F}})\, dV - \int_\Omega (\bar{\bar{k}}^2\mathrm{E}) \cdot \bar{\mathrm{F}}\, dV = -j\omega \int_\Omega \mathrm{J}^{imp} \cdot \bar{\mathrm{F}}\, dV \\ \displaystyle +j\omega \int_{\Gamma_N} \mathrm{J}^{imp}_{\Gamma_N} \cdot \bar{\mathrm{F}}_t\, dS - \int_\Omega (\bar{\bar{\mu}}^{-1}\mathrm{M}^{imp}) \cdot (\nabla \times \bar{\mathrm{F}})\, dV \quad \forall\, \mathrm{F} \in H_D(\mathrm{curl};\Omega) \end{array} \right.$$

MAXWELL'S EQUATIONS

2D Variational Formulation (Axi-symmetric Problems)

E_ϕ -Variational Formulation (Azimuthal)

$$\begin{cases} \text{Find } E_\phi \in E_{\phi,D} + \tilde{H}^1_D(\Omega) \text{ such that:} \\ \int_\Omega (\bar{\bar{\mu}}^{-1}_{\rho,z} \nabla \times \mathrm{E}_\phi) \cdot (\nabla \times \bar{\mathrm{F}}_\phi)\, dV - \int_\Omega (\bar{\bar{k}}^2_\phi \mathrm{E}_\phi) \cdot \bar{\mathrm{F}}_\phi \, dV = -j\omega \int_\Omega J^{imp}_\phi \bar{F}_\phi \, dV \\ \quad + j\omega \int_{\Gamma_N} J^{imp}_{\phi,\Gamma_N} \bar{F}_\phi \, dS - \int_\Omega (\bar{\bar{\mu}}^{-1}_{\rho,z} \mathrm{M}^{imp}_{\rho,z}) \cdot \bar{\mathrm{F}}_\phi \, dV \qquad \forall\, F_\phi \in \tilde{H}^1_D(\Omega) \end{cases}$$

$\mathrm{E}_{\rho,z}$ -Variational Formulation (Meridian)

$$\begin{cases} \text{Find } (E_\rho, E_z) \in \mathrm{E}_D + \tilde{H}_D(\mathrm{curl};\Omega) \text{ such that:} \\ \int_\Omega (\bar{\bar{\mu}}^{-1}_\phi \nabla \times \mathrm{E}_{\rho,z}) \cdot (\nabla \times \bar{\mathrm{F}}_{\rho,z})\, dV - \int_\Omega (\bar{\bar{k}}^2_{\rho,z} \mathrm{E}_{\rho,z}) \cdot \bar{\mathrm{F}}_{\rho,z} \, dV = \\ \quad -j\omega \int_\Omega J^{imp}_\rho \bar{F}_\rho + J^{imp}_z \bar{F}_z \, dV + j\omega \int_{\Gamma_N} J^{imp}_{\rho,\Gamma_N} \bar{F}_\rho + J^{imp}_{z,\Gamma_N} \bar{F}_z \, dS \\ \quad - \int_\Omega (\bar{\bar{\mu}}^{-1}_\phi \mathrm{M}^{imp}_\phi) \cdot \bar{\mathrm{F}}_{\rho,z} \, dV \qquad \forall\, (F_\rho, F_z) \in \tilde{H}_D(\mathrm{curl};\Omega) \end{cases}$$

MODEL PROBLEMS OF INTEREST

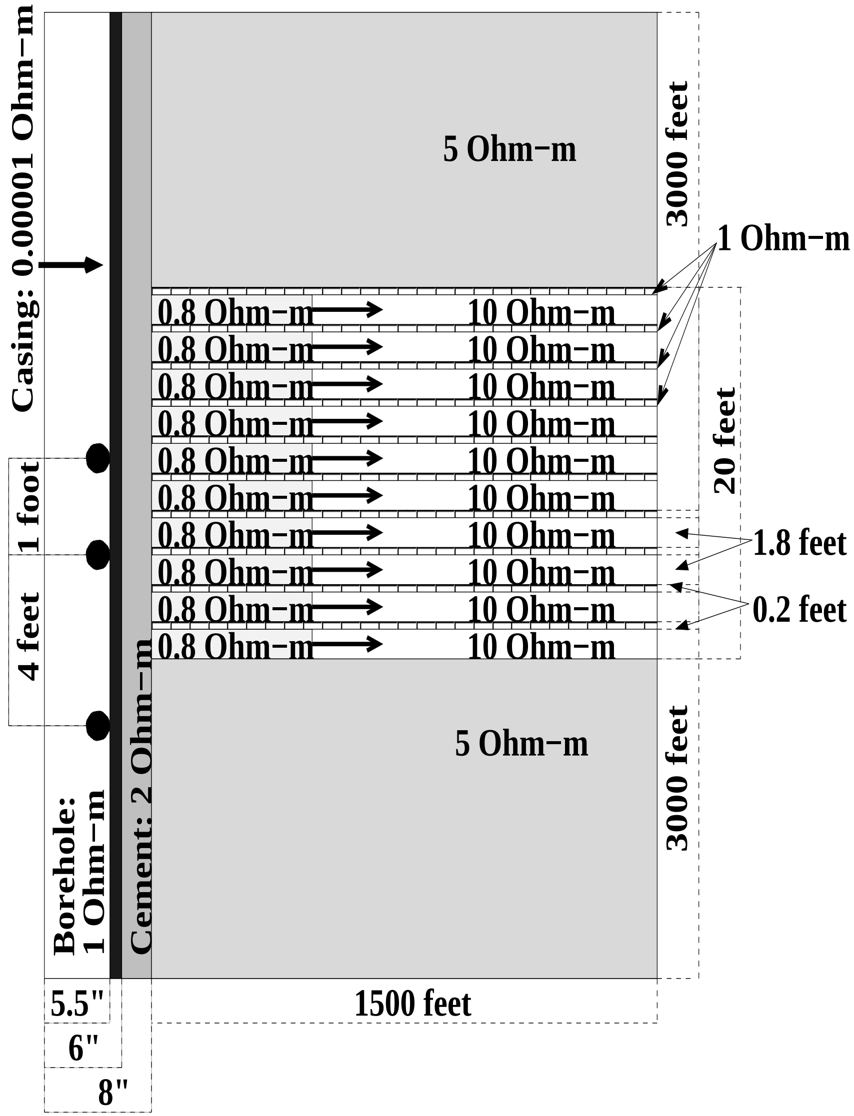

Axisymmetric 3D problem.

Seven different materials.

Through casing resistivity instrument.

Large variations on resistivity.

Objective: Study the effect of invasion THROUGH CASING on laminated sands.

MODEL PROBLEMS OF INTEREST

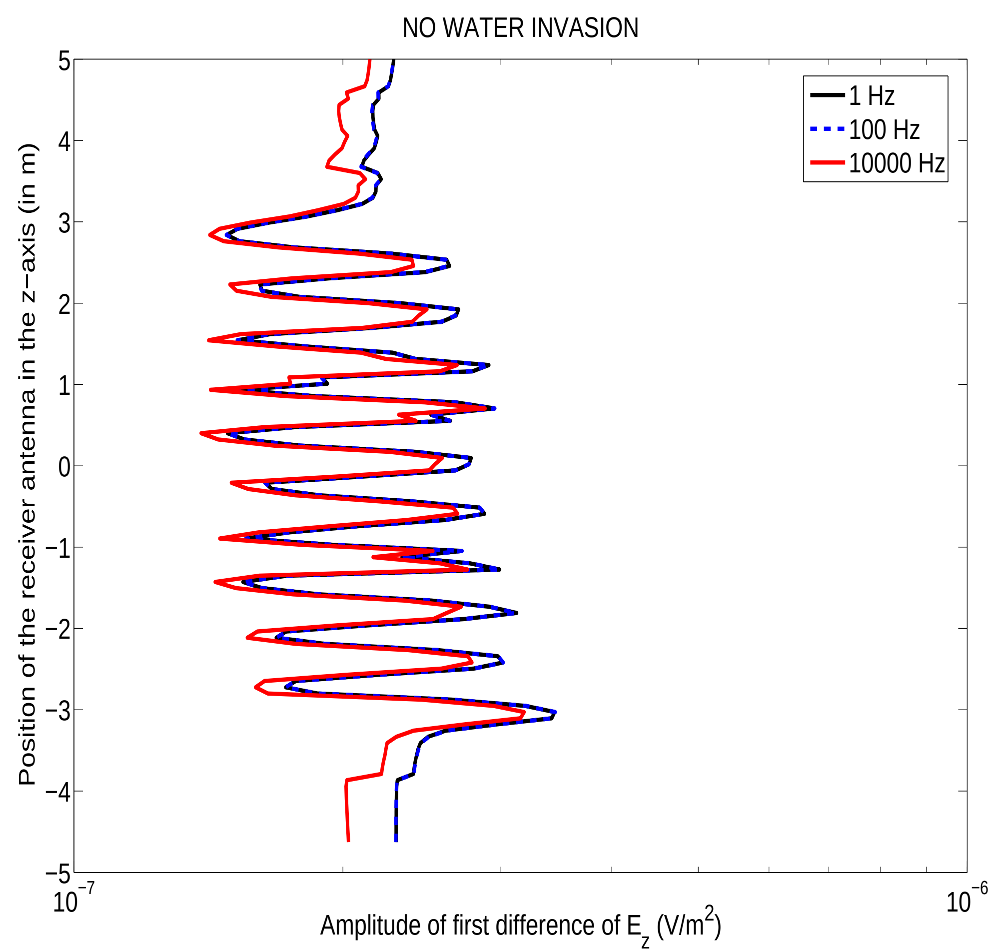

Variations due to frequency are small (below 5%)

MODEL PROBLEMS OF INTEREST

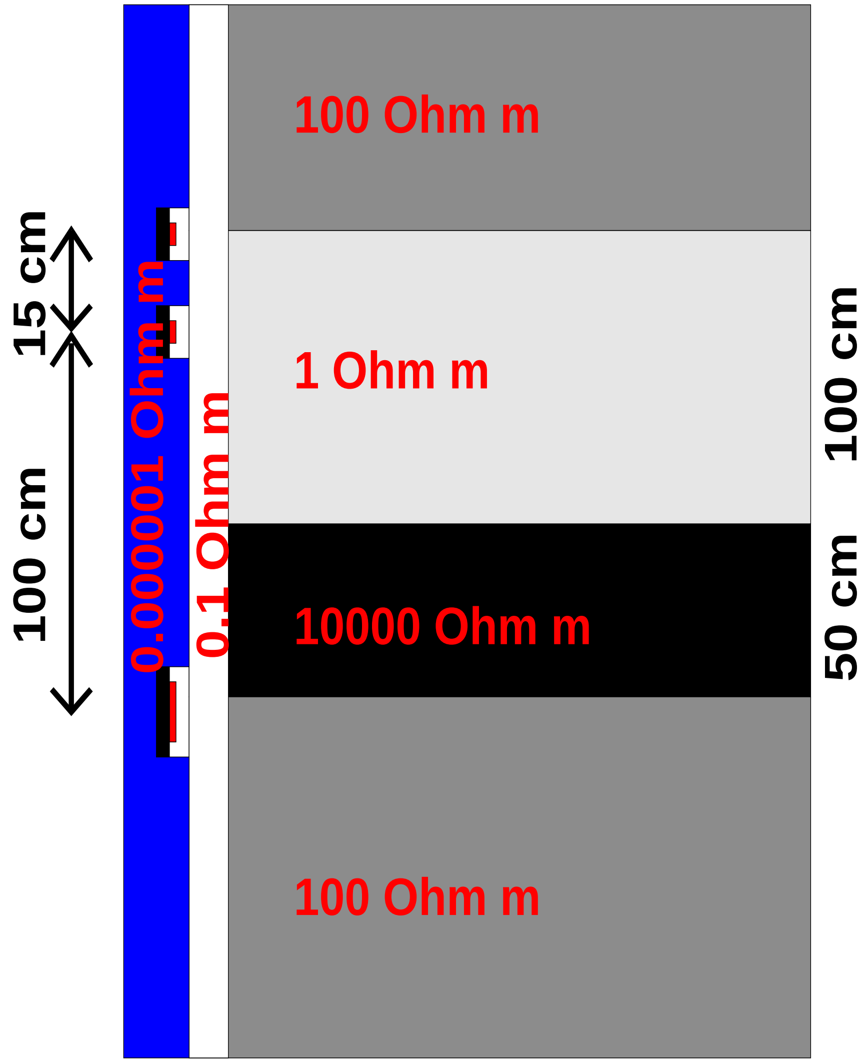

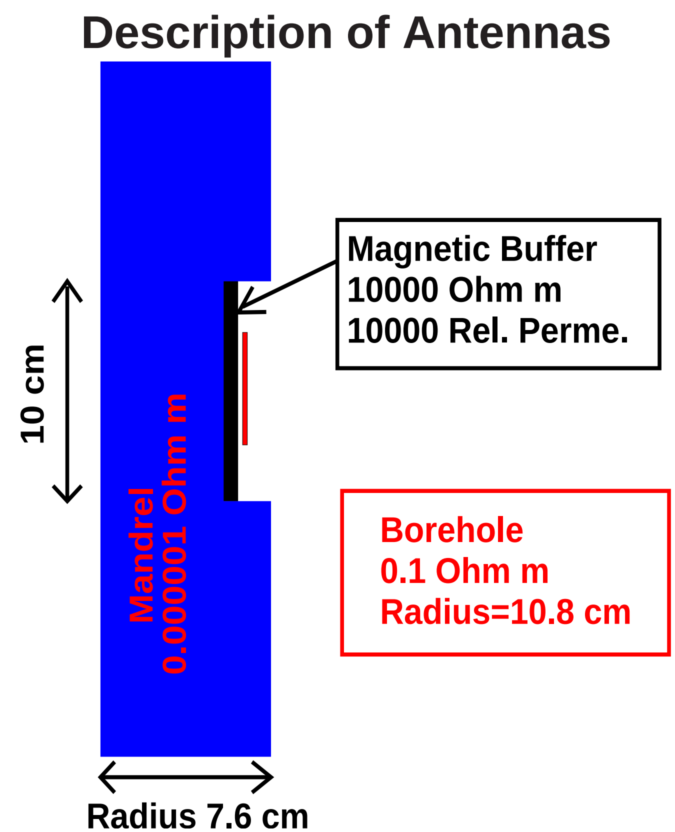

Goal: To Study the Effect of Invasion, Anistotropy, and Magnetic Permeability.

THE hp-FINITE ELEMENT METHOD (FEM)

The h-Finite Element Method

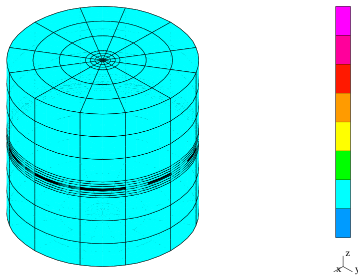

1. Convergence limited by the polynomial degree, and large material contrasts.
2. Optimal *h*-grids do NOT converge exponentially in real applications.
3. They may "lock" (100$\%$ error).

The p-Finite Element Method

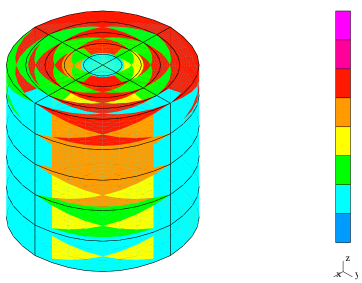

1. Exponential convergence feasible for analytical ("nice") solutions.
2. Optimal *p*-grids do NOT converge exponentially in real applications.
3. If initial *h*-grid is not adequate, the *p*-method will fail miserably.

The hp-Finite Element Method

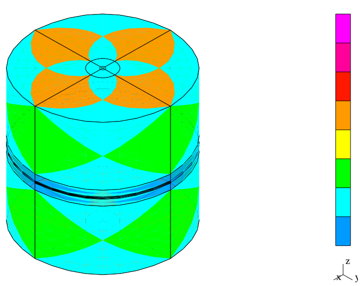

1. Exponential convergence feasible for ALL solutions.
2. Optimal *hp*-grids DO converge exponentially in real applications.
3. If initial *hp*-grid is not adequate, results will still be great.

GOAL-ORIENTED ADAPTIVITY

Motivation (Goal-Oriented Adaptivity)

Test Problem

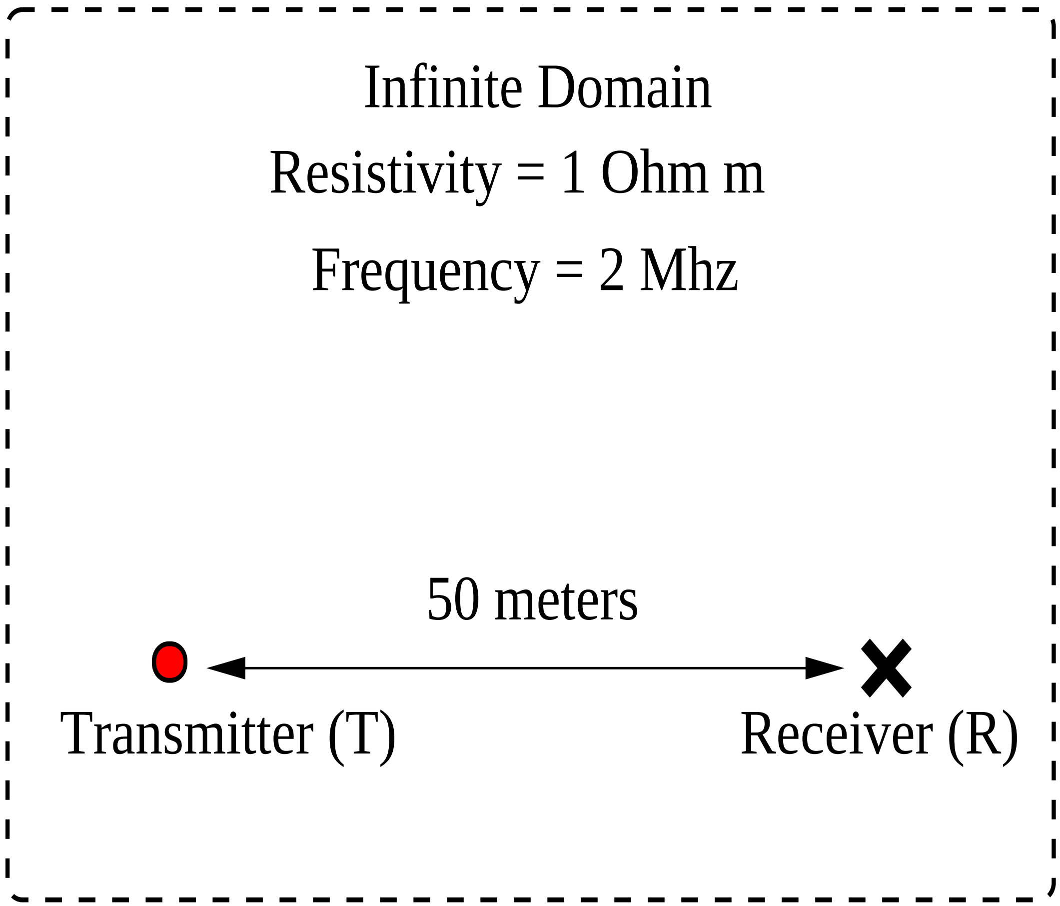

GOAL-ORIENTED ADAPTIVITY

Motivation (Goal-Oriented Adaptivity)

Test Problem

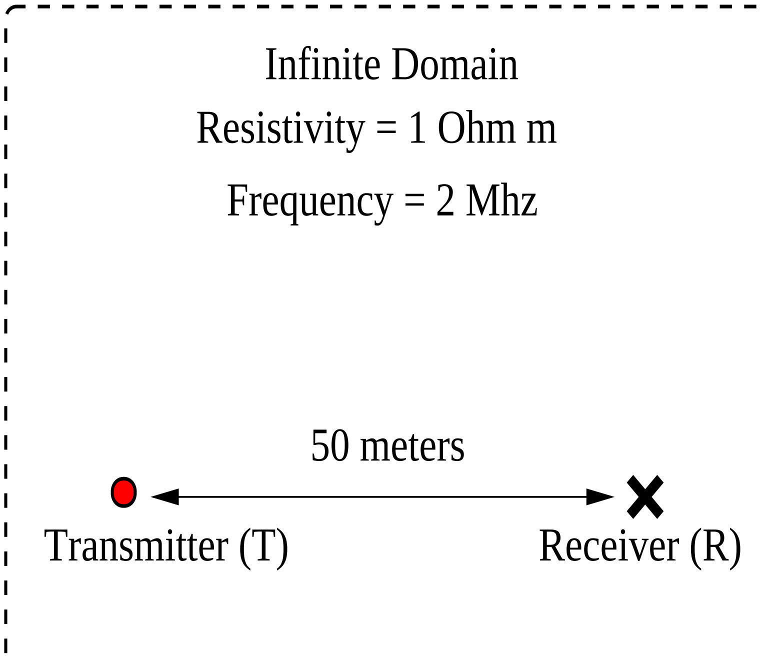

- **Solution decays exponentially.**
- $\frac{|E(T)|}{|E(R)|} \approx 10^{60}$
- **Results using energy-norm adaptivity:**
  - **Energy-norm error:** 0.001%
  - **Relative error in the quantity of interest** $> 10^{30}\ \%$.

GOAL-ORIENTED ADAPTIVITY

Motivation (Goal-Oriented Adaptivity)

Test Problem

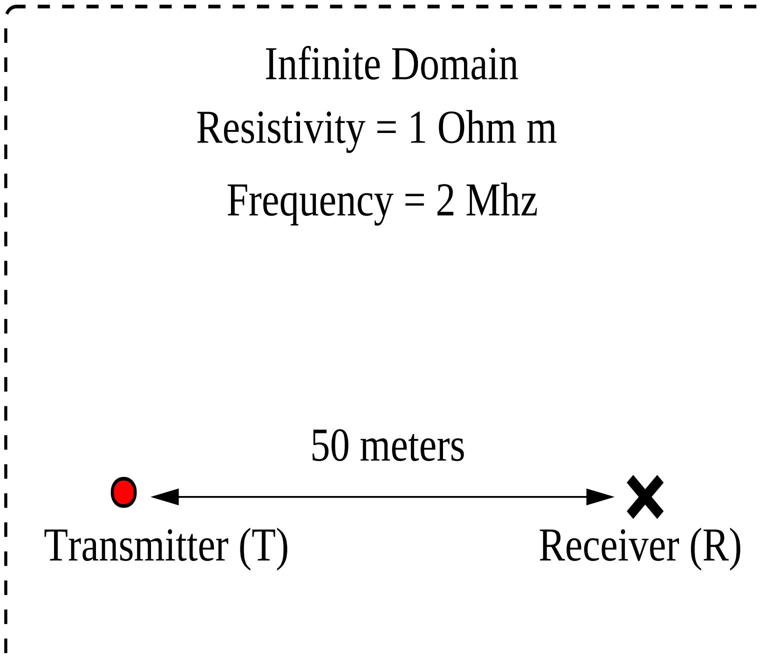

- **Solution decays exponentially.**
- $\dfrac{|E(T)|}{|E(R)|} \approx 10^{60}$
- **Results using energy-norm adaptivity:**
  - **Energy-norm error:** 0.001%
  - **Relative error in the quantity of interest** $> 10^{30}$ **%.**

Goal-oriented adaptivity is needed

Becker-Rannacher (1995,1996), Rannacher-Stuttmeier (1997), Cirak-Ramm (1998), Paraschivoiu-Patera (1998), Peraire-Patera (1998), Prudhomme-Oden (1999, 2001), Heuveline-Rannacher (2003), Solin-Demkowicz (2004).

GOAL-ORIENTED ADAPTIVITY

Motivation (Goal-Oriented Adaptivity)

Test Problem

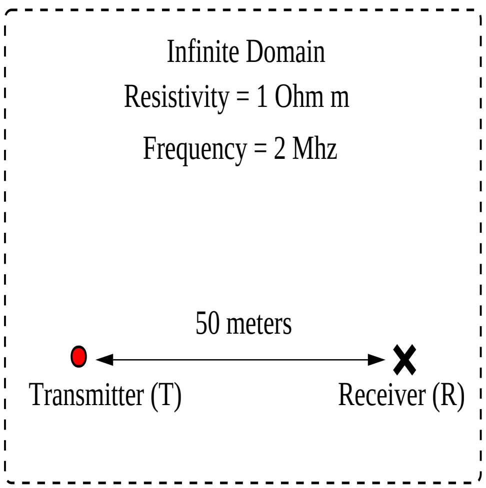

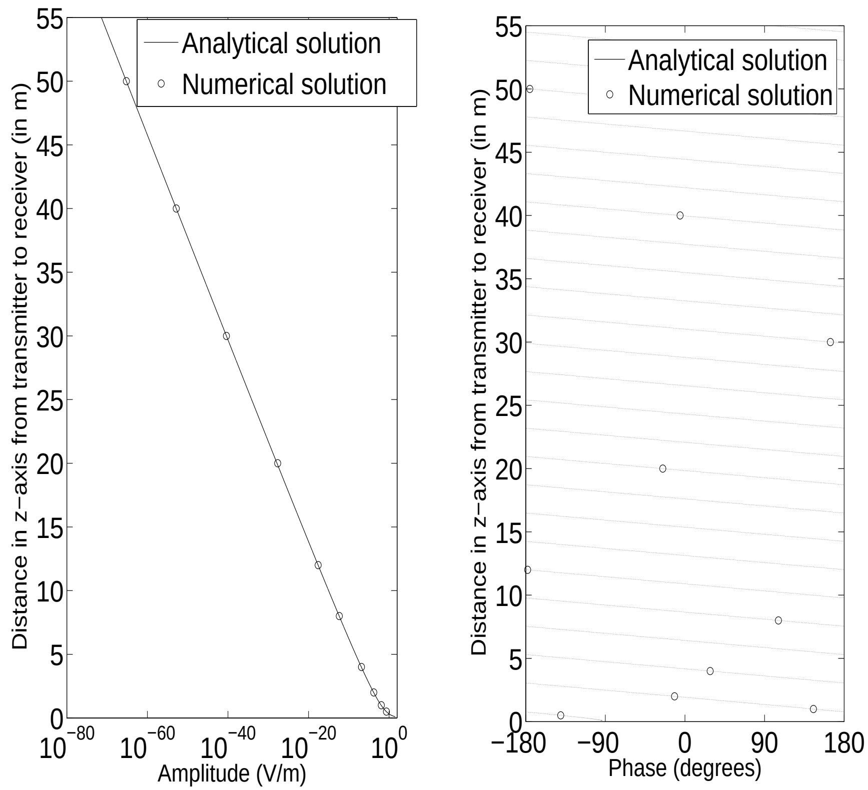

Goal-oriented adaptivity is needed

GOAL-ORIENTED ADAPTIVITY

Mathematical Formulation (Goal-Oriented Adaptivity)

Let's L be the quantity of interest (Ex.: first vertical difference of electric field).

We consider the following problem (in variational form):

$$\left\{ \begin{array}{l} \text{Find } L(\Psi)\text{, where } \Psi \in V \text{ such that :} \\ b(\Psi, \xi) = f(\xi) \quad \forall \xi \in V \ . \end{array} \right.$$

We define residual $r_e(\xi) = b(e, \xi)$. We seek for solution G of:

$$\left\{ \begin{array}{l} \text{Find } G \in V'' \sim V \text{ such that :} \\ G(r_e) = L(e) \ . \end{array} \right.$$

This is necessarily solved if we find the solution of the *dual* problem:

$$\left\{ \begin{array}{l} \text{Find } G \in V \text{ such that :} \\ b(\Psi, G) = L(\Psi) \quad \forall \Psi \in V \ . \end{array} \right.$$

Notice that $L(e) = b(e, G)$.

GOAL-ORIENTED ADAPTIVITY

Mathematical Formulation (Goal-Oriented Adaptivity)

DIRECT PROBLEM - Ψ -
2D Cross-Section

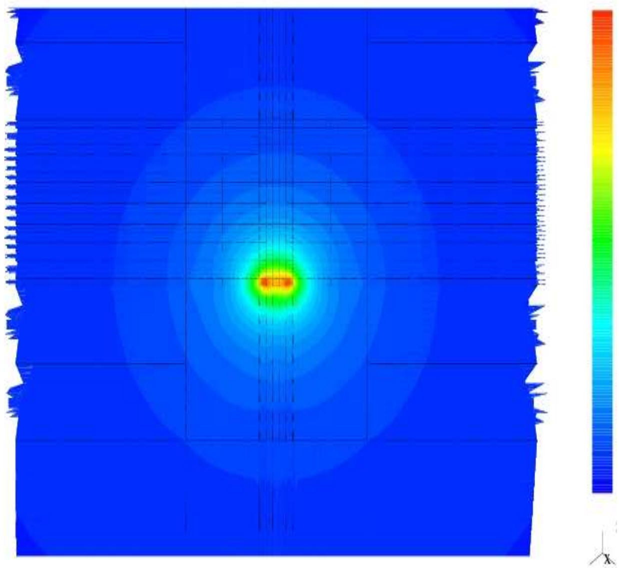

DUAL PROBLEM - G -
2D Cross-Section

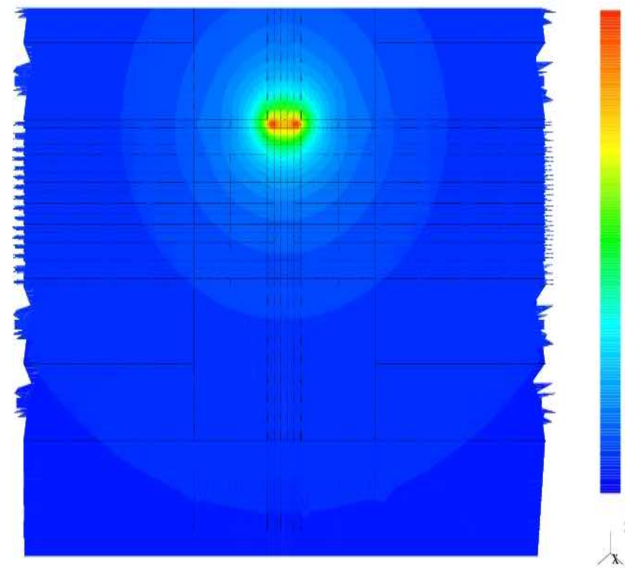

Representation Formula for the Error in the Quantity of Interest:

$$L(\Psi)=b(\Psi,G) = \int_\Omega \sigma \, \nabla\Psi \, \nabla G \, dV$$ **(electrostatics)**

SELF-ADAPTIVE GOAL-ORIENTED hp-FEM

Algorithm for Goal-Oriented Adaptivity - STEP I -

Solve Direct and Dual Problems on Grid hp

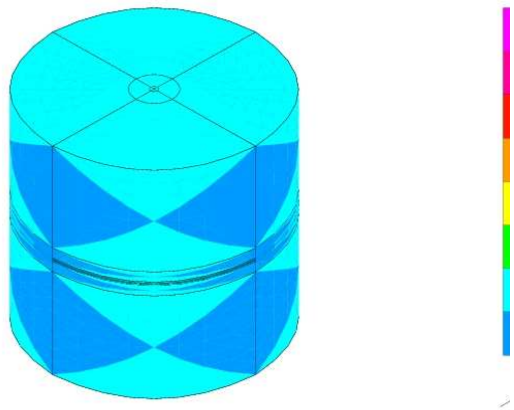

$\longrightarrow$

Solve Direct and Dual Problems on Grid $h/2, p+1$

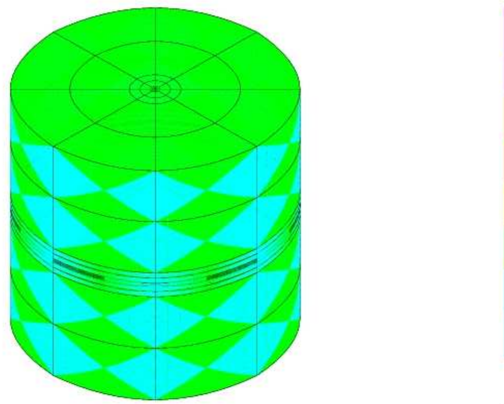

Use the fine grid solution to estimate the coarse grid error function.
Apply the fully automatic goal-oriented hp-adaptive algorithm.

Next optimal hp-grid:

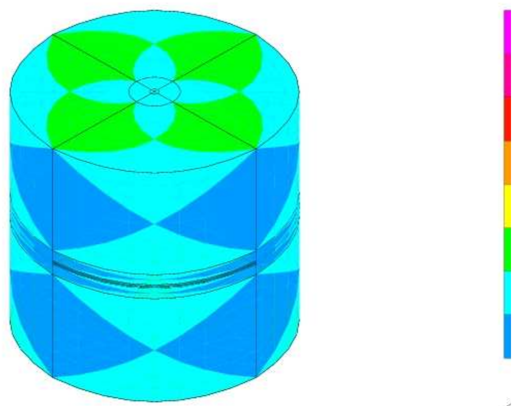

SELF-ADAPTIVE GOAL-ORIENTED hp-FEM

Algorithm for Goal-Oriented Adaptivity - STEP II -

Solve Direct and Dual Problems on Grid hp

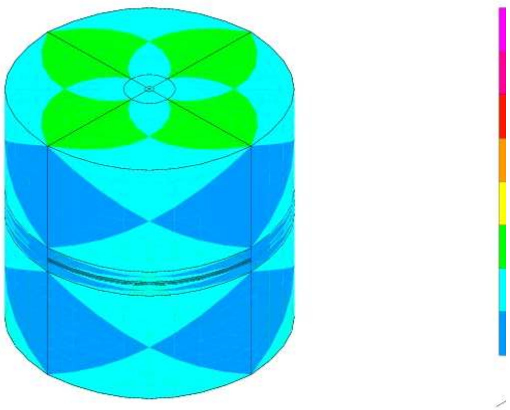

$\longrightarrow$

Solve Direct and Dual Problems on Grid $h/2, p+1$

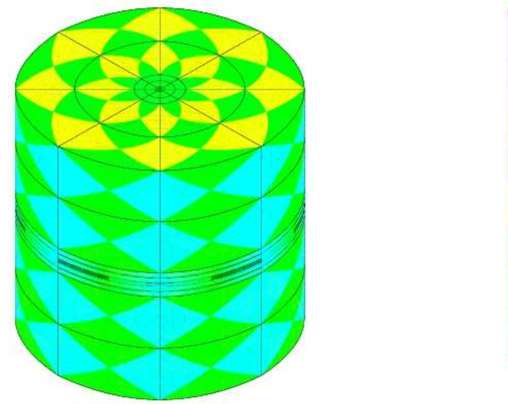

Use the fine grid solution to estimate the coarse grid error function.
Apply the fully automatic goal-oriented hp-adaptive algorithm.

Next optimal hp-grid:

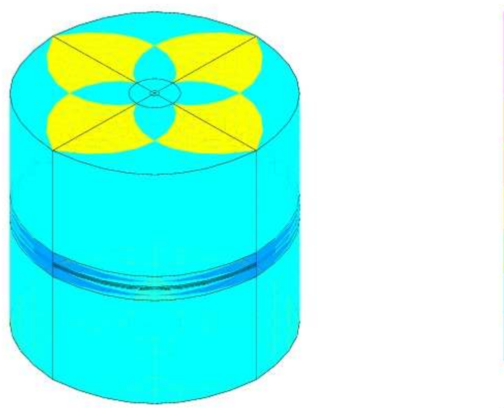

SELF-ADAPTIVE GOAL-ORIENTED hp-FEM

Algorithm for Goal-Oriented Adaptivity - STEP III -

Solve Direct and Dual Problems on Grid hp

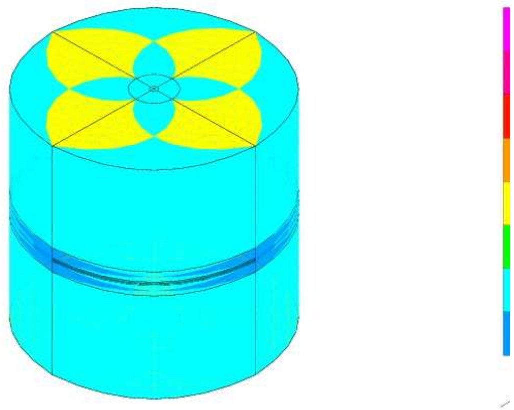

$\longrightarrow$

Solve Direct and Dual Problems on Grid $h/2, p+1$

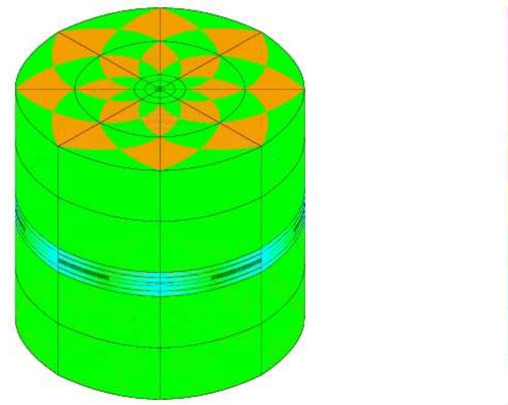

Use the fine grid solution to estimate the coarse grid error function.
Apply the fully automatic goal-oriented hp-adaptive algorithm.

Next optimal hp-grid:

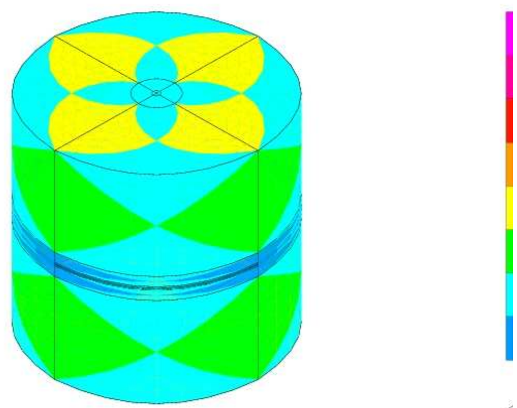

SELF-ADAPTIVE GOAL-ORIENTED hp-FEM

Algorithm for Goal-Oriented Adaptivity - STEP IV -

Solve Direct and Dual Problems on Grid hp

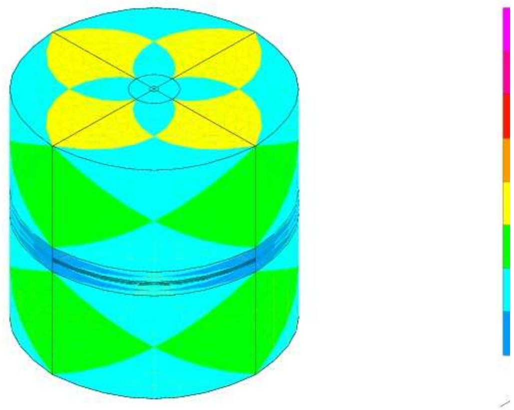

$\longrightarrow$

Solve Direct and Dual Problems on Grid $h/2, p+1$

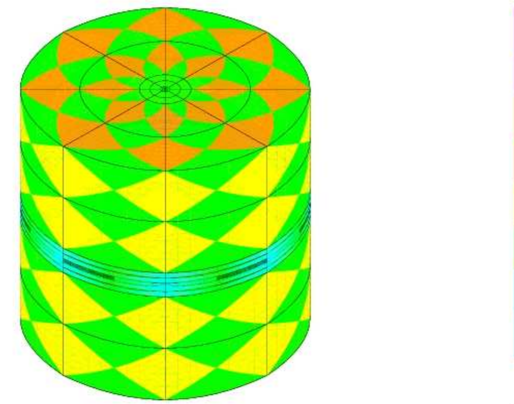

Use the fine grid solution to estimate the coarse grid error function.
Apply the fully automatic goal-oriented hp-adaptive algorithm.

Next optimal hp-grid:

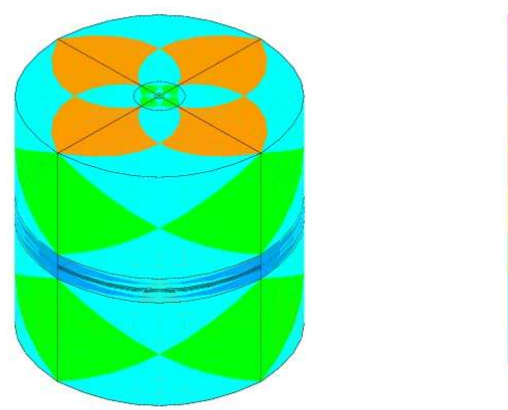

2D hp-FEM: NUMERICAL RESULTS

Type of Problems We Can Solve with 2Dhp90

Physical Devices	Magnetic Buffers	Insulators	Displacement Currents
	Casing	Casing Imperfections	Combination of all
Materials	Isotropic	Anisotropic*	
Sources	Toroidal Antennas	Solenoidal Antennas	Dipoles in Any Direction
	Electrodes	Finite Size Antennas	Combination of All
Logging Instruments	LWD/MWD	Laterolog	Normal
	Induction	Dielectric Instruments	Cross-well
Frequency	0-10 Ghz.		
Invasion	Water	Oil	etc.

ALL AXISYMMETRIC RESISTIVITY LOGGING PROBLEMS

2D hp-FEM: VERIFICATION OF RESULTS

- **Comparison Against Analytical Results.**
  1. Exact solution in a homogeneous media.
  2. Exact solution in a homogeneous media with a mandrel.
  3. Exact solution in a homogeneous media with casing.
- **Comparison Against Semi-Analytical 1D Codes.**
  1. Comparison against 1D ’radial’ code.
  2. Comparison against 1D ’hybrid’ code.
- **Comparison Against 2D Codes.**
  1. Comparison against a 2D FE code (Dr. Wei Yang).
  2. Comparison between continuous elements vs. edge elements.
- **Verification of Physical Properties.**
  1. Reciprocity principle.
  2. Discrete divergence free approximation for edge elements.
  3. Sensitivity with respect to different size of domain and antennas.
- **Built-in Numerical Verifications.**
  1. Error control provided by the fine grid.
  2. Comparison between continuous elements vs. edge elements.

2D hp-FEM: VERIFICATION OF RESULTS

Validation against a 1D 'radial' code (T. Habashy)

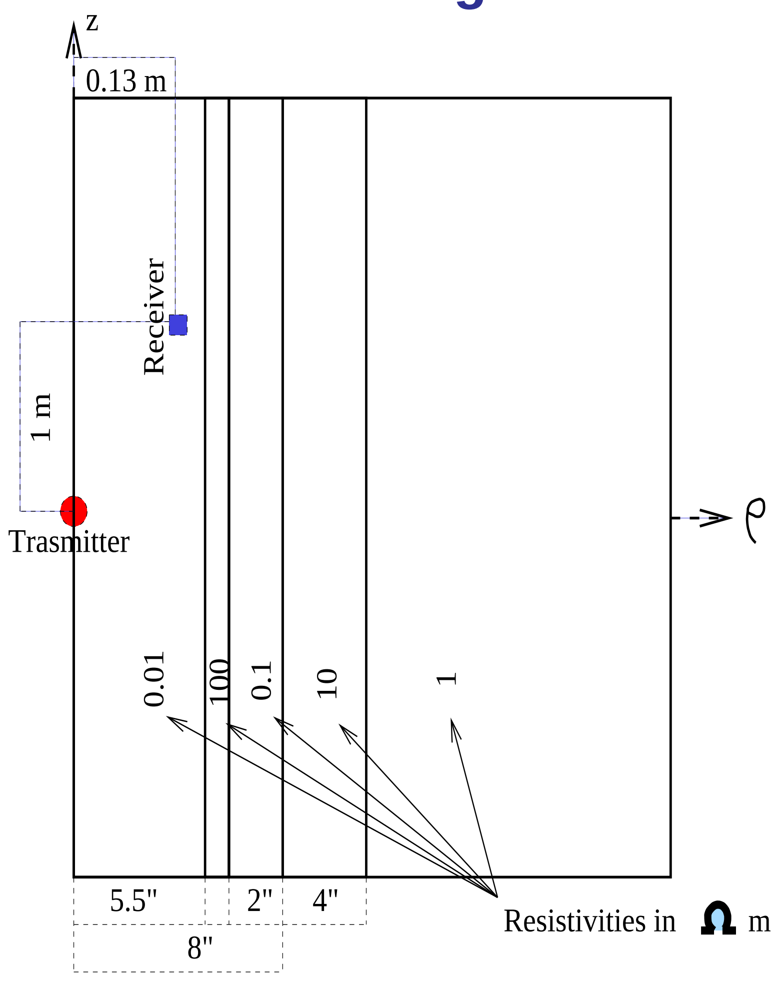

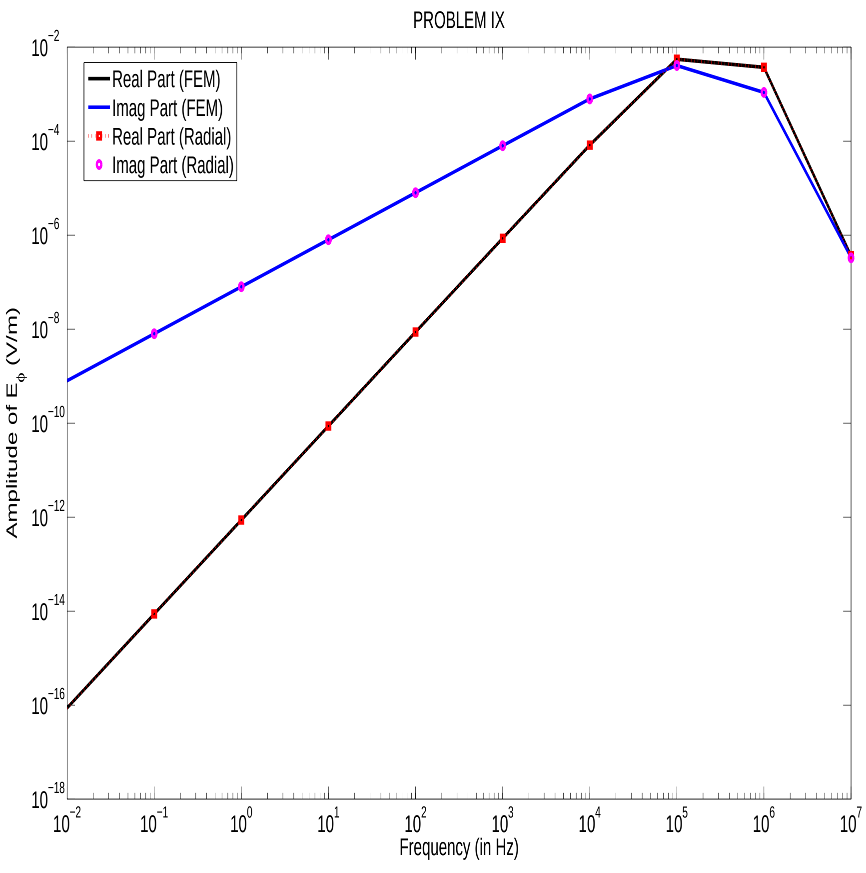

2D hp-FEM: VERIFICATION OF RESULTS

Validation against a 1D 'hybrid' code (G. L. Wang)

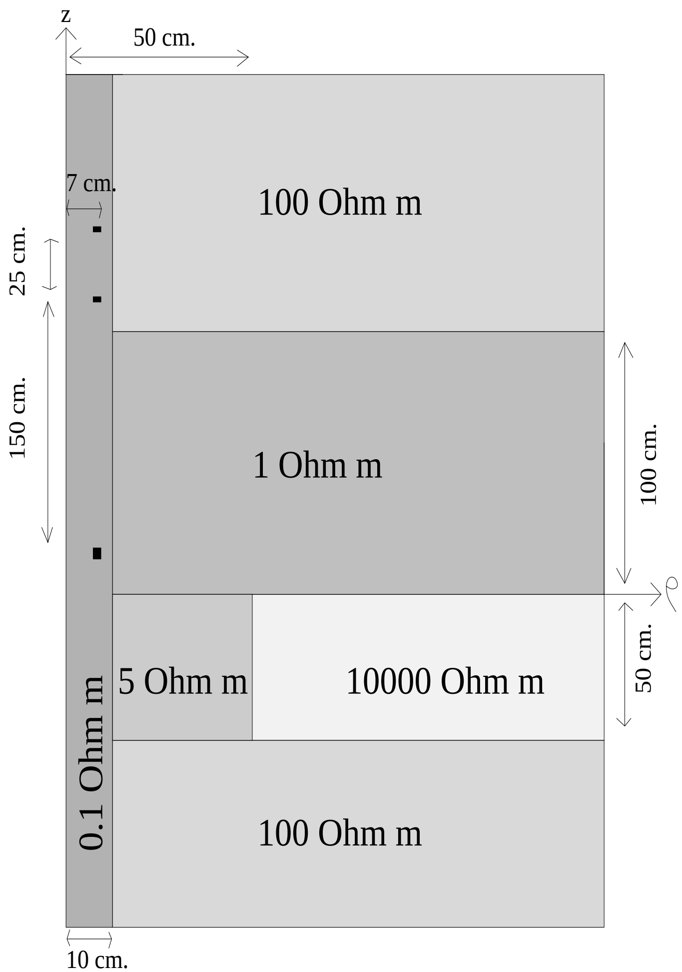

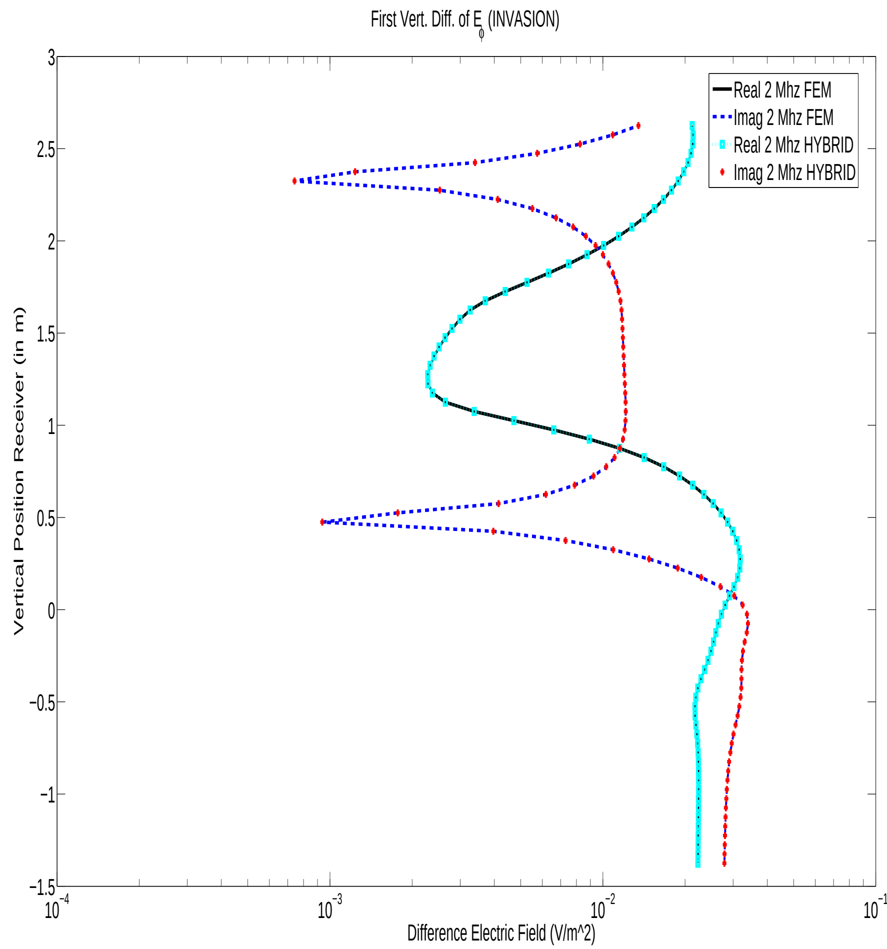

2D hp-FEM: VERIFICATION OF RESULTS

Ring of Vert. Dipoles vs. One Vertical Dipole in a Homogeneous Media of Resistivity 5 $\Omega \cdot$ m

Vertical Distance from Transmitter to Receiver: 499 m.

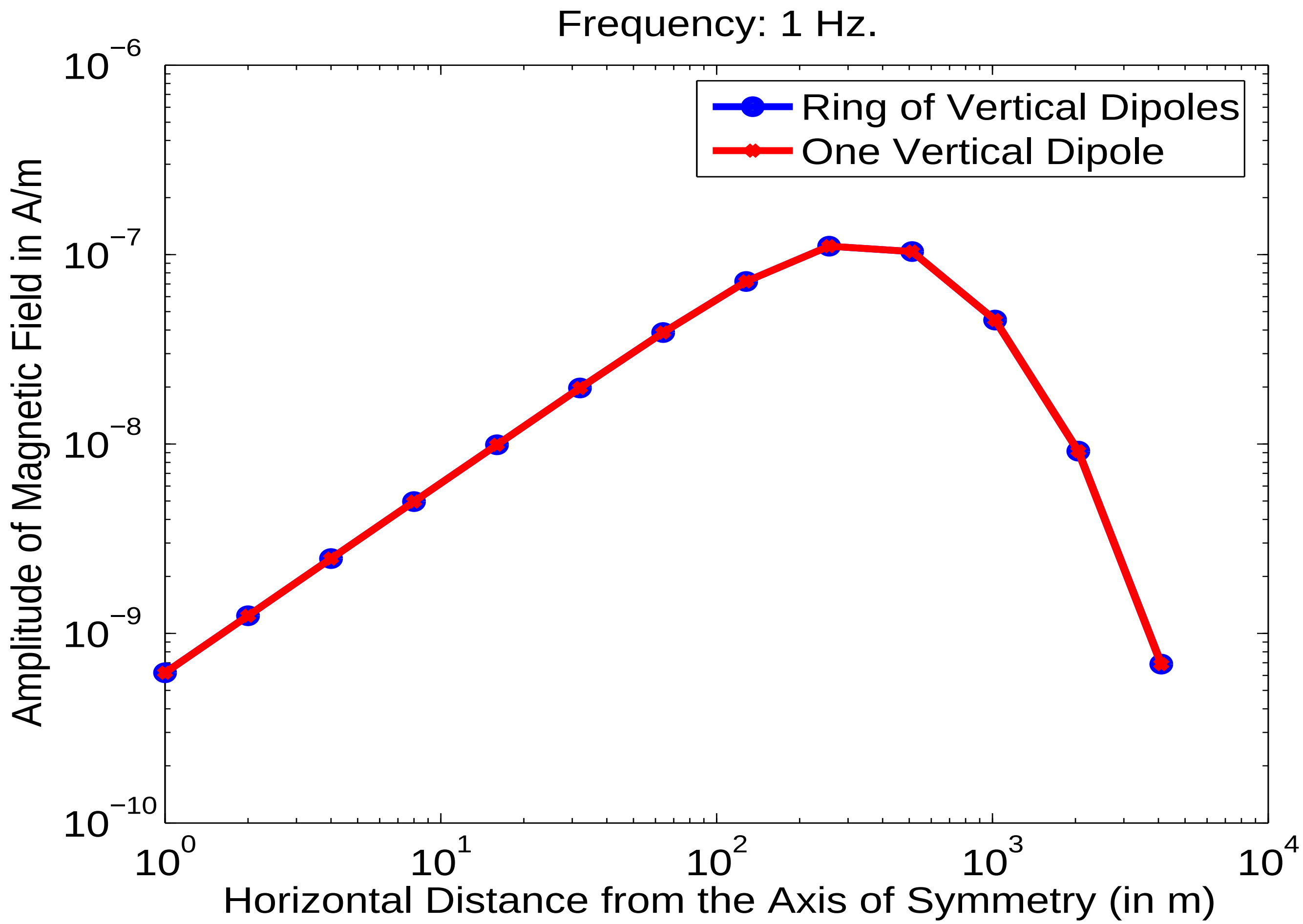

2D hp-FEM: VERIFICATION OF RESULTS

Comparison Against Analytical Solutions

Solutions in a Homogeneous Lossy ($1\ \Omega\ m$) Media (2 Mhz)

Solenoid Antenna **Toroid Antenna**

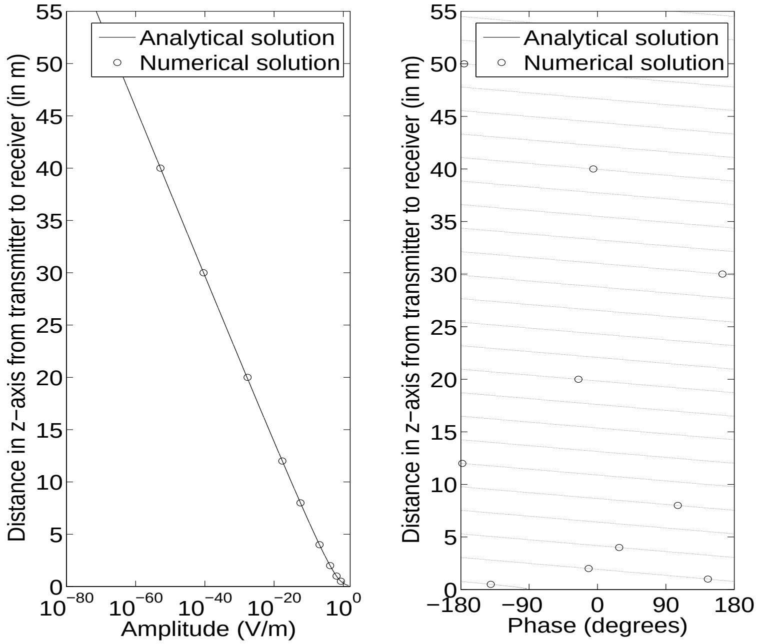

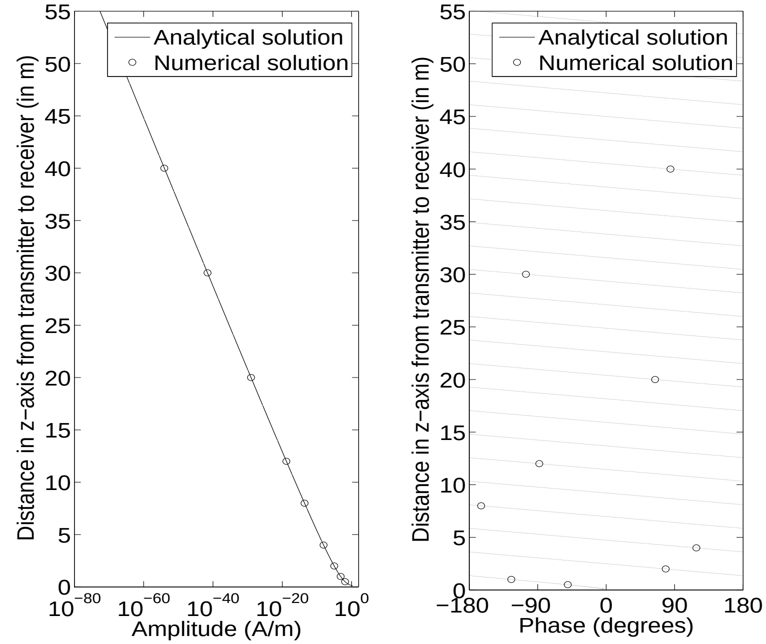

Electric Field **Magnetic Field**

2D hp-FEM: VERIFICATION OF RESULTS

Comparison Against Analytical Solutions

Solutions in a Homogeneous Lossy ($1\ \Omega\ m$) Media (2 Mhz) in Presence of a Conductive Mandrel

Solenoid Antenna

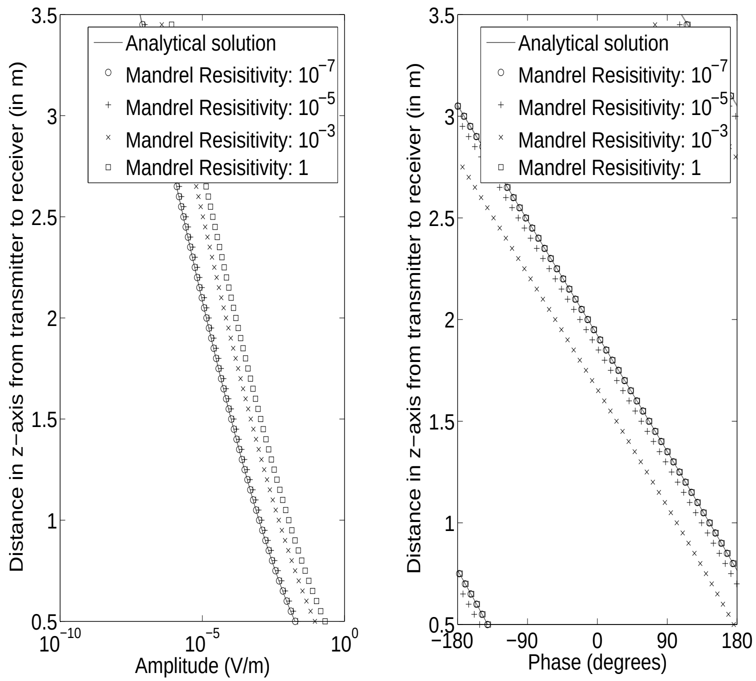

Electric Field

Toroid Antenna

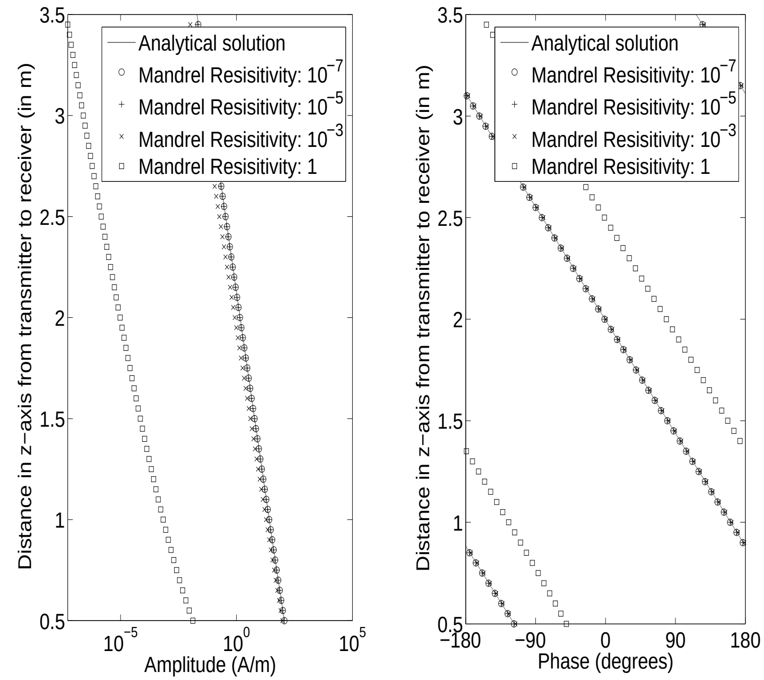

Magnetic Field

2D hp-FEM: INDUCTION INSTRUMENTS

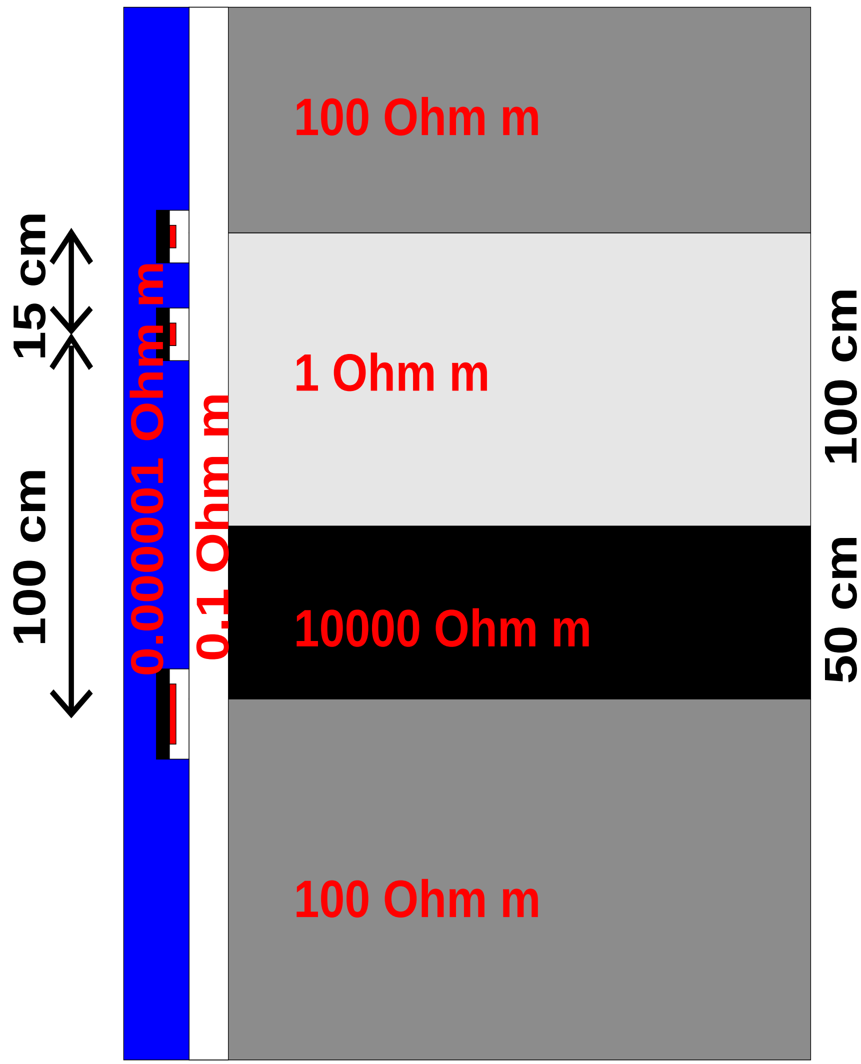

Description of Antennas

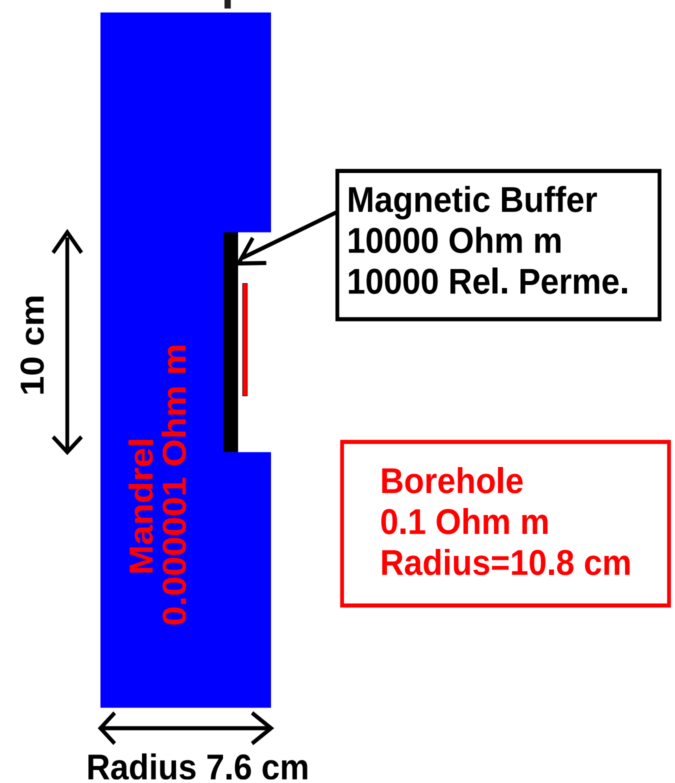

Goal: To Study the Effect of Invasion, Anistotropy, and Magnetic Permeability.

2D hp-FEM: INDUCTION INSTRUMENTS

First. Vert. Diff. E_ϕ (solenoid). Position: 0.475m

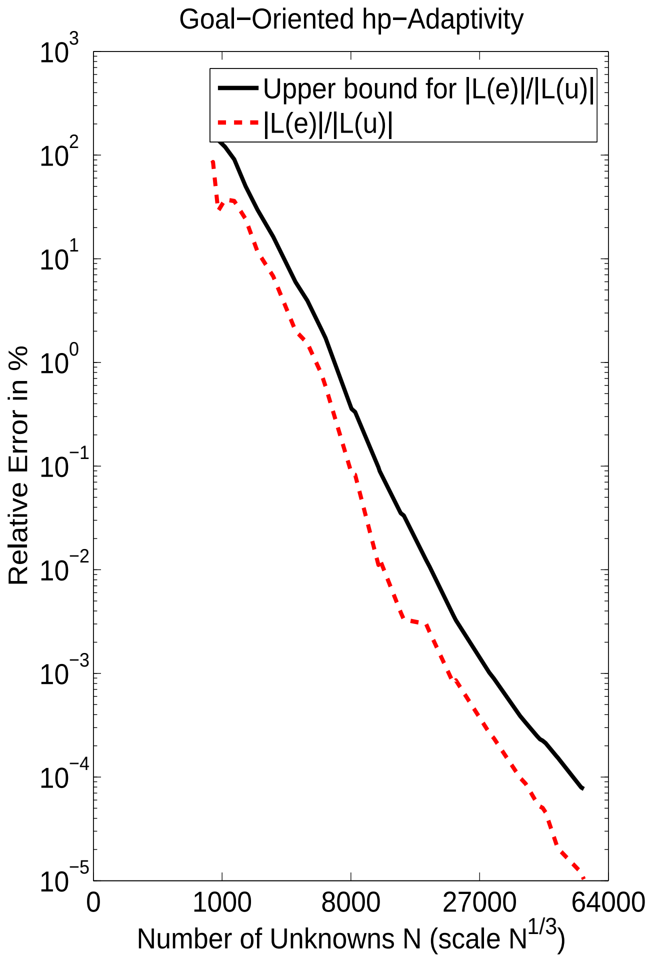

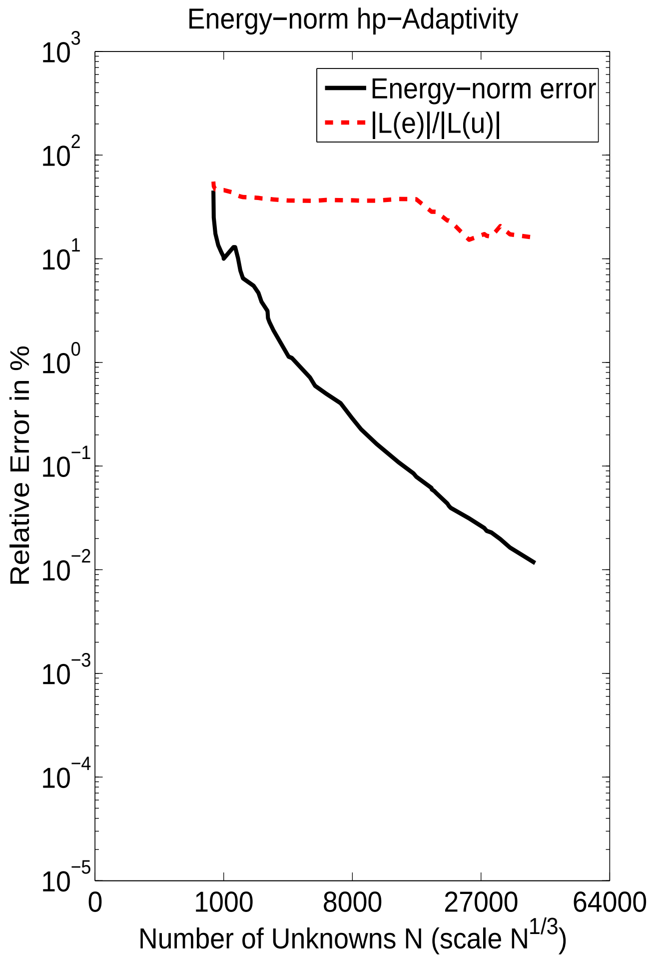

2D hp-FEM: INDUCTION INSTRUMENTS

Goal-Oriented vs. Energy-norm hp-Adaptivity

Problem with Mandrel at 2 Mhz.

Continuous Elements (Goal-Oriented Adaptivity)

Quantity of Interest	Real Part	Imag Part
COARSE GRID	-0.1629862203E-01	-0.4016944732E-02
FINE GRID	-0.1629862347E-01	-0.4016944223E-02

Continuous Elements (Energy-norm Adaptivity)

Quantity of Interest	Real Part	Imag Part
0.01% ENERGY ERROR	-0.1382759158E-01	-0.2989492851E-02

It is critical to use GOAL-ORIENTED adaptivity.

2D hp-FEM: INDUCTION INSTRUMENTS

First. Vert. Diff. E_ϕ (solenoid). Position: 0.475m

GOAL-ORIENTED HP-ADAPTIVITY (Quadrilateral Elements)

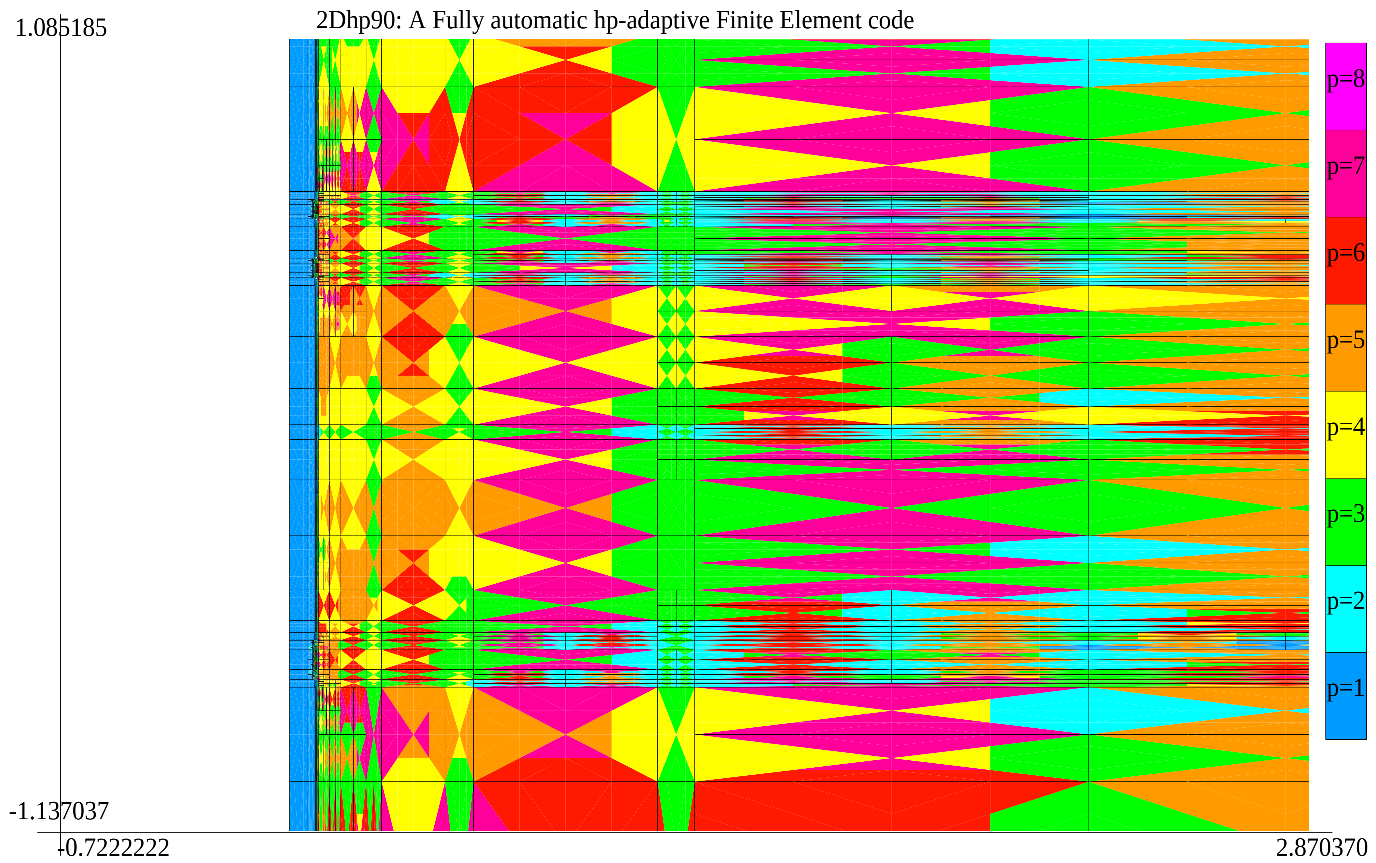

2D hp-FEM: INDUCTION INSTRUMENTS

First. Vert. Diff. E_ϕ (solenoid). Position: 0.475m

GOAL-ORIENTED HP-ADAPTIVITY (ZOOM TOWARDS FIRST RECEIVER ANTENNA)

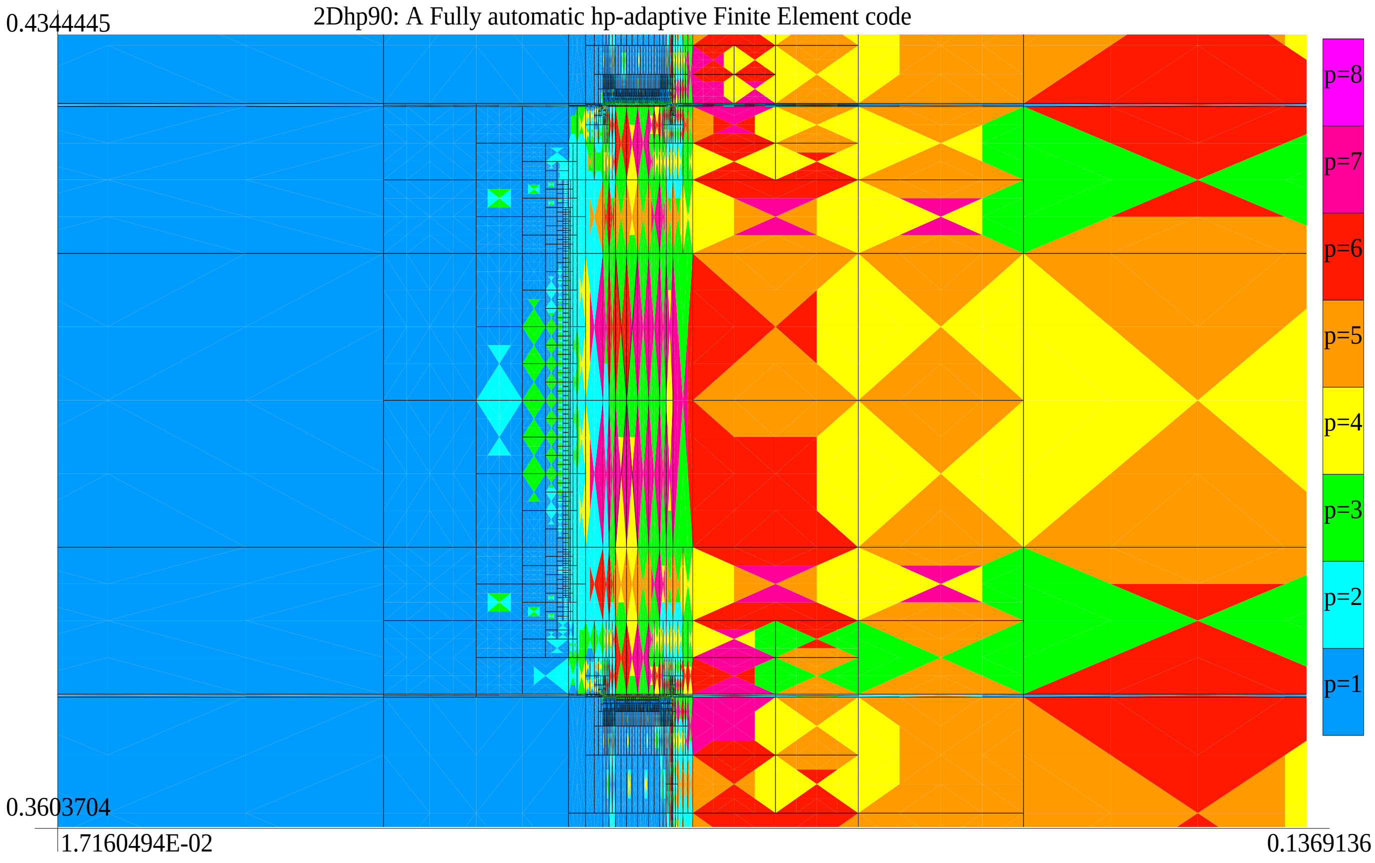

2D hp-FEM: INDUCTION INSTRUMENTS

First Vert. Diff. H_ϕ for different antennas

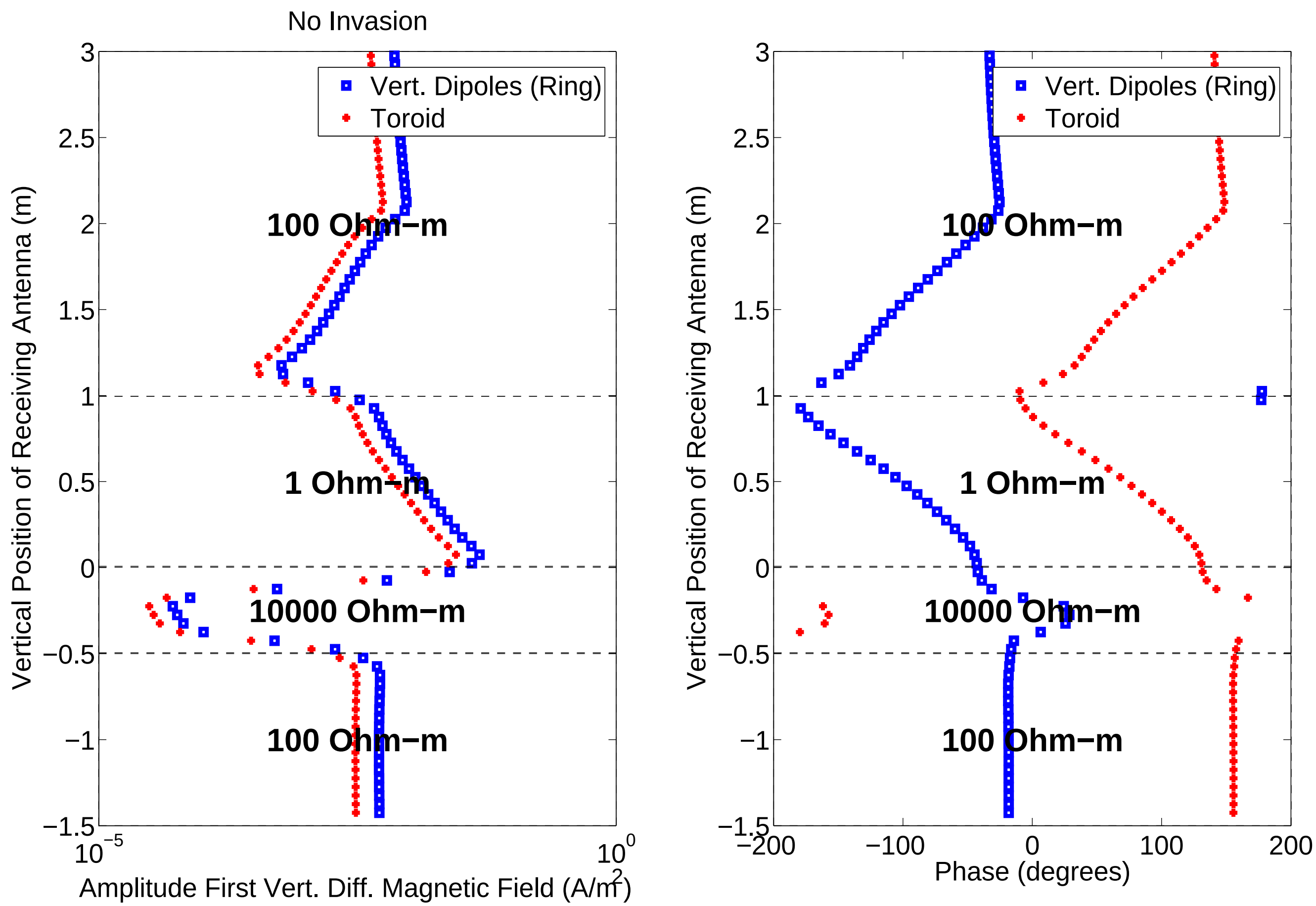

In LWD instruments, we obtain similar results using toroids or a ring of vert. dipoles

2D hp-FEM: INDUCTION INSTRUMENTS

First Vert. Diff. E_z for a toroid antenna

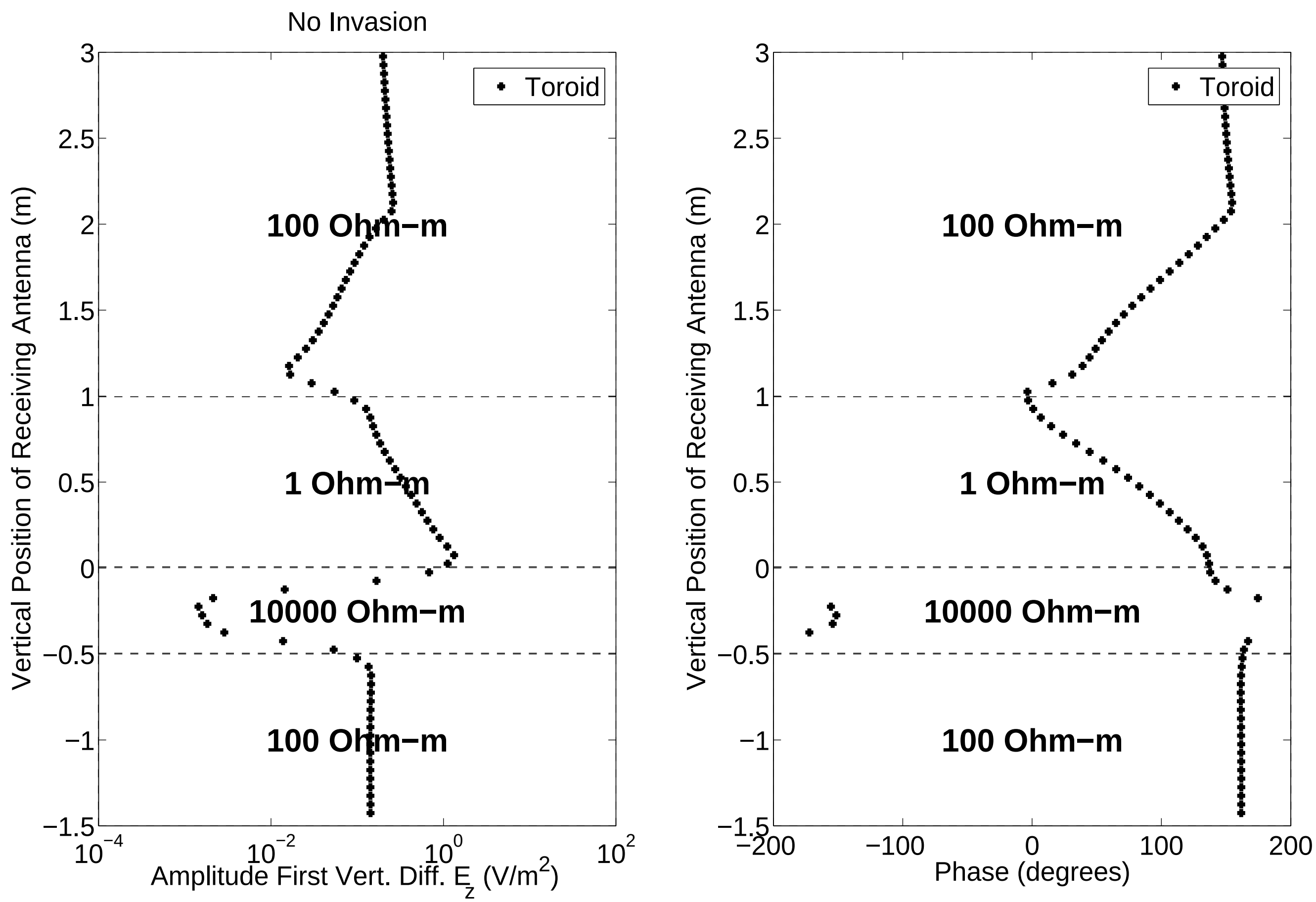

Toroids are adequate for identifying highly resistive layers

2D hp-FEM: INDUCTION INSTRUMENTS

First Vert. Diff. E_ϕ for a solenoid antenna

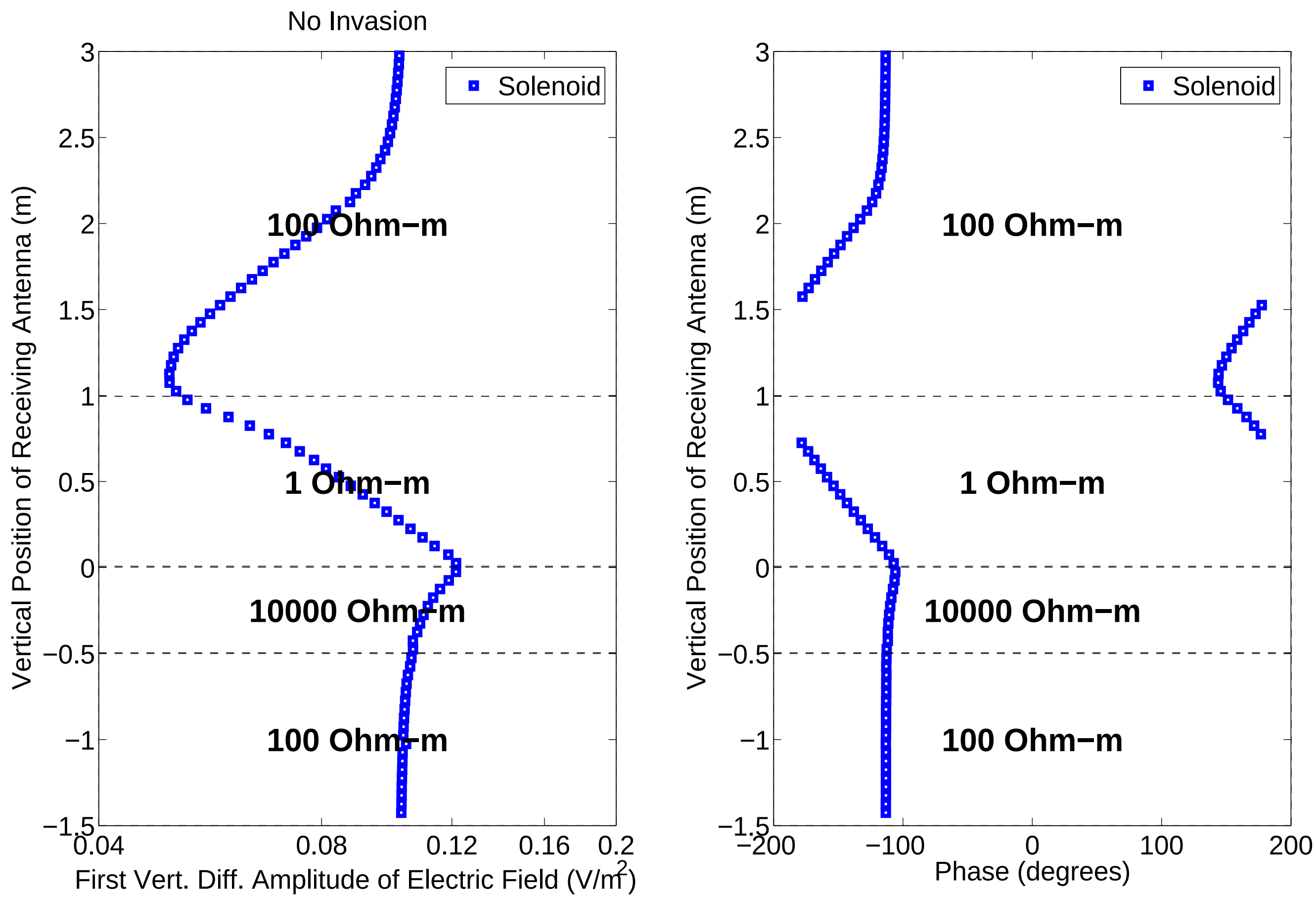

Solenoids are adequate for identifying low resistive layers

2D hp-FEM: INDUCTION INSTRUMENTS

Use of Magnetic Buffers (E_ϕ for a solenoid)

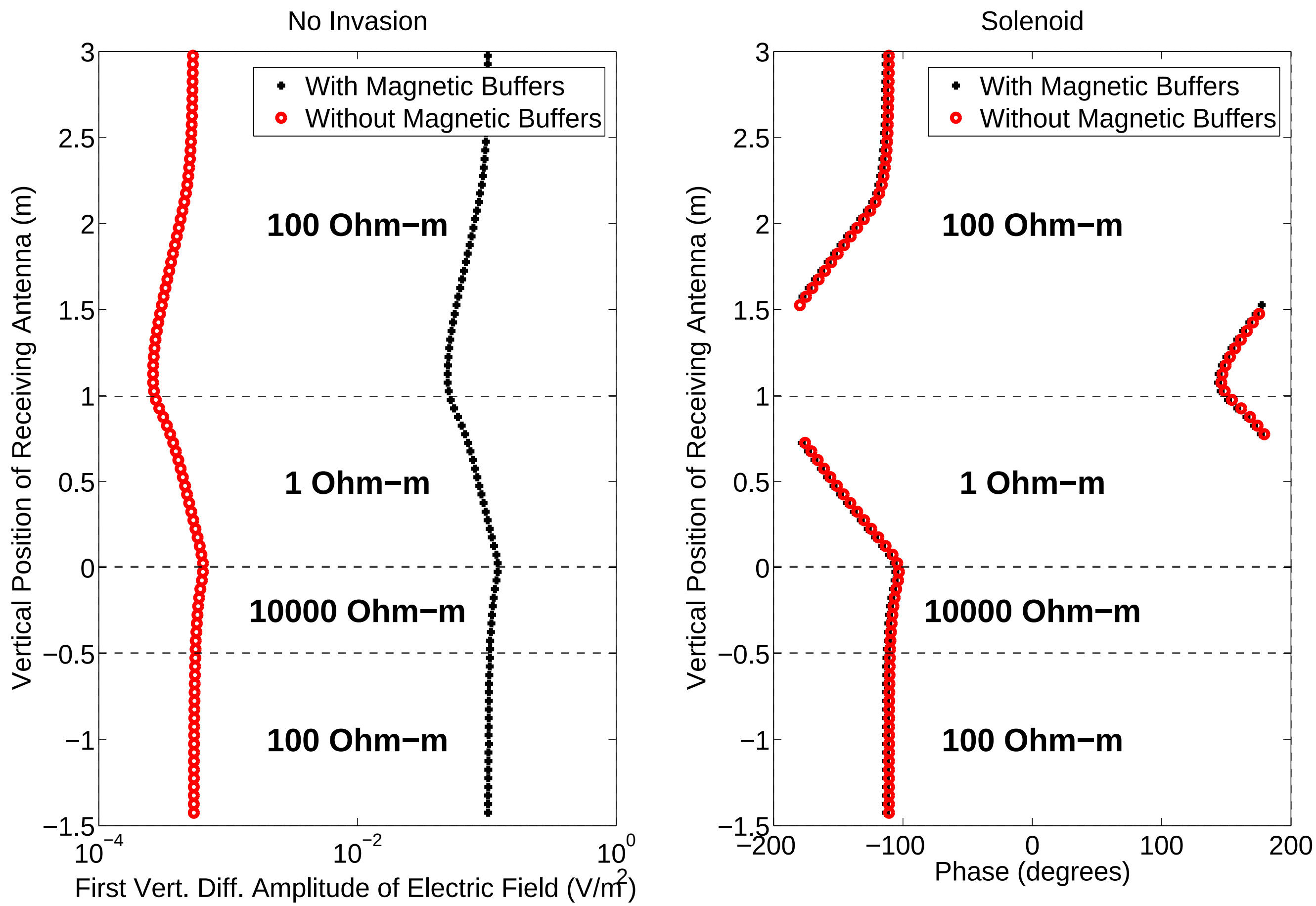

Use of magnetic buffers strengthen the signal in combination with solenoids

2D hp-FEM: INDUCTION INSTRUMENTS

Use of Magnetic Buffers (H_ϕ for a toroid)

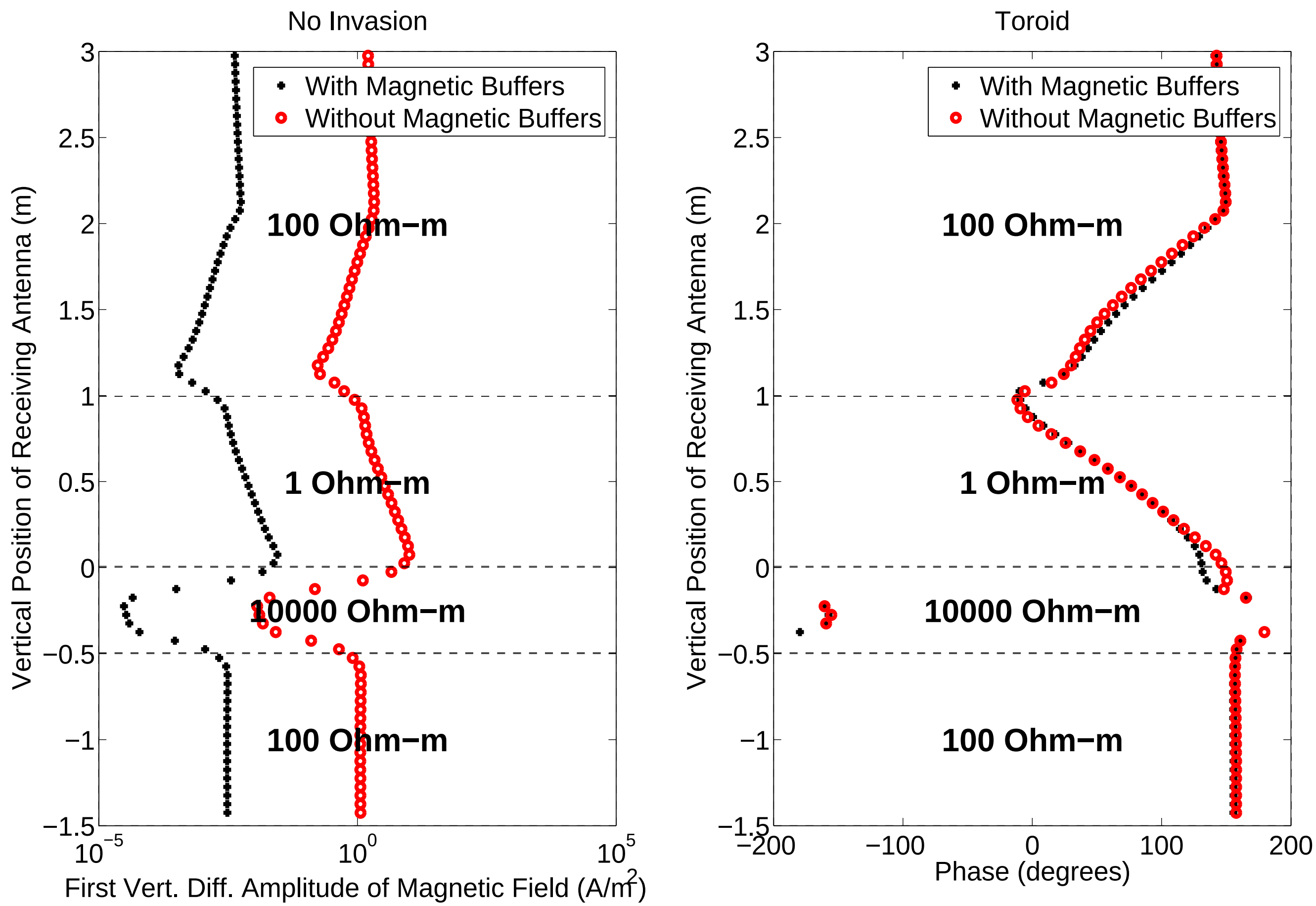

However, magnetic buffers weaken the signal in combination with toroids

2D hp-FEM: INDUCTION INSTRUMENTS

Invasion study (E_ϕ for a solenoid)

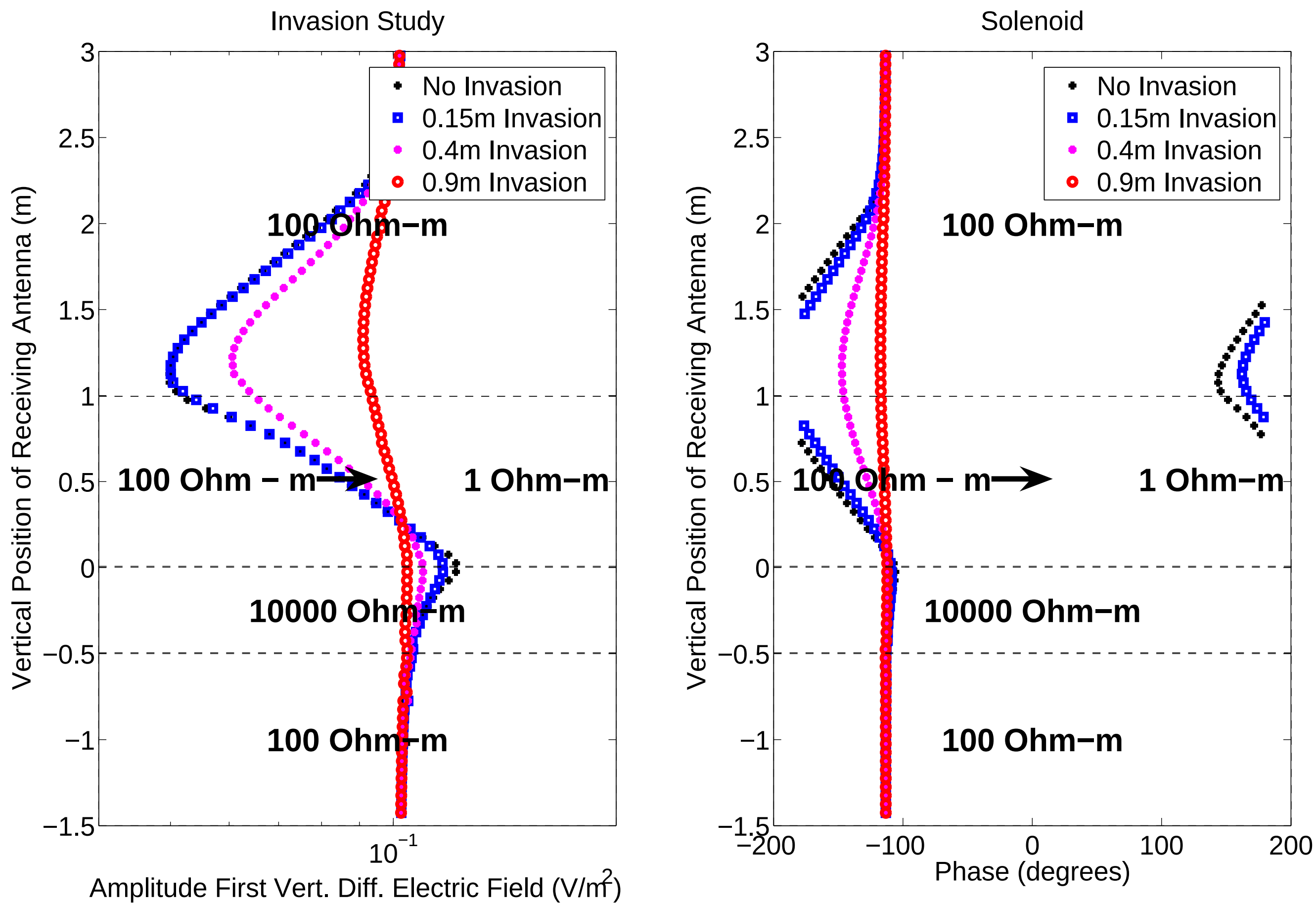

Large invasion effects can be sensed using solenoids

2D hp-FEM: INDUCTION INSTRUMENTS

Invasion study (H_ϕ for a toroid)

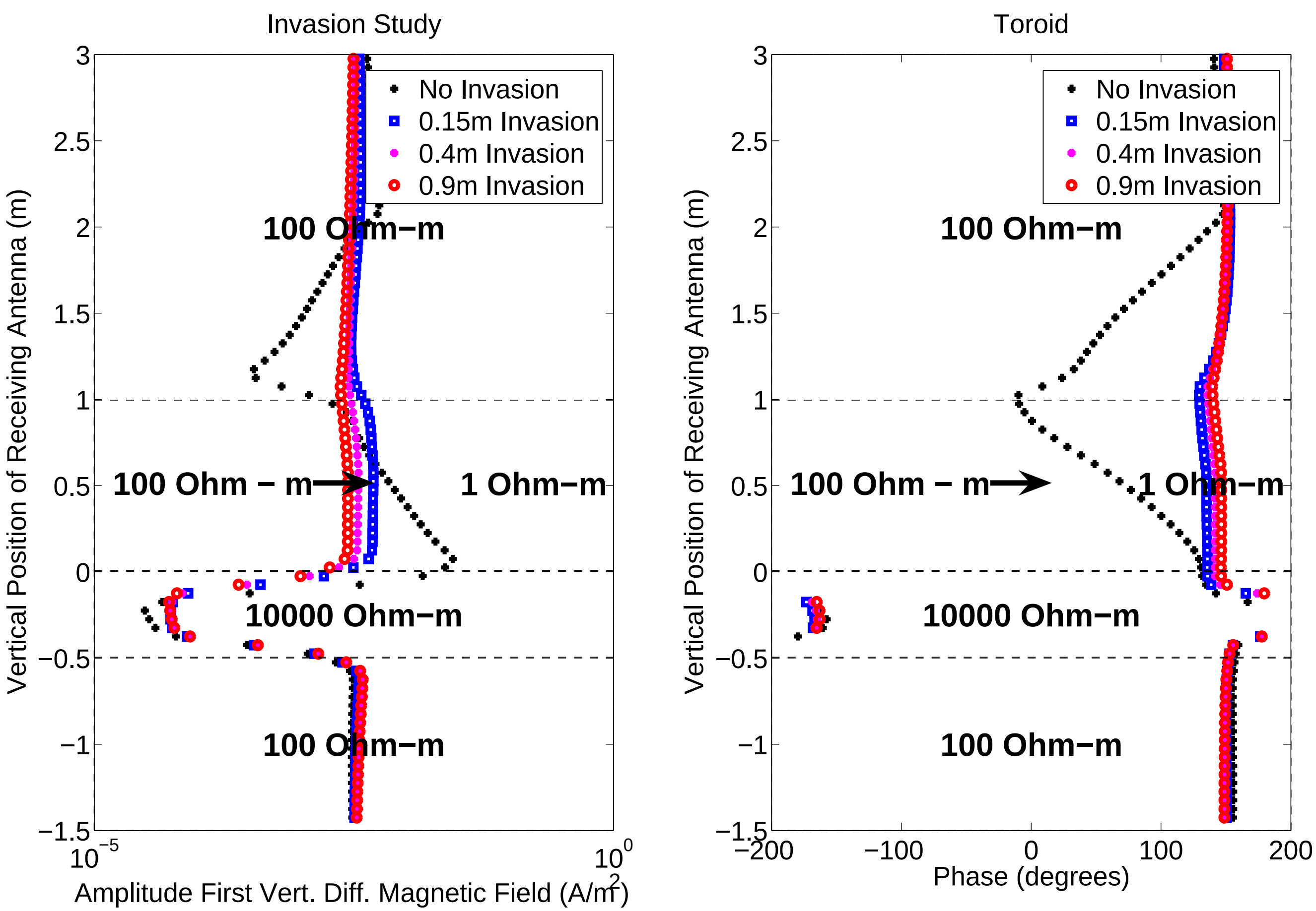

Small invasion effects can be sensed using toroids

2D hp-FEM: INDUCTION INSTRUMENTS

Invasion study (E_ϕ for a solenoid)

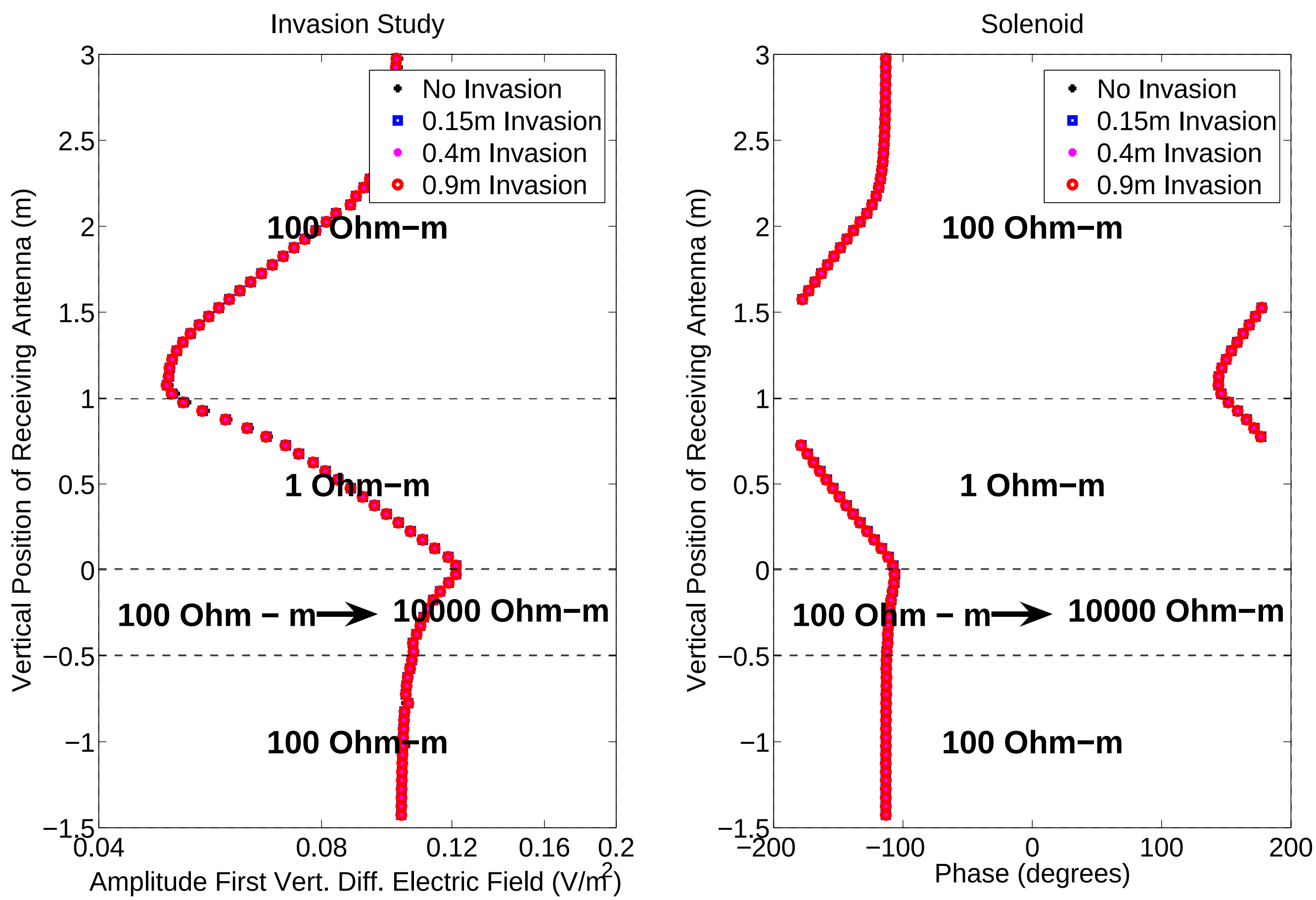

Invasion in resistive layers cannot be sensed using solenoids

2D hp-FEM: INDUCTION INSTRUMENTS

Invasion study (H_ϕ for a toroid)

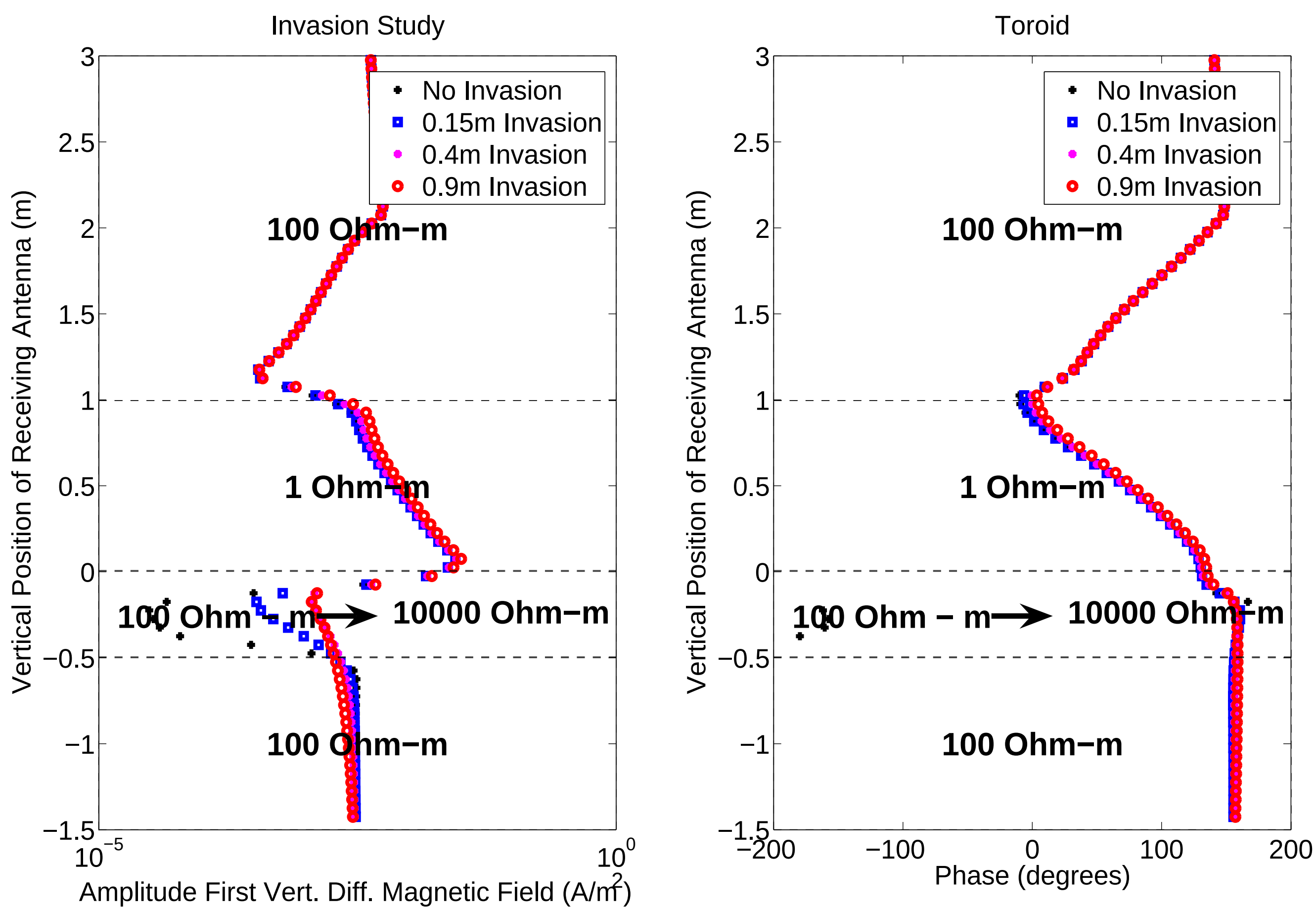

Invasion in resistive layers should be studied using toroids

2D hp-FEM: INDUCTION INSTRUMENTS

Invasion and mandrel magnetic permeab. (E_ϕ)

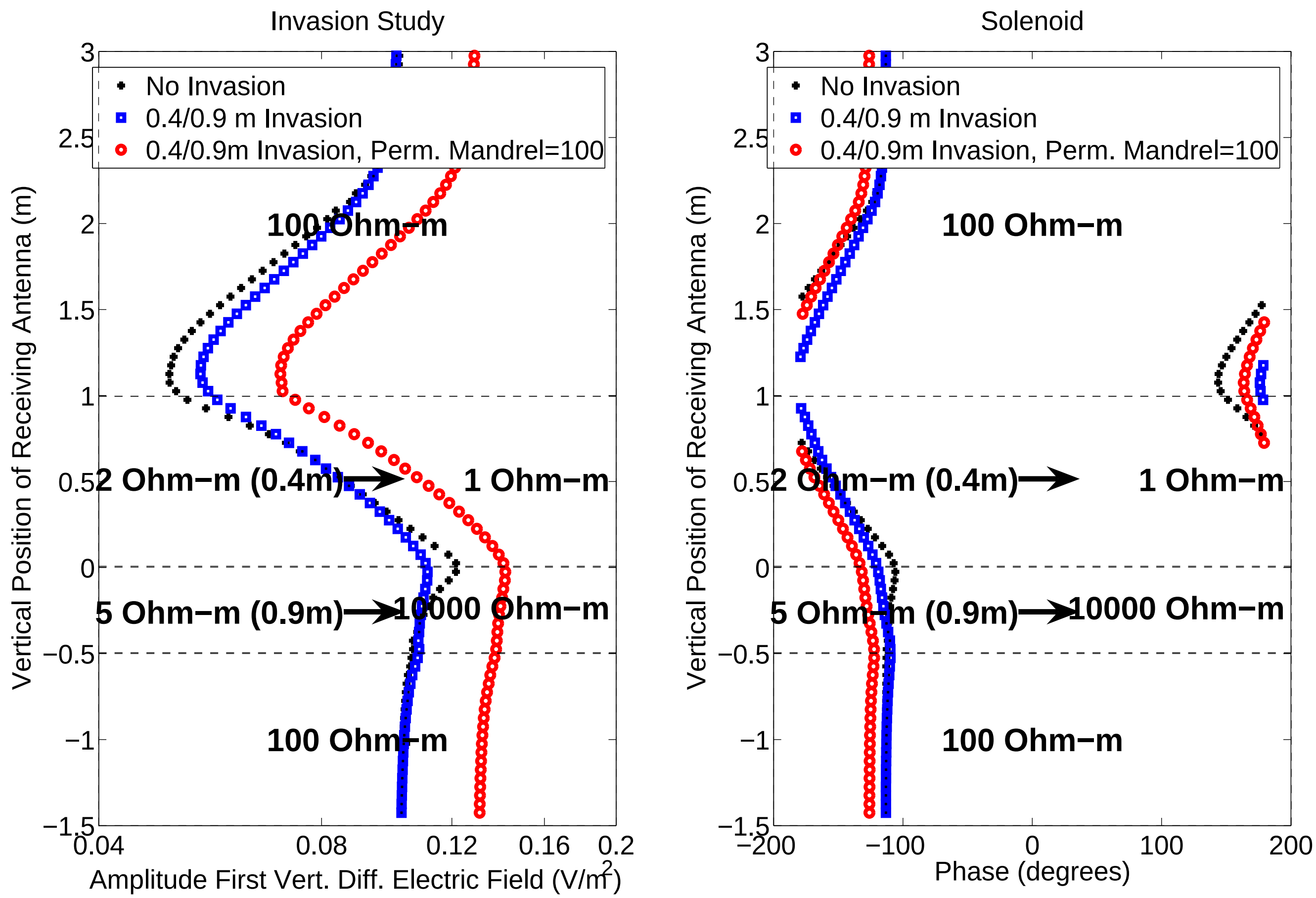

The effect of magnetic permeability on the mandrel is similar to the effect of magnetic buffers

2D hp-FEM: INDUCTION INSTRUMENTS

Anisotropy (H_ϕ)

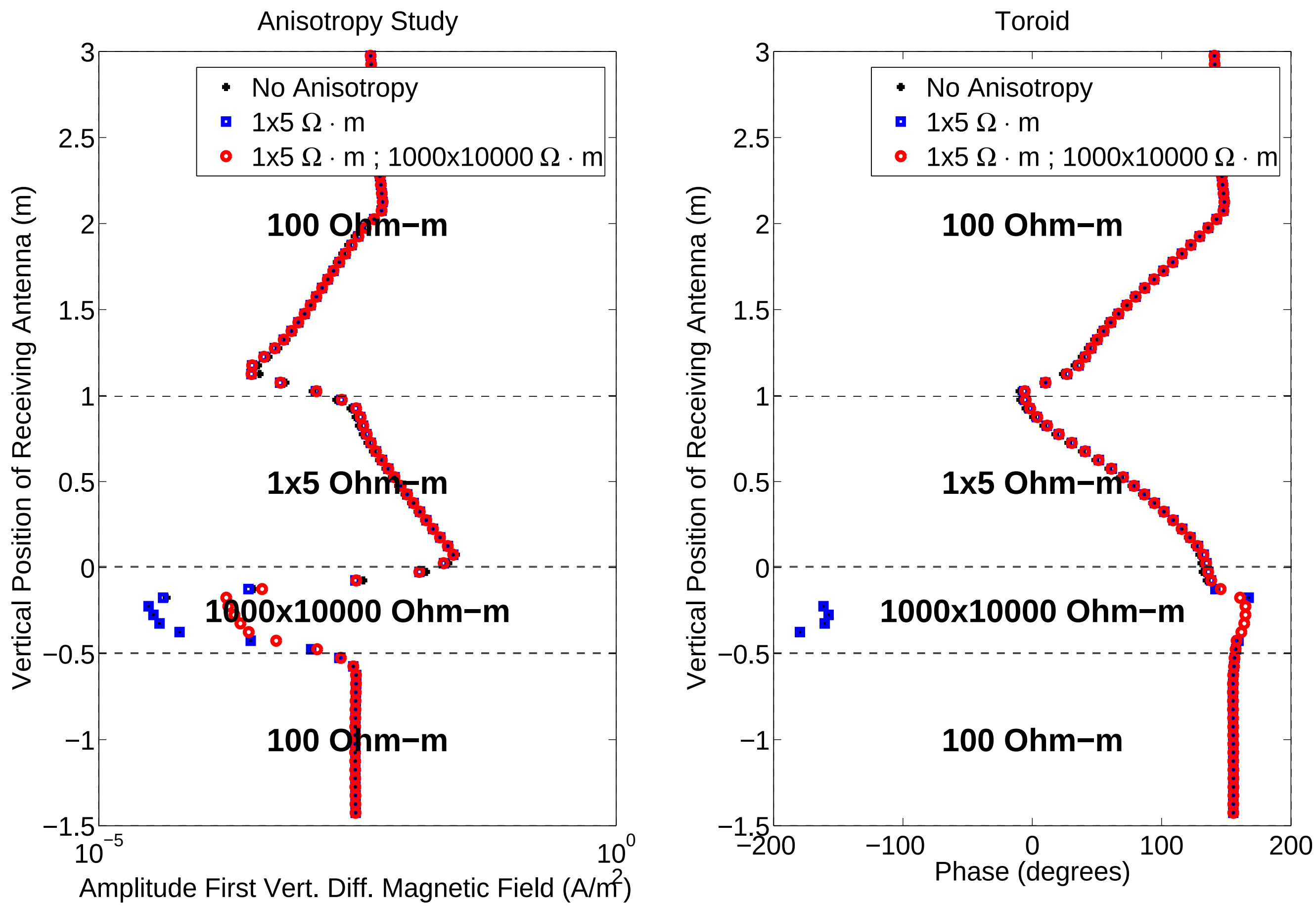

Anisotropy effects may be important when studying resistive layers

2D hp-FEM: THROUGH CASING INSTRUMENTS

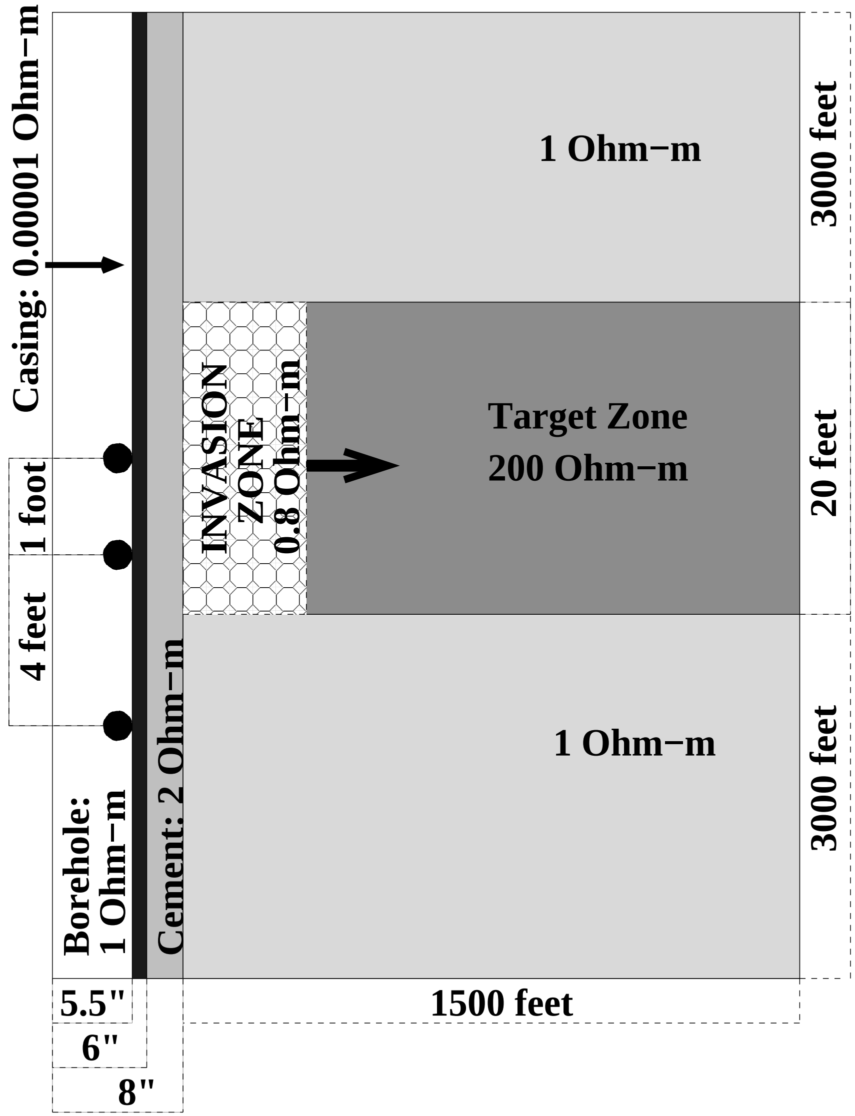

Axisymmetric 3D problem.

Seven different materials.

Through casing resistivity instrument.

Objective: Study the effect of water invasion THROUGH CASING.

2D hp-FEM: THROUGH CASING INSTRUMENTS

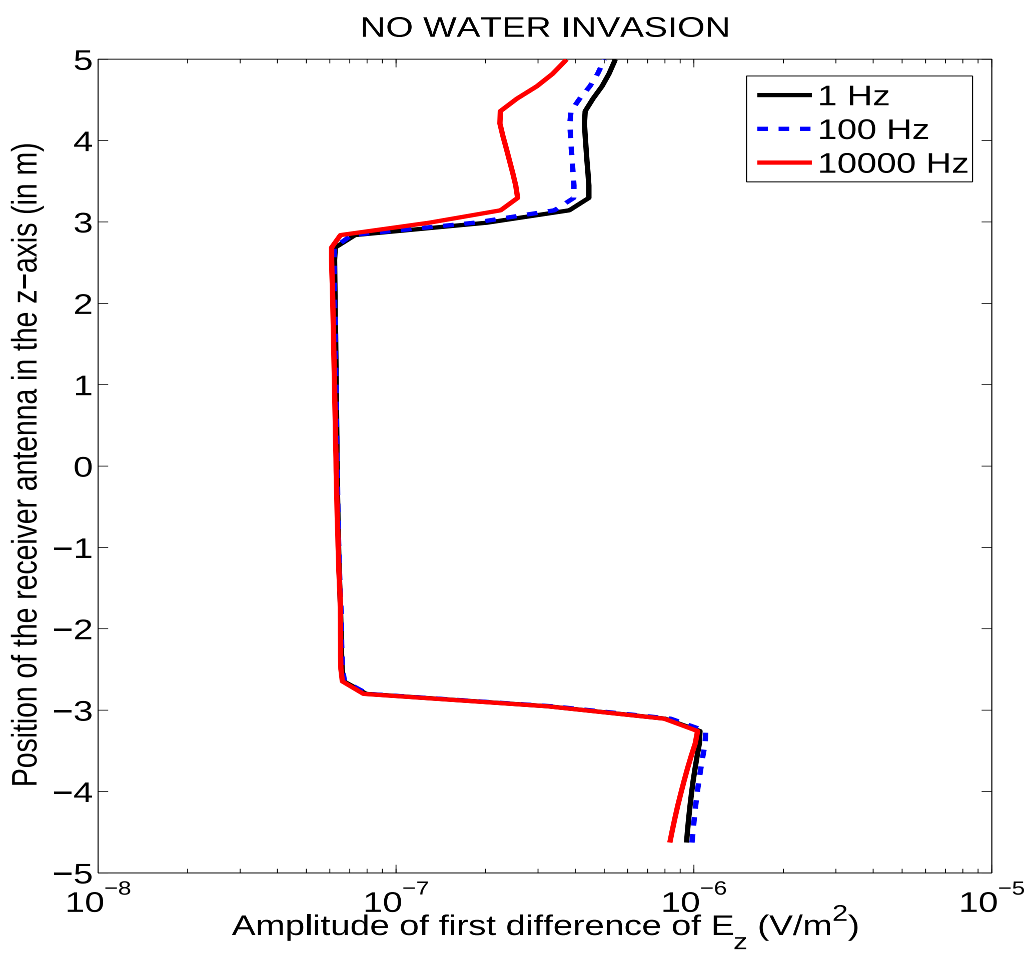

Variations due to frequency are small (below 5%)

2D hp-FEM: THROUGH CASING INSTRUMENTS

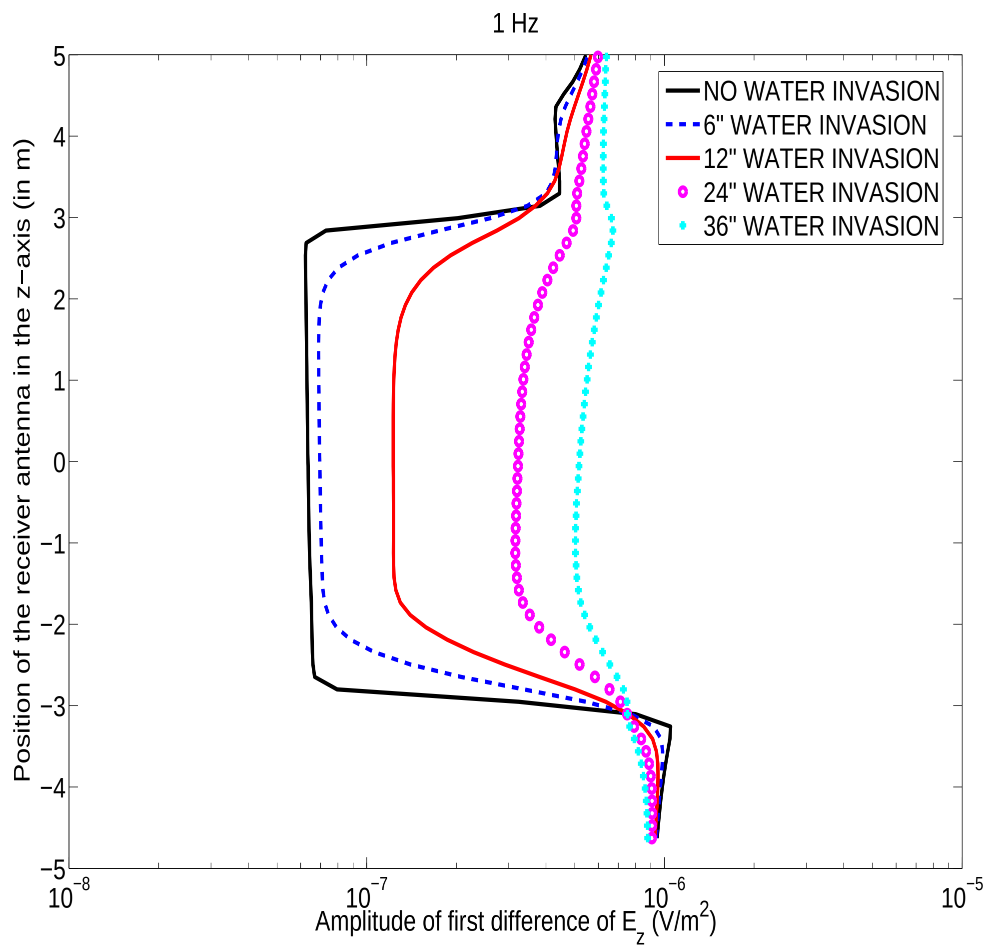

Water invasion through casing can be accurately assessed

2D hp-FEM: THROUGH CASING INSTRUMENTS

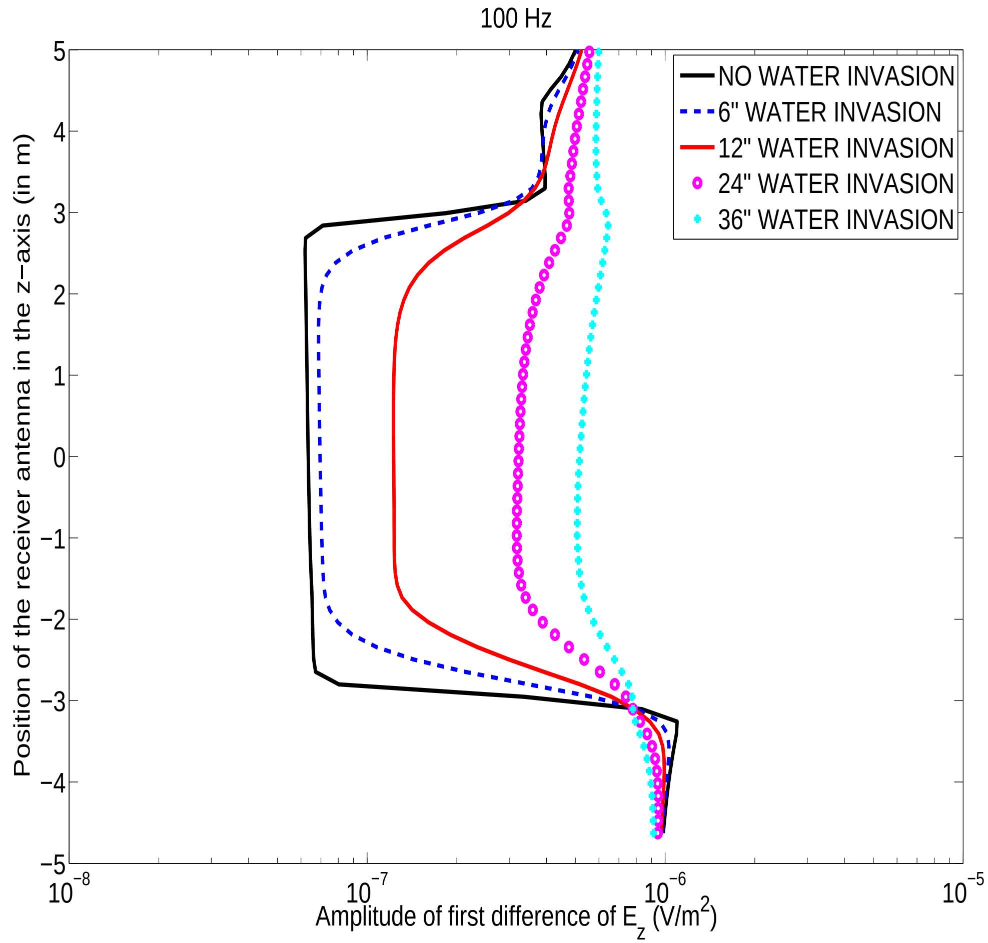

Water invasion through casing can be accurately assessed

2D hp-FEM: THROUGH CASING INSTRUMENTS

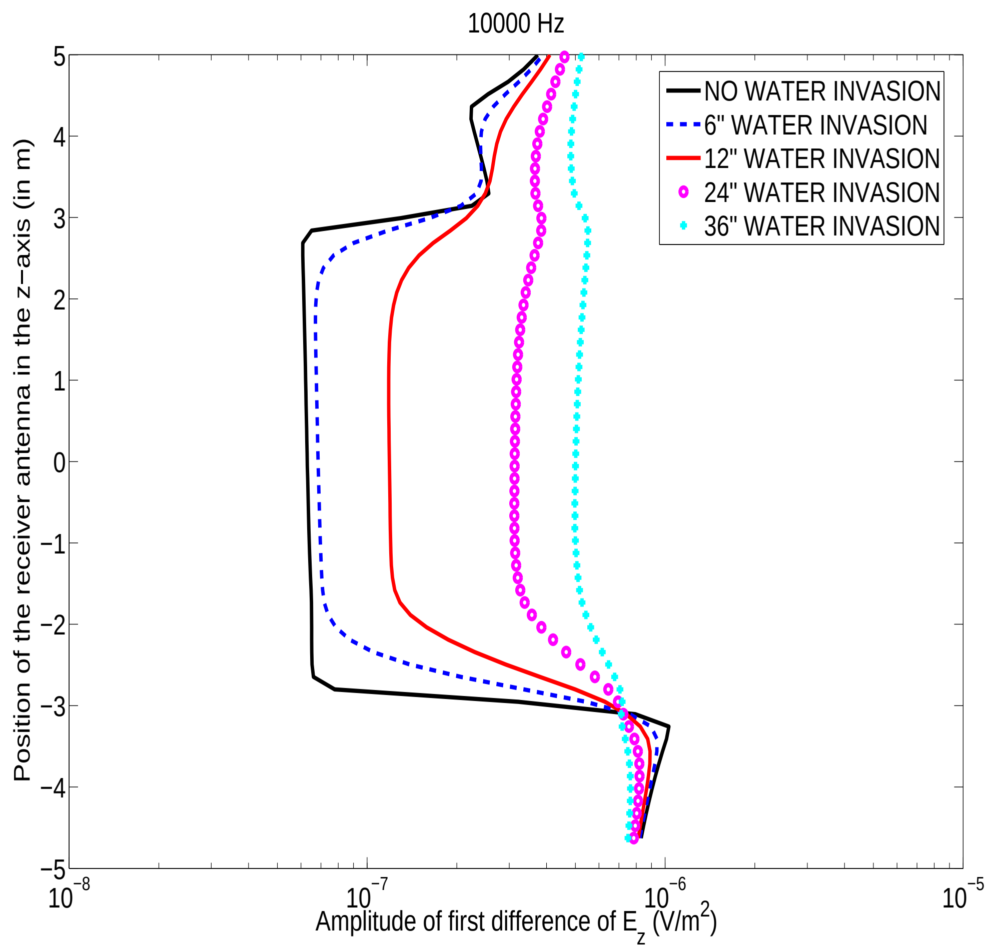

Water invasion through casing can be accurately assessed

2D hp-FEM: THROUGH CASING INSTRUMENTS

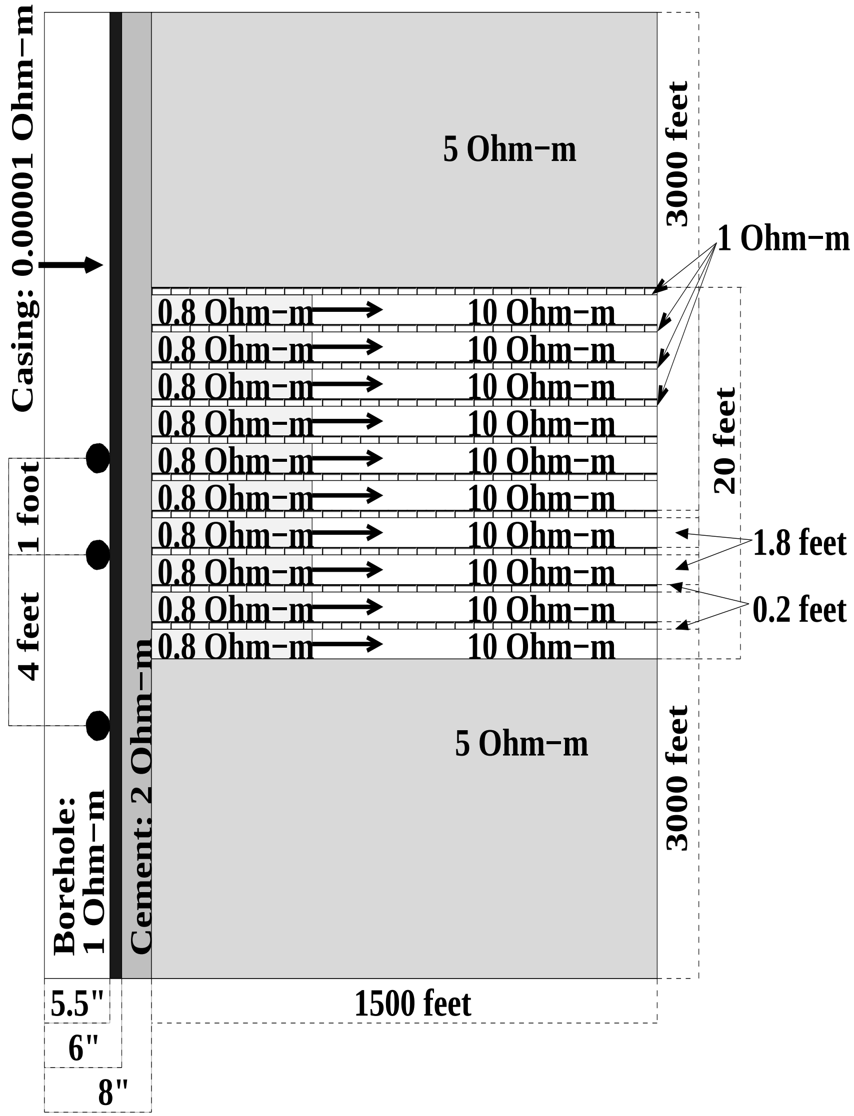

Axisymmetric 3D problem.

Seven different materials.

Through casing resistivity instrument.

Large variations on resistivity.

Objective: Study the effect of invasion THROUGH CASING on laminated sands.

2D hp-FEM: THROUGH CASING INSTRUMENTS

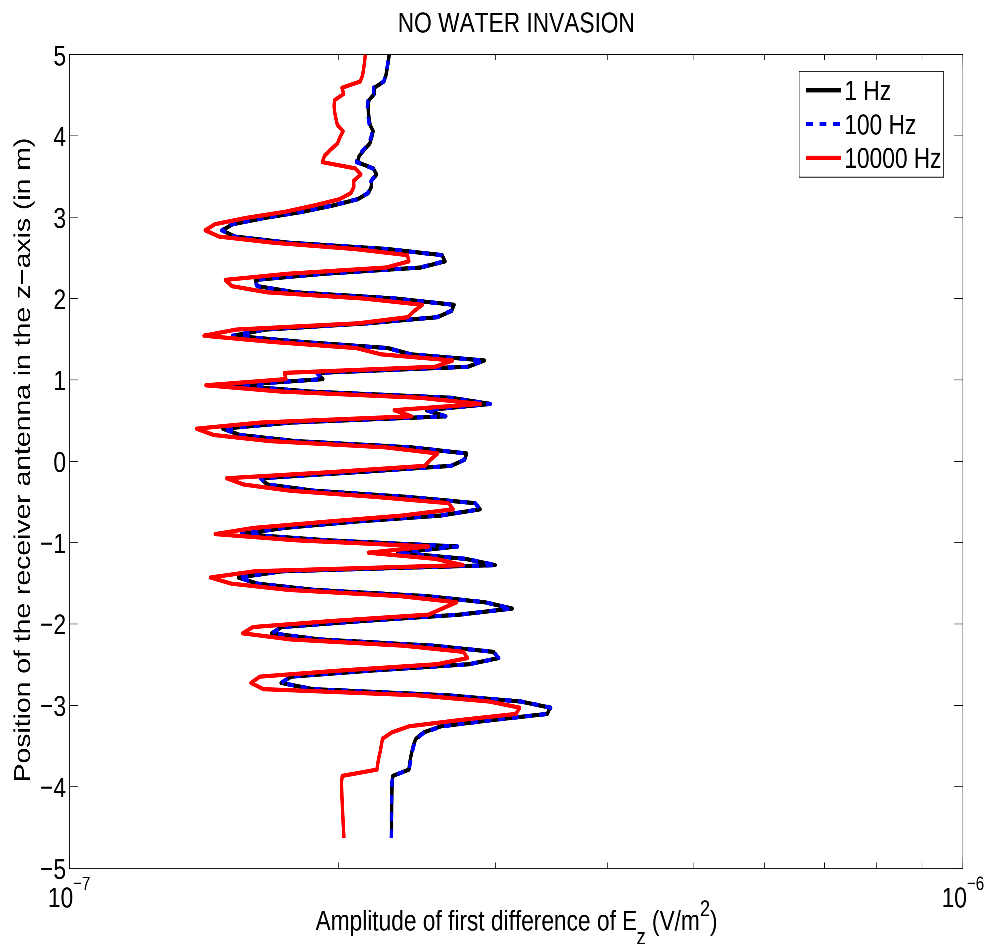

Variations due to frequency are small (below 5%)

2D hp-FEM: THROUGH CASING INSTRUMENTS

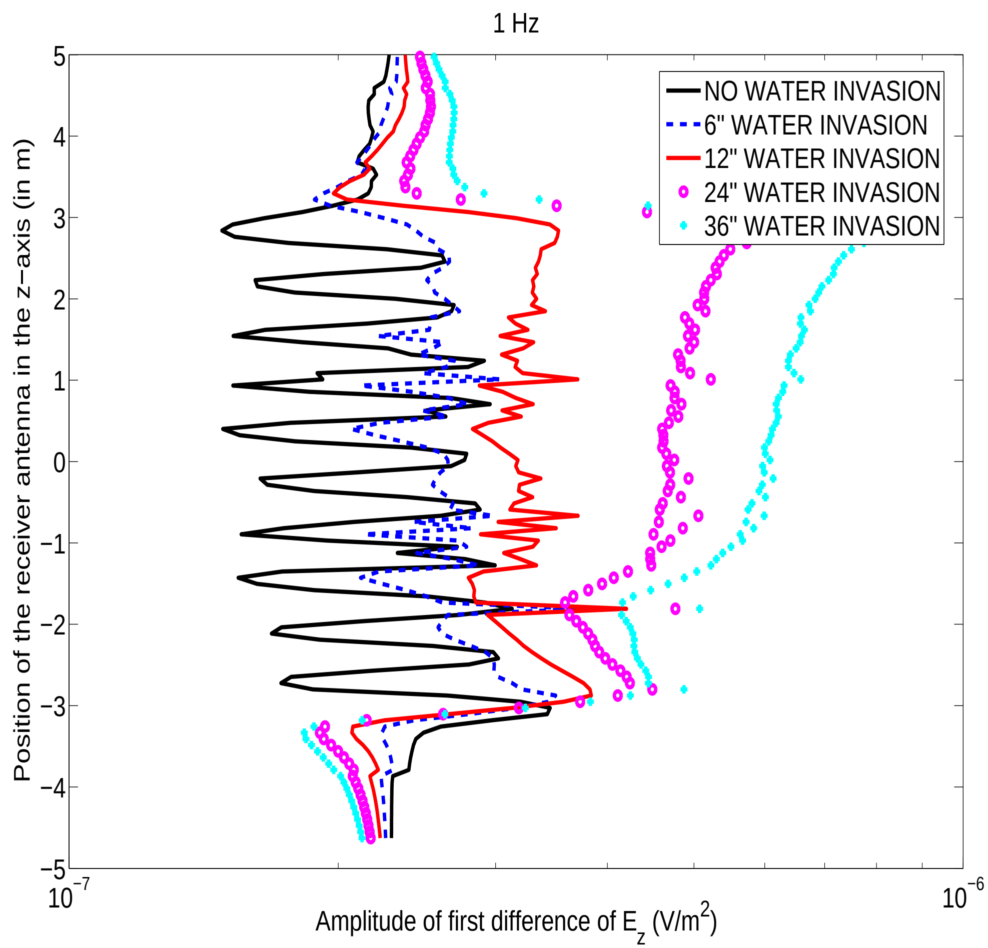

Variations due to water ivasion are large

2D hp-FEM: THROUGH CASING INSTRUMENTS

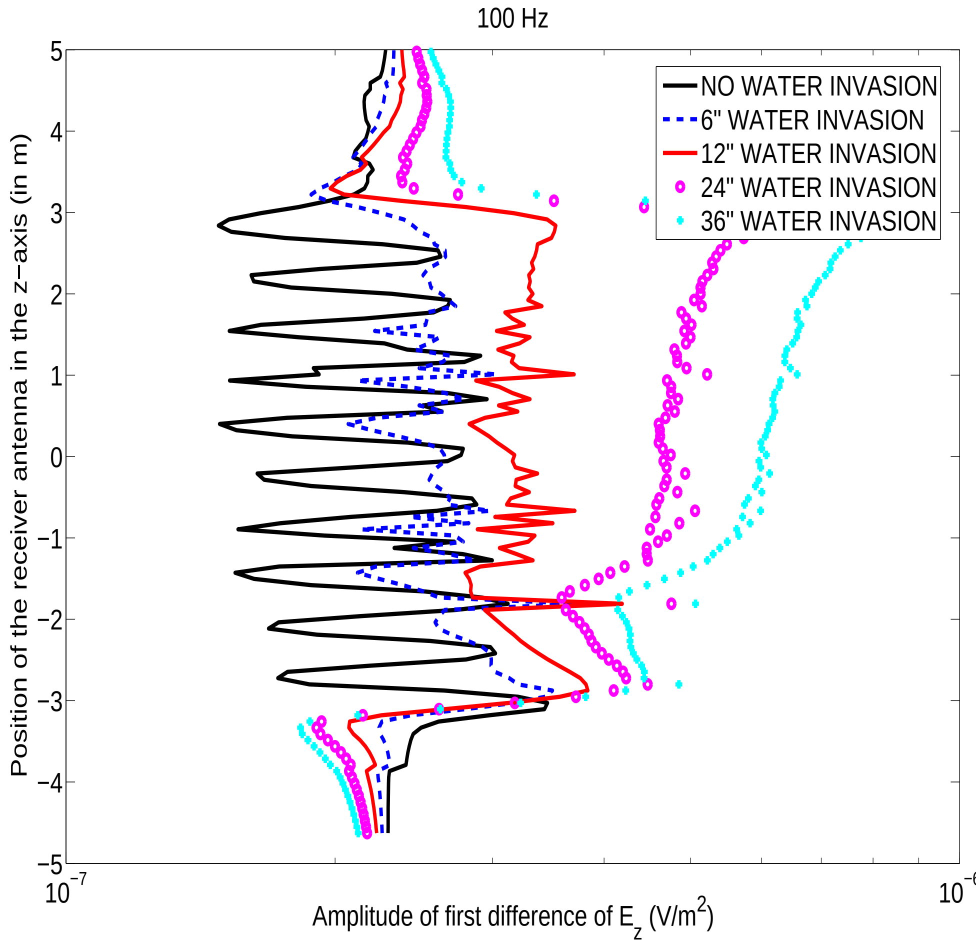

Variations due to water ivasion are large

2D hp-FEM: THROUGH CASING INSTRUMENTS

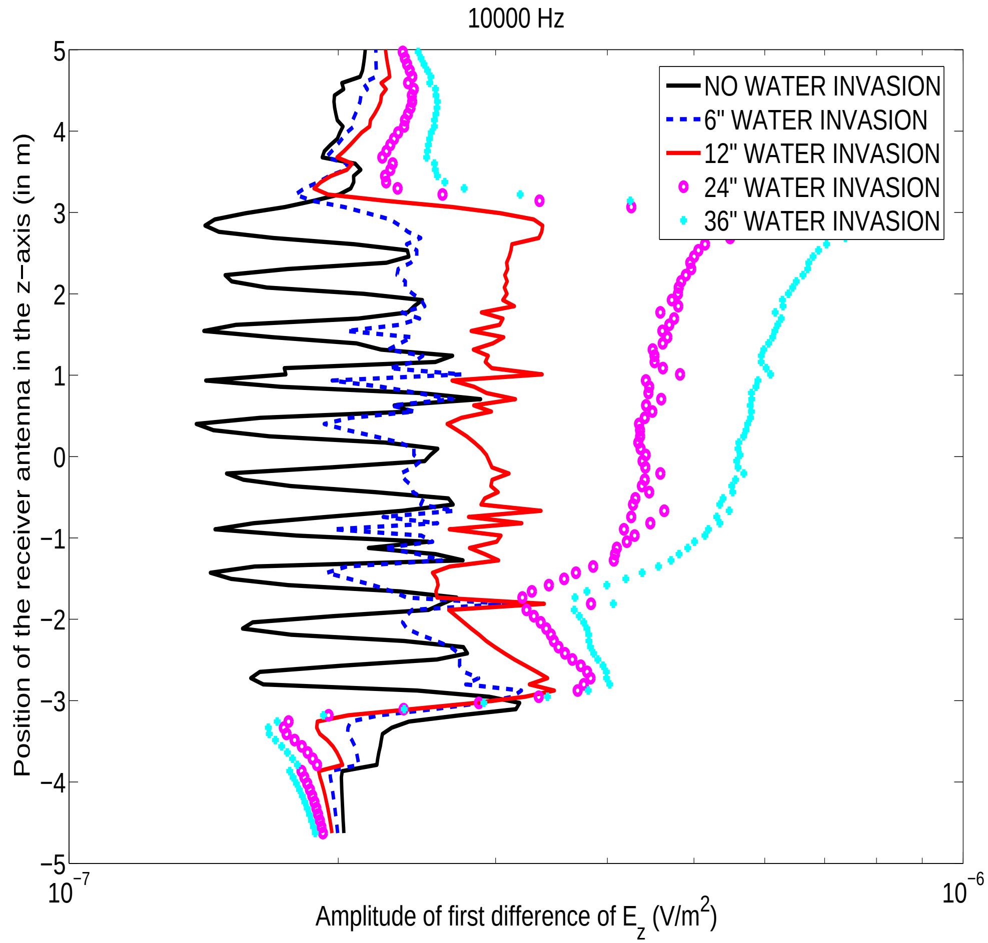

Variations due to water ivasion are large

2D hp-FEM: THROUGH CASING INSTRUMENTS

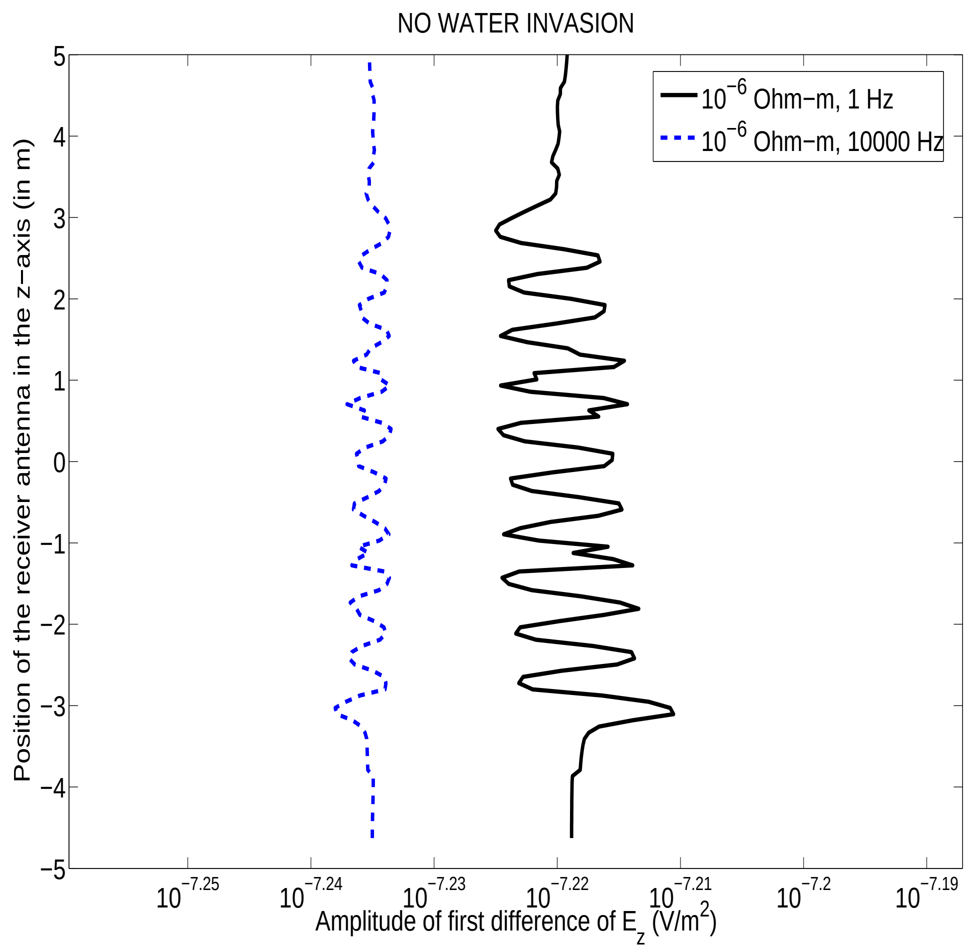

Casing resistivity can be analyzed from different frequency measurements

2D hp-FEM: THROUGH CASING INSTRUMENTS

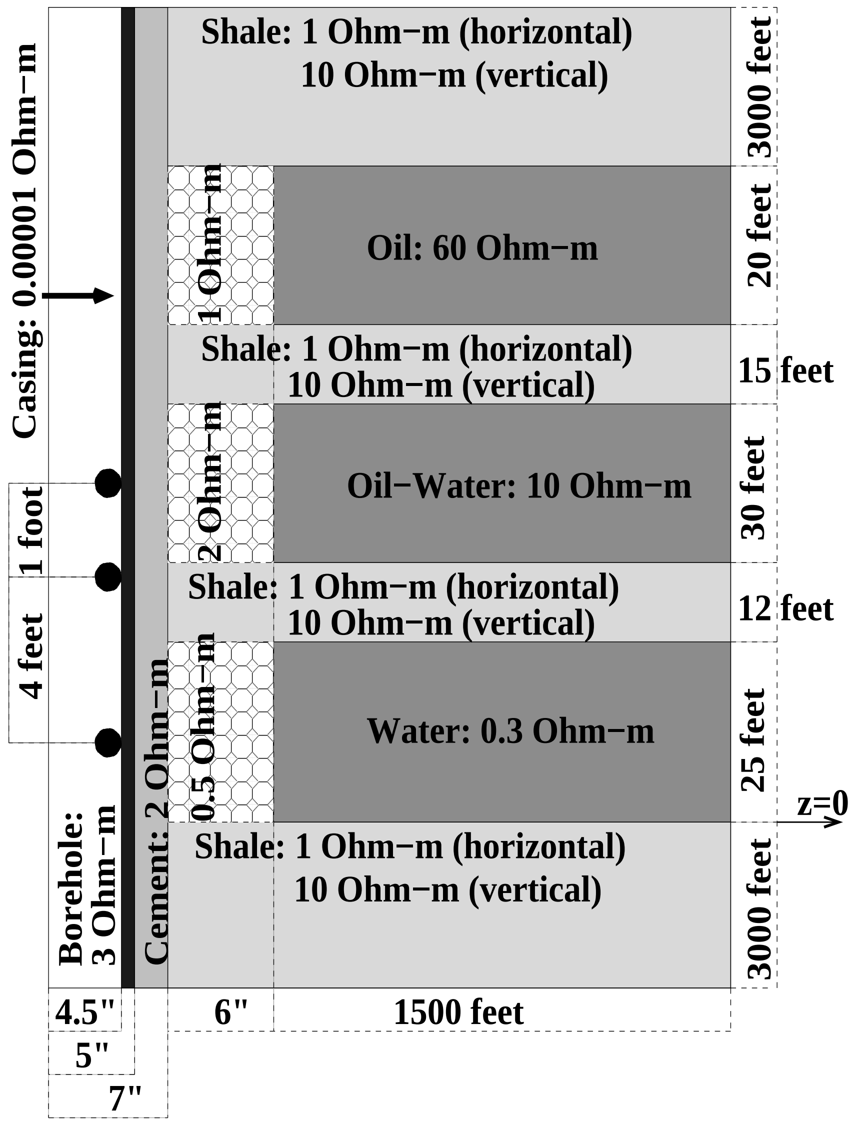

Axisymmetric 3D problem.

Seven different materials with high contrast on resistivity.

Through casing resistivity instrument.

Objective: Study the effect of invasion and anisotropy THROUGH CASING.

2D hp-FEM: THROUGH CASING INSTRUMENTS

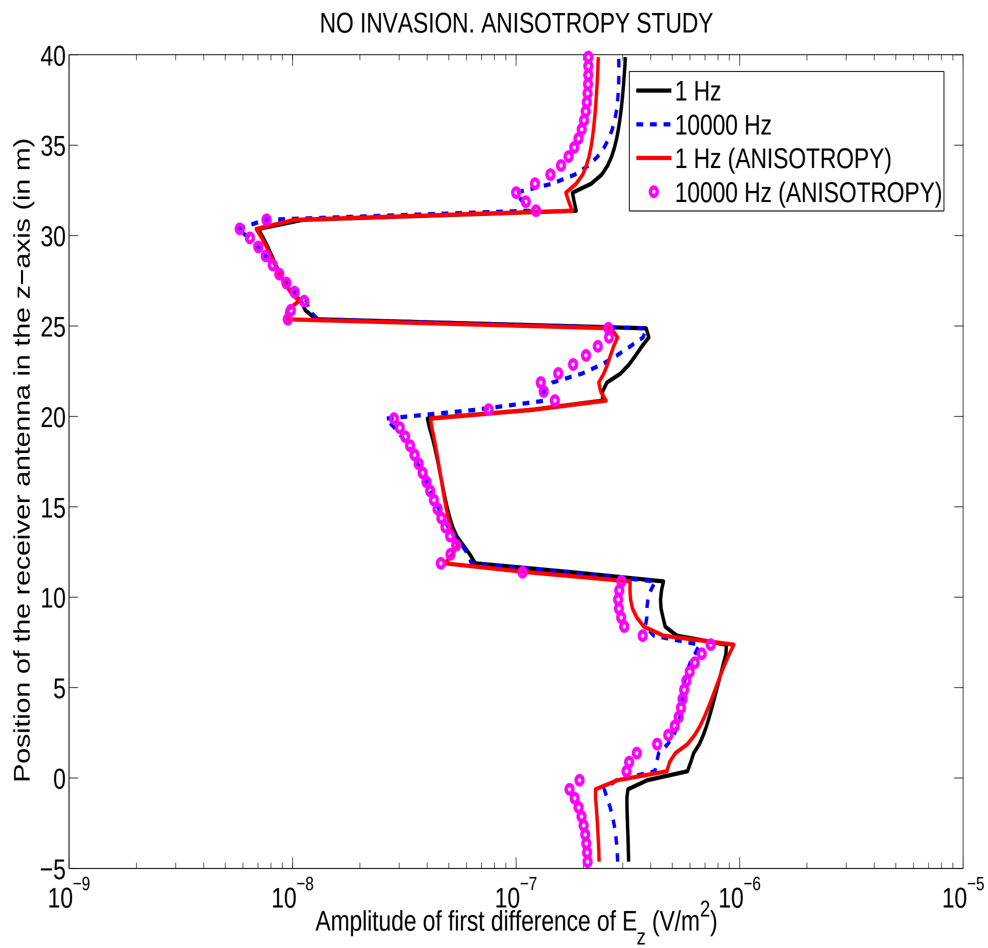

Study of anisotropy and frequency effects require from high accuracy simulations

2D hp-FEM: THROUGH CASING INSTRUMENTS

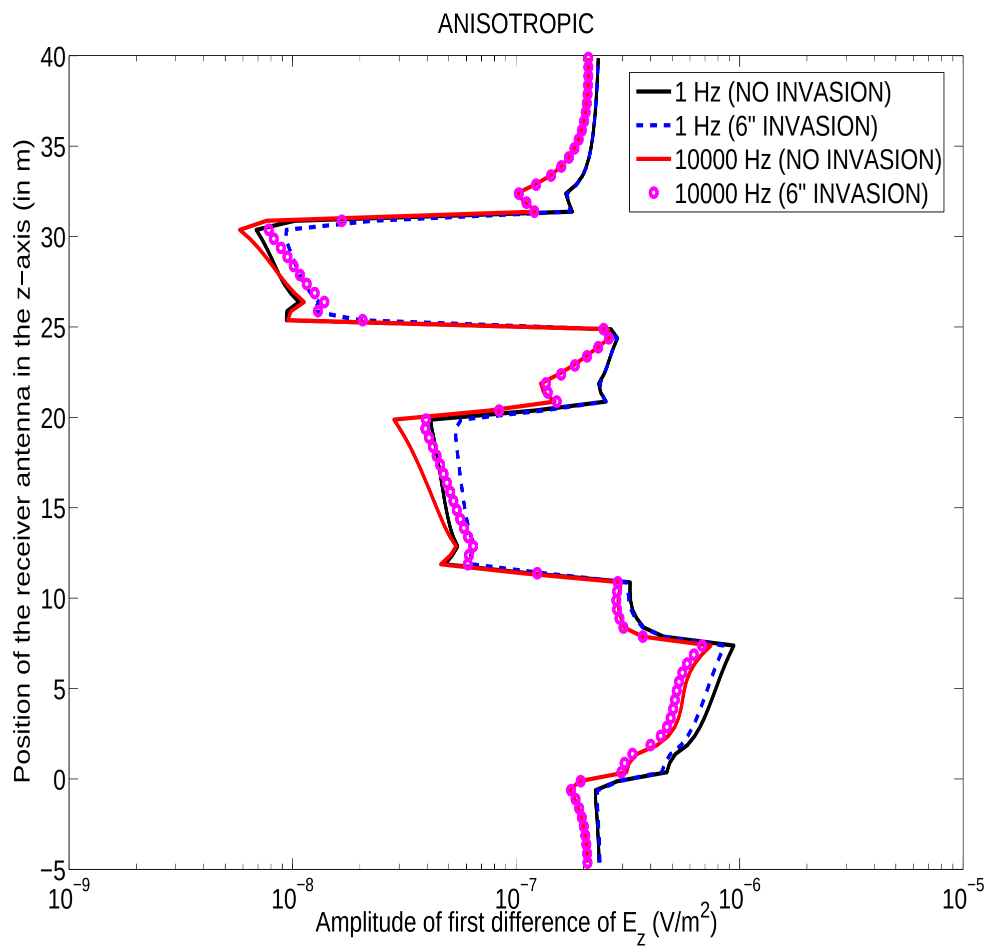

Variations due to invasion are below 20%.

2D hp-FEM: THROUGH CASING CROSS-WELL

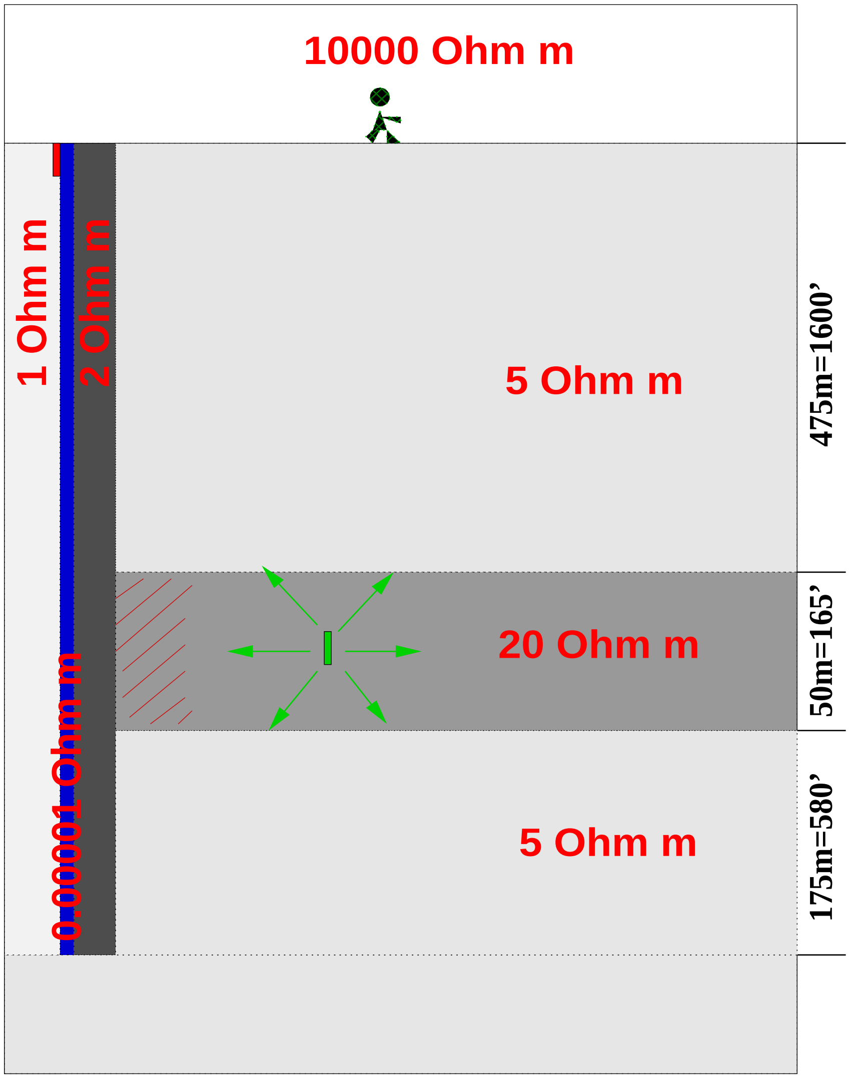

5.5" Borehole radio ; 0.5" Casing ; 2" Cement

Axisymmetric 3D problem.

Six different materials.

Different positions of receiving antenna.

Transmitter antenna located 3 m. below surface (inside and outside borehole).

Objective: Identify physical effects ocurring on this EM logging problem.

2D hp-FEM: THROUGH CASING CROSS-WELL

Different Types of Source Antennas

GALVANIC SOURCES

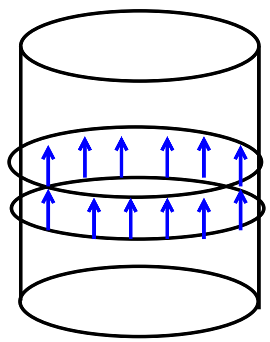

Vertical Dipoles (Ring)

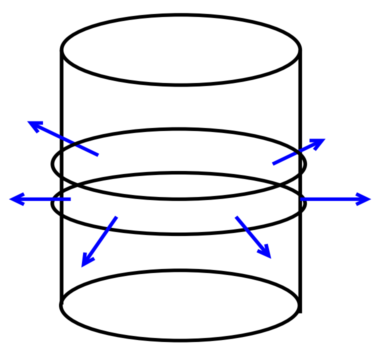

Horizontal Dipoles (Ring)

INDUCTION SOURCES

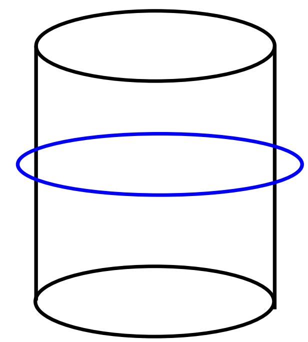

Solenoid

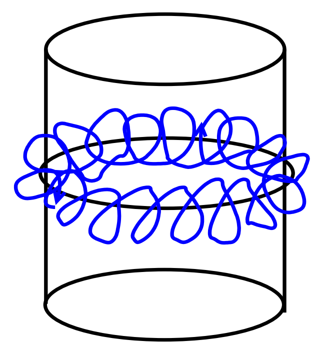

Toroid

2D hp-FEM: THROUGH CASING CROSS-WELL

A Cross-Well Study with One Cased Well: Toroid Antennas

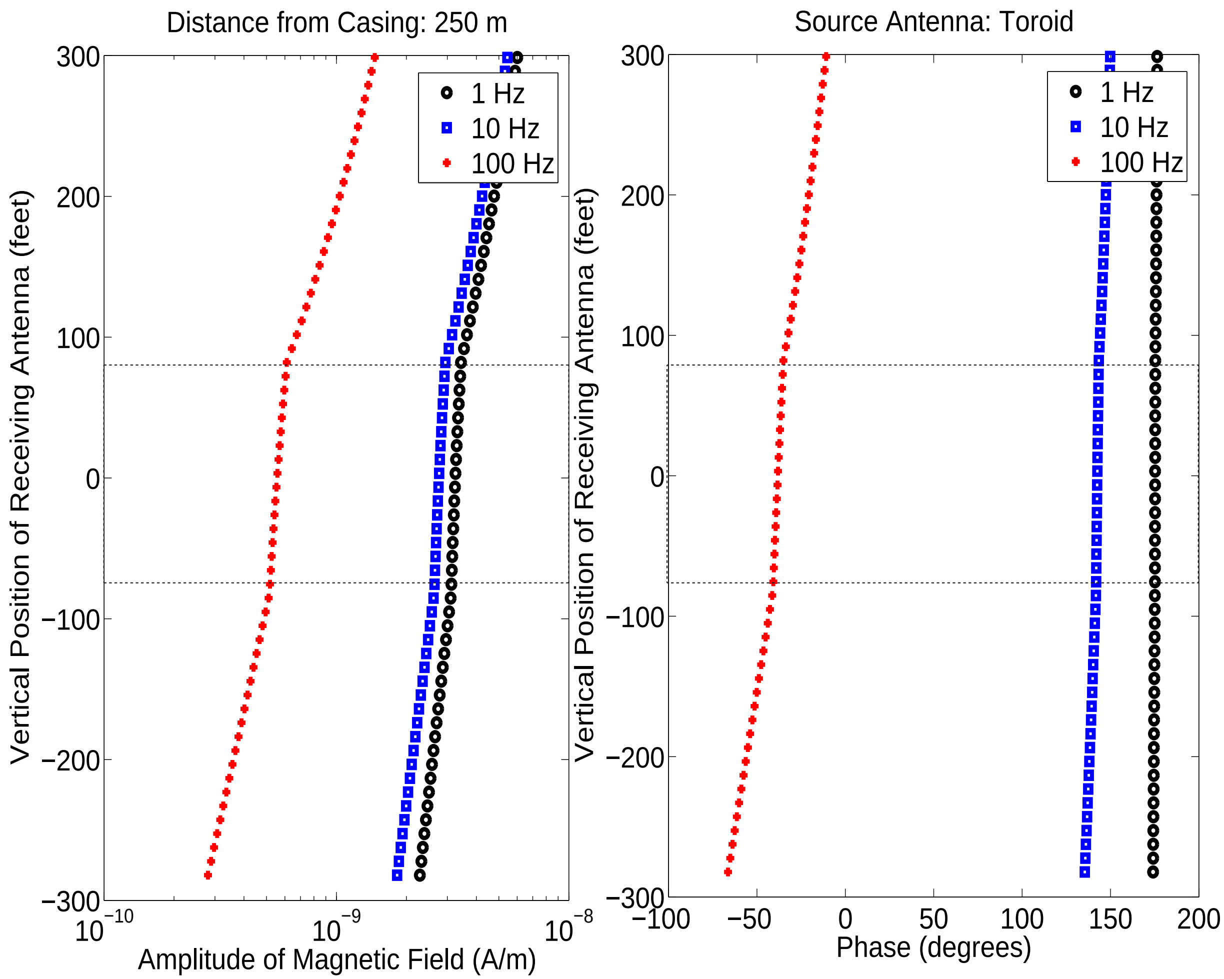

2D hp-FEM: THROUGH CASING CROSS-WELL

A Cross-Well Study: Vertical Dipoles

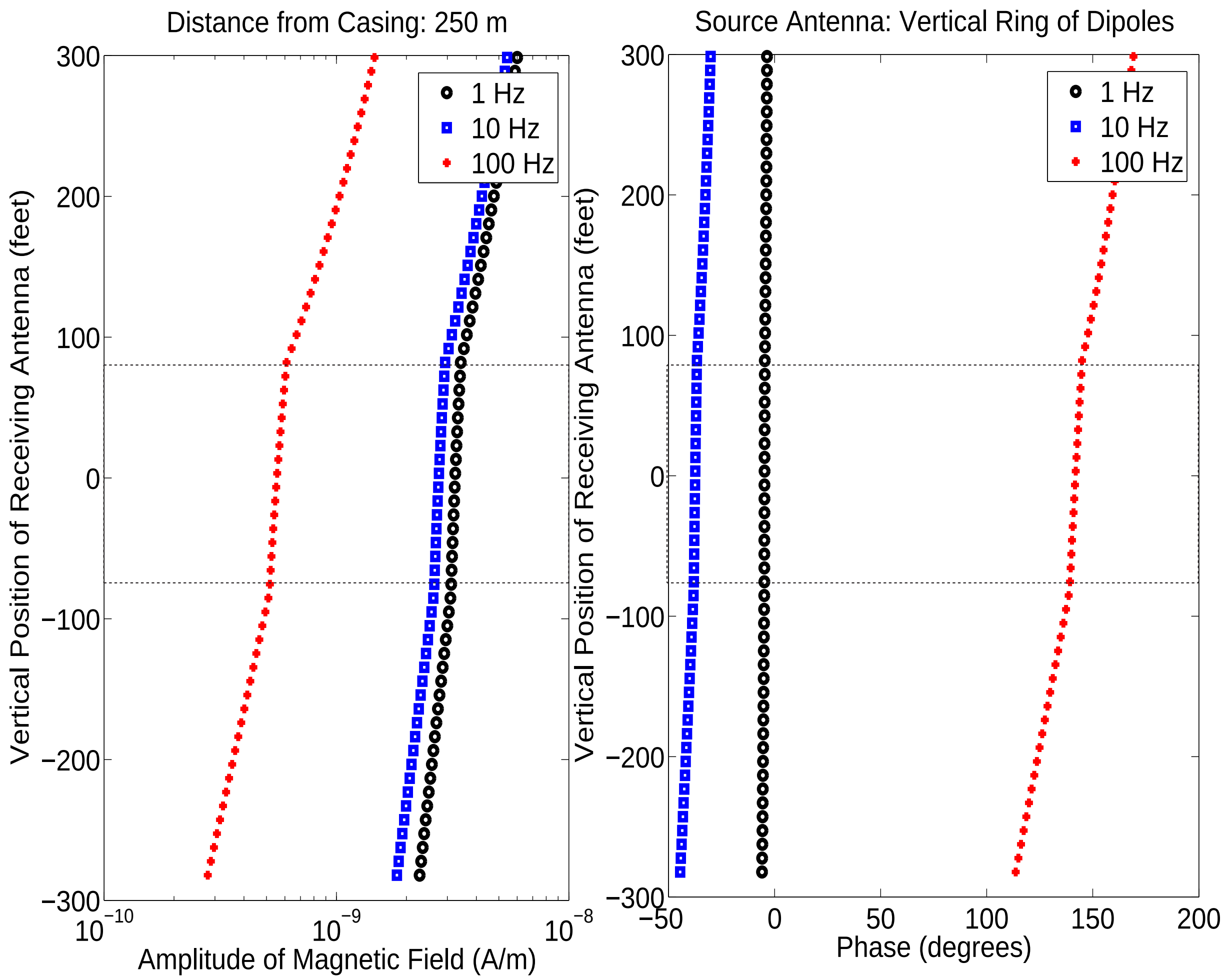

2D hp-FEM: THROUGH CASING CROSS-WELL

A Cross-Well Study: Horizontal Dipoles

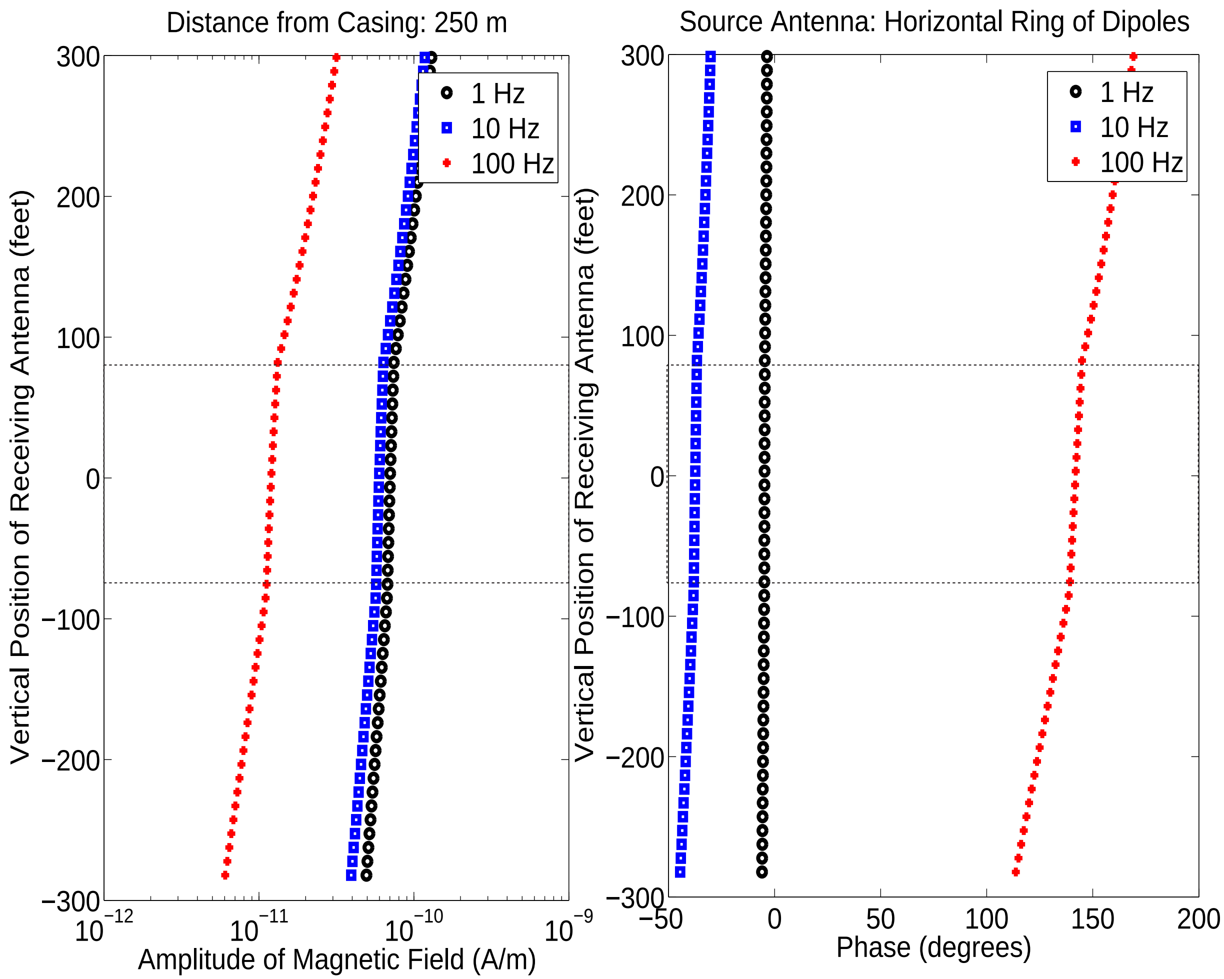

2D hp-FEM: THROUGH CASING CROSS-WELL

A Cross-Well Study: Different Antennas

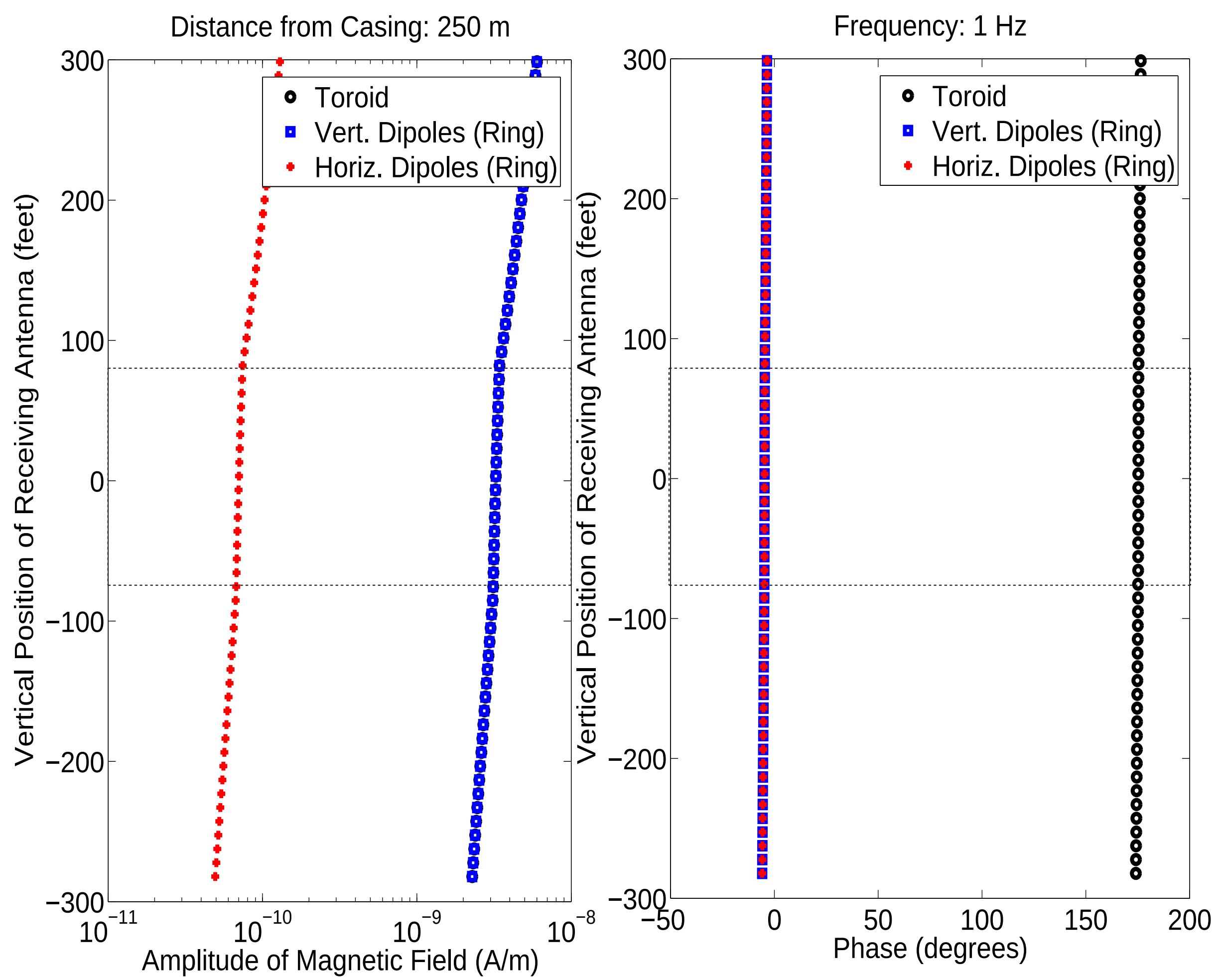

2D hp-FEM: THROUGH CASING CROSS-WELL

A Cross-Well Study: Toroid Antennas (Outside Borehole)

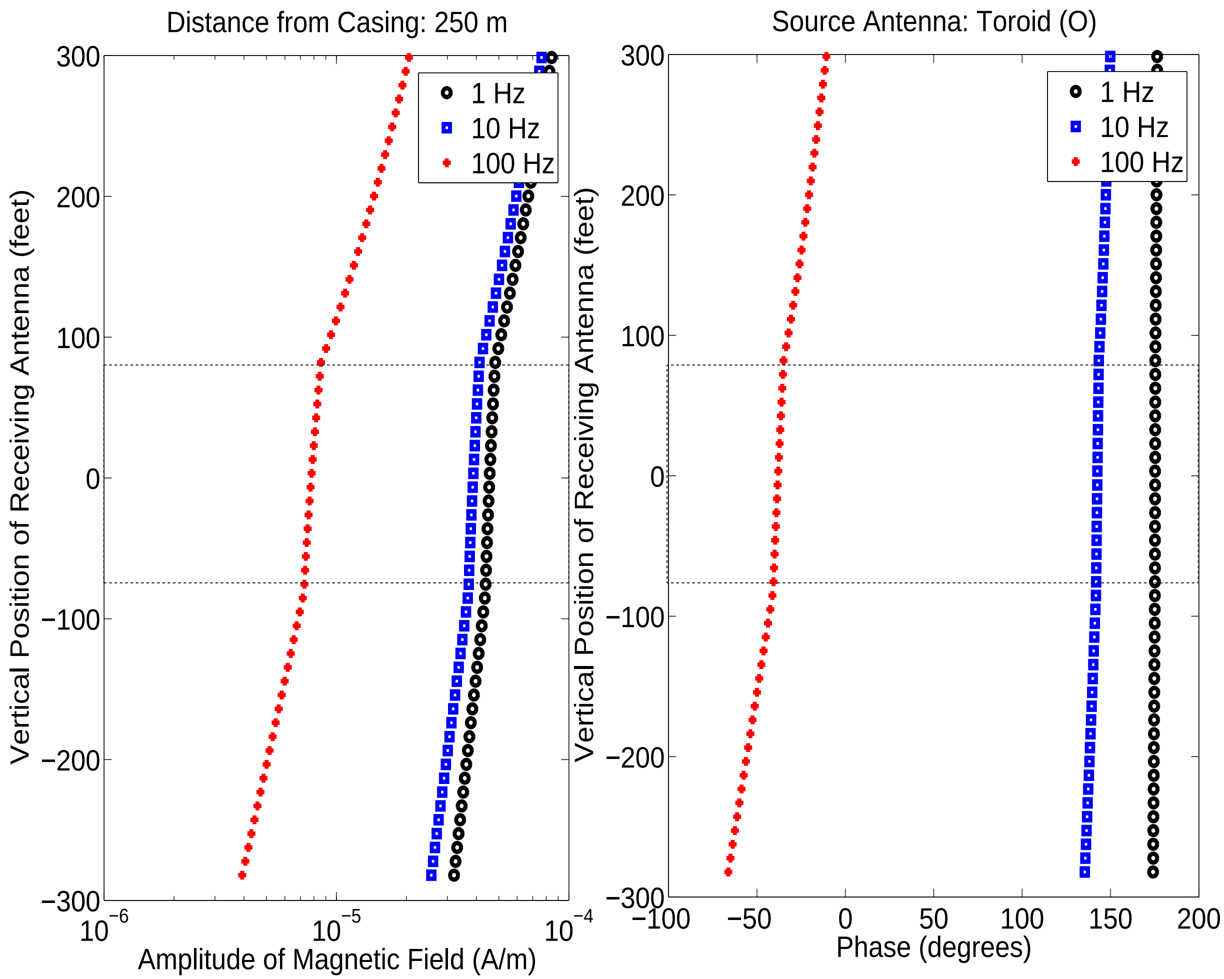

2D hp-FEM: THROUGH CASING CROSS-WELL

A Cross-Well Study: Vertical Dipoles (Outside Borehole)

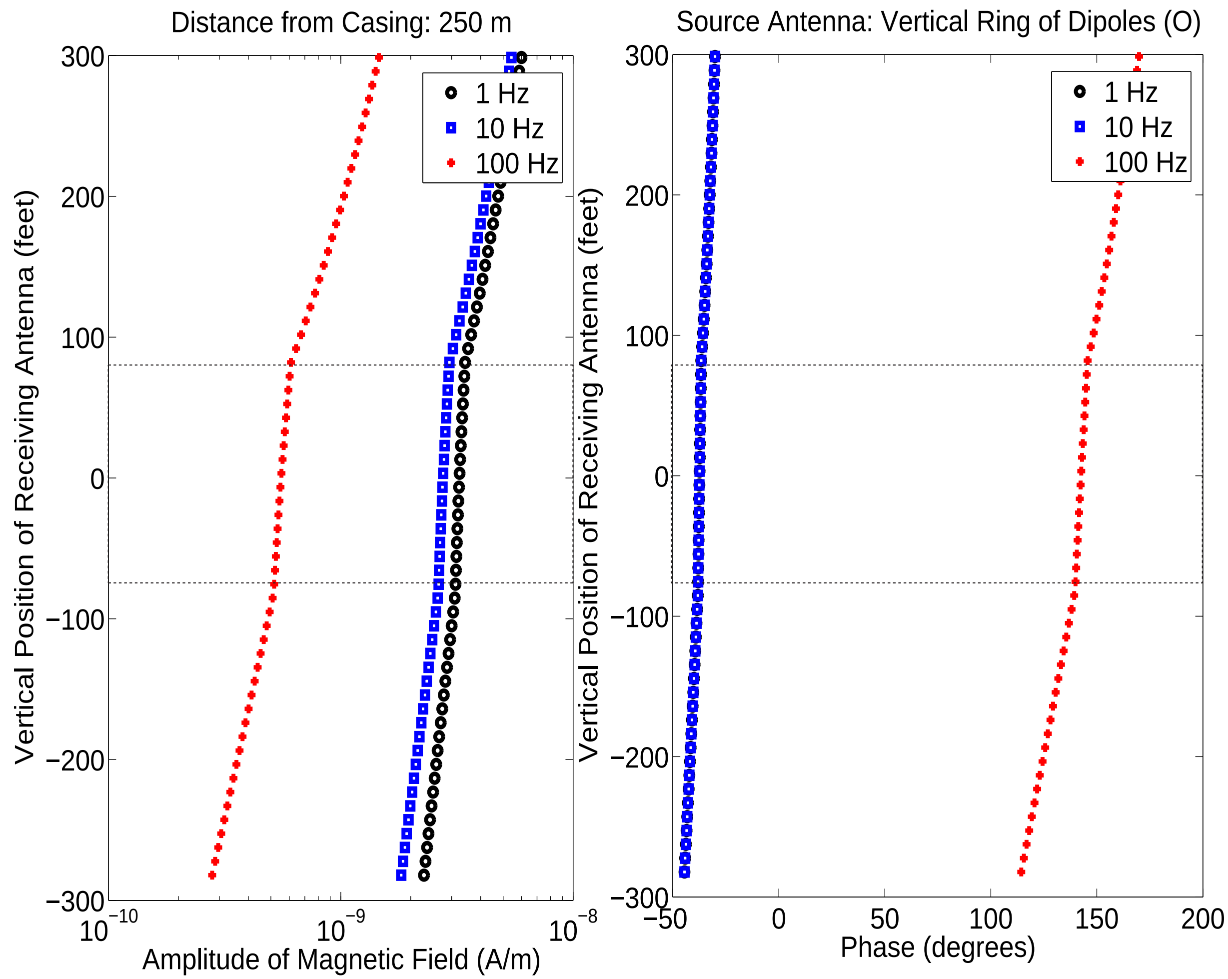

2D hp-FEM: THROUGH CASING CROSS-WELL

A Cross-Well Study: Horizontal Dipoles (Outside Borehole)

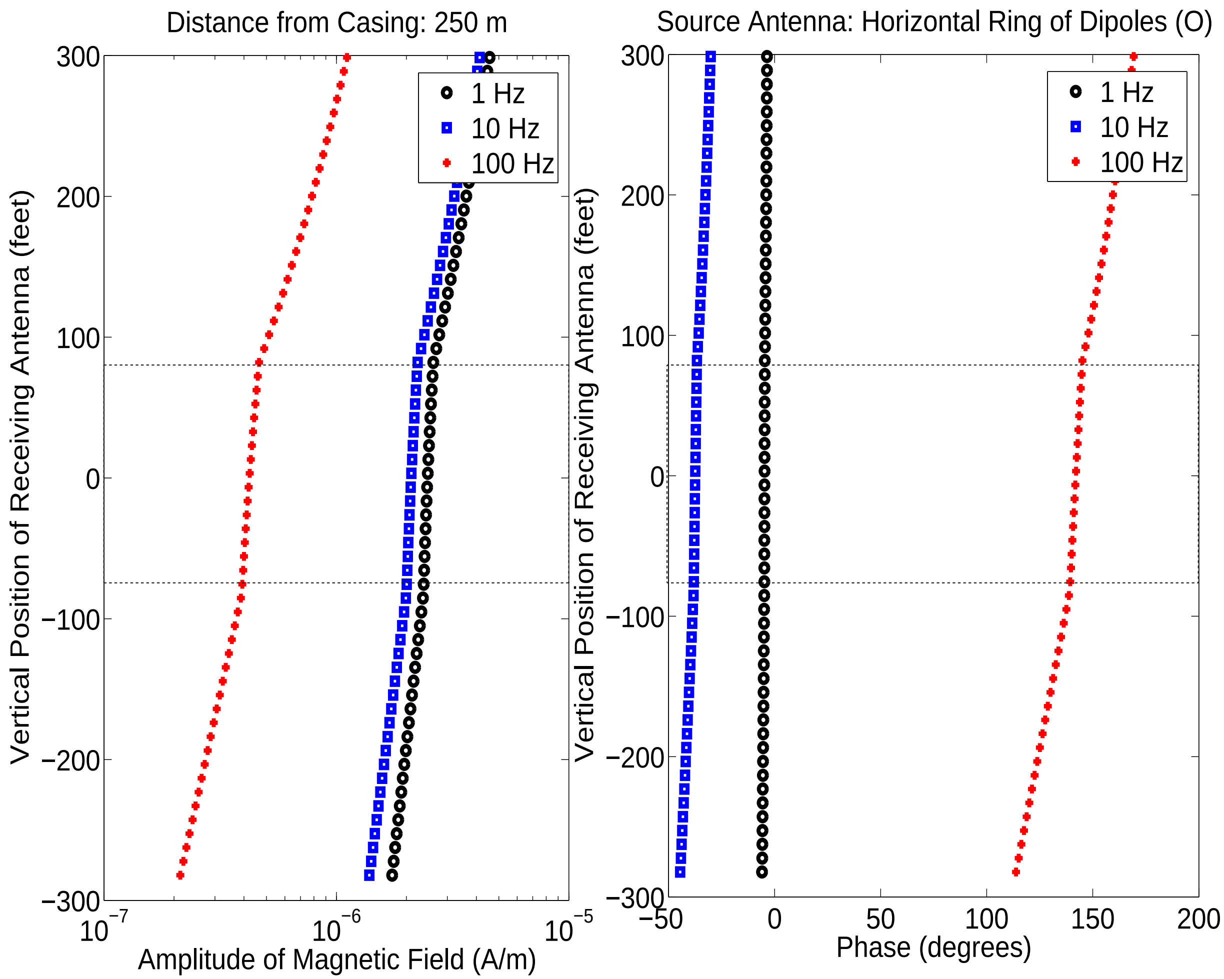

2D hp-FEM: THROUGH CASING CROSS-WELL

A Cross-Well Study: Different Antennas (Outside Borehole)

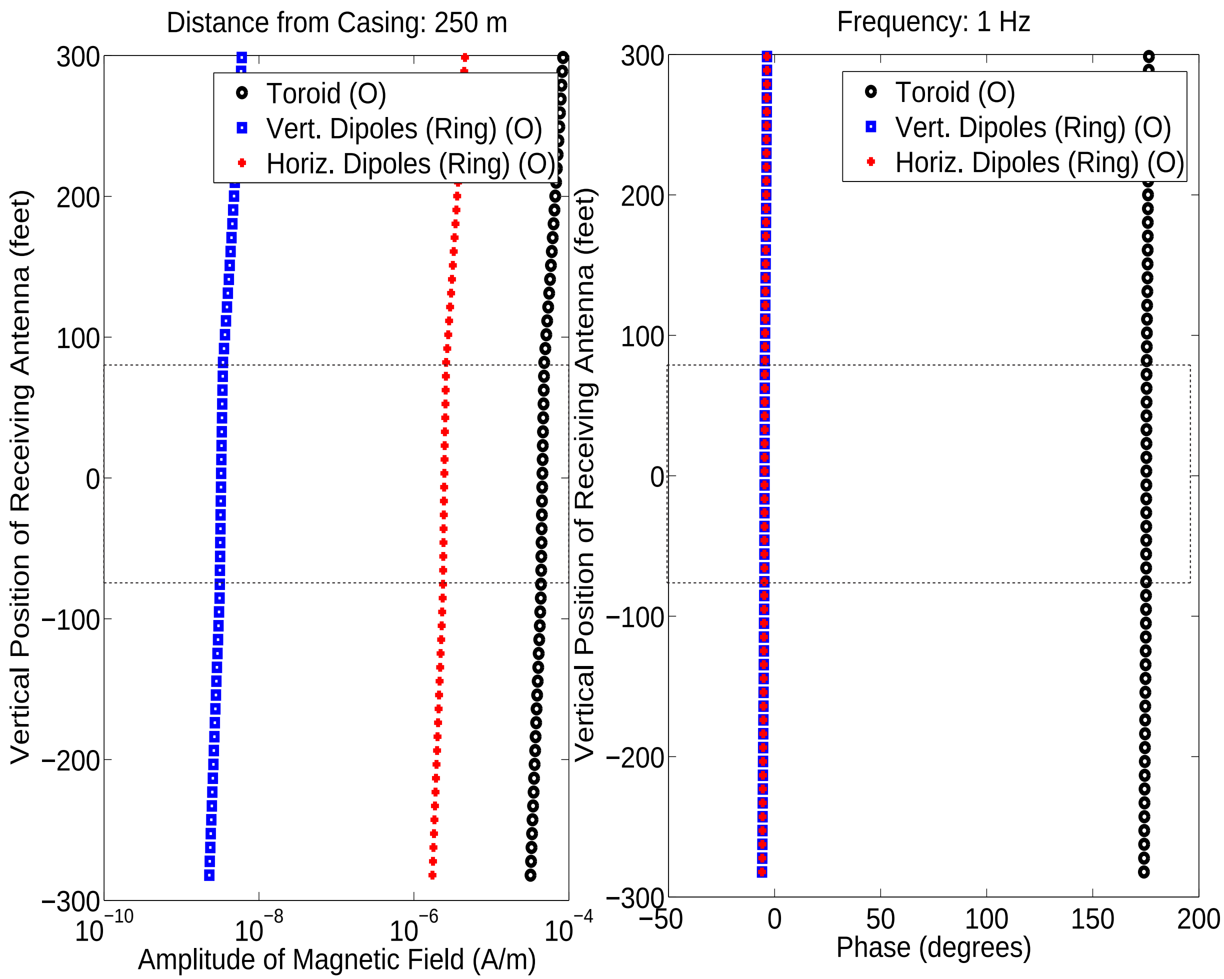

2D hp-FEM: THROUGH CASING CROSS-WELL

A Cross-Well Study: Antennas Inside and Outside Borehole

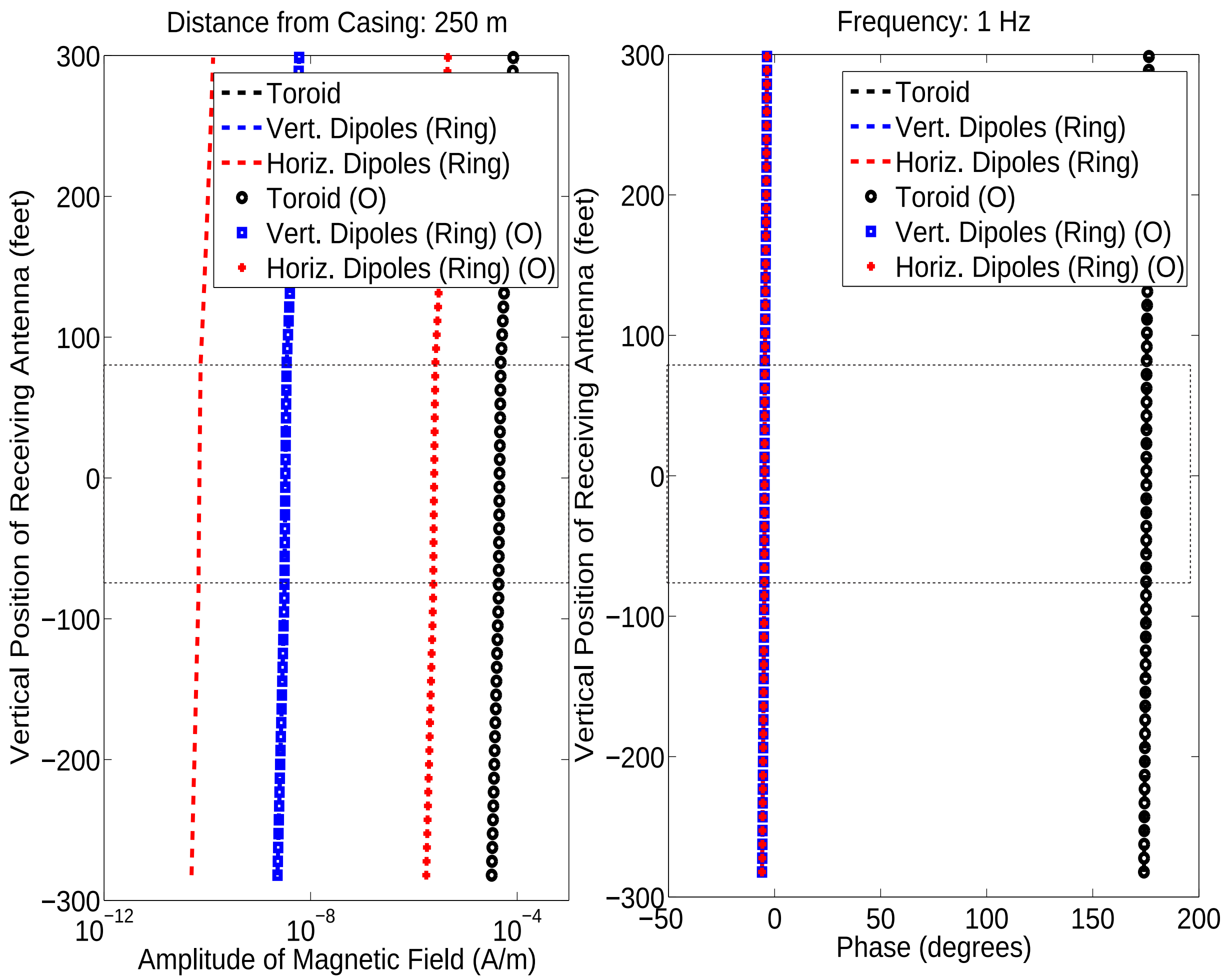

2D hp-FEM: THROUGH CASING CROSS-WELL

A Cross-Well Study: Receivers at 500 m (Horizontal Distance)

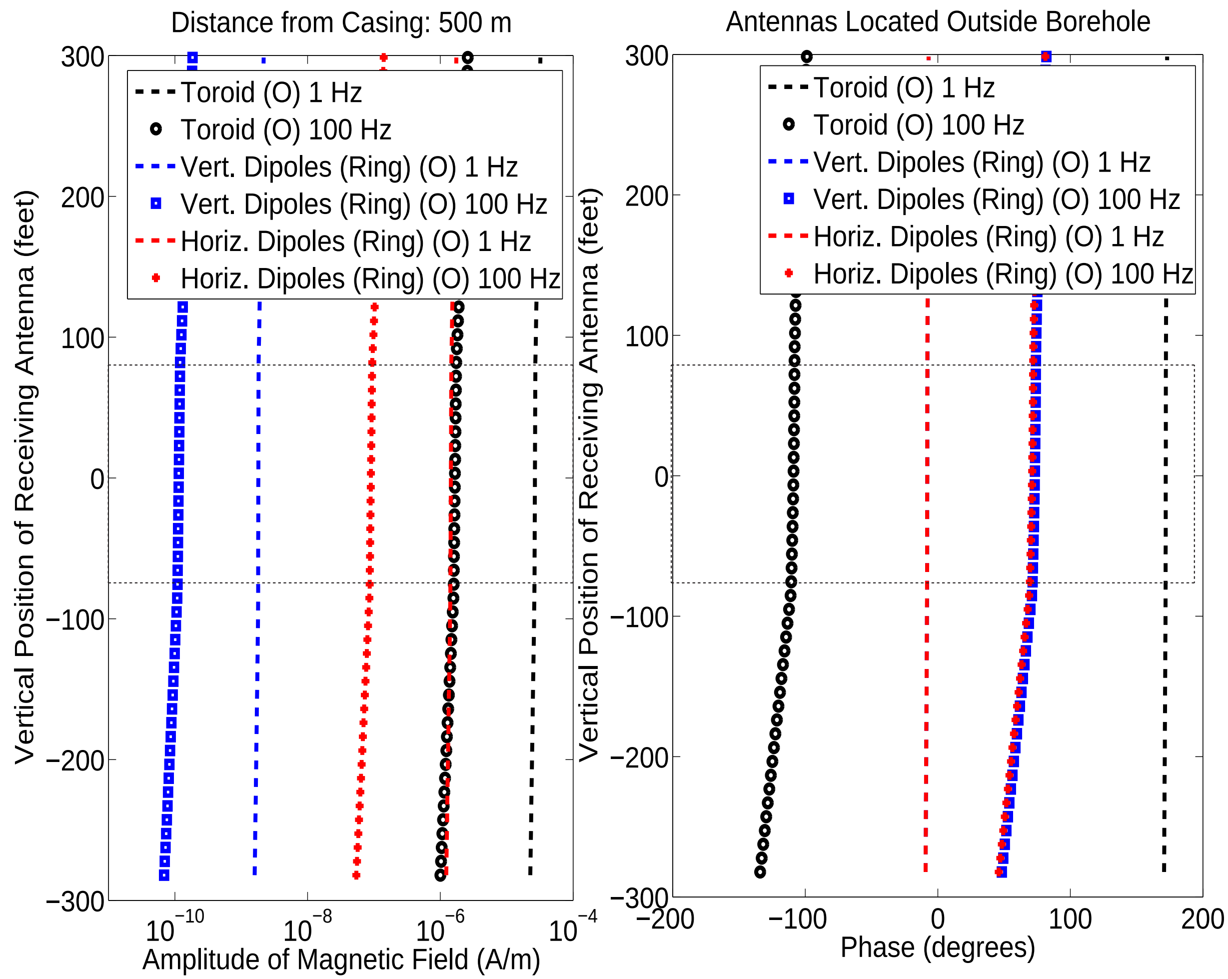

2D hp-FEM: THROUGH CASING CROSS-WELL

A Cross-Well Study: First Vertical Diff. of Magnetic Field

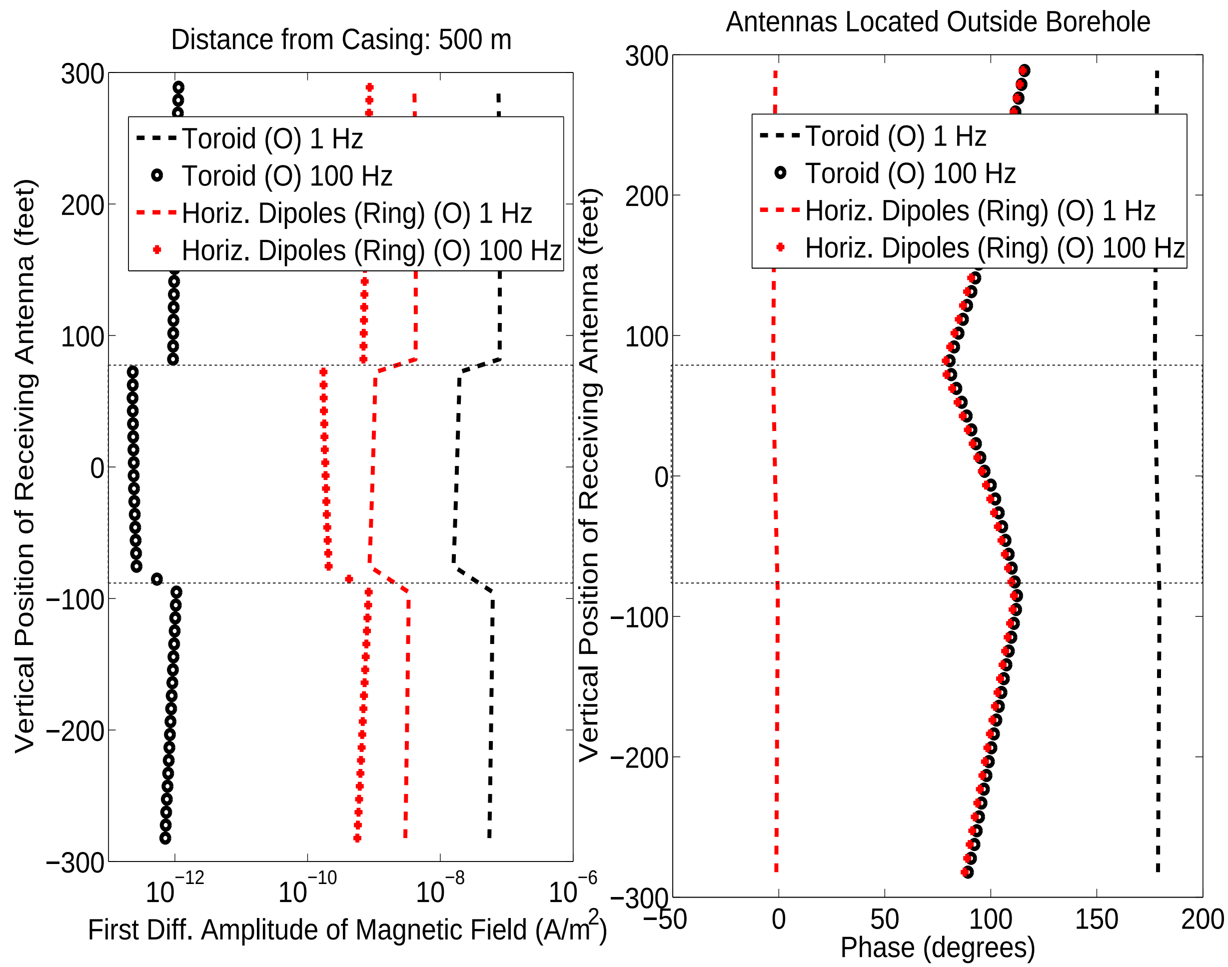

2D hp-FEM: THROUGH CASING CROSS-WELL

A Cross-Well Study: First Vert. Diff. Magnetic Field (50 m)

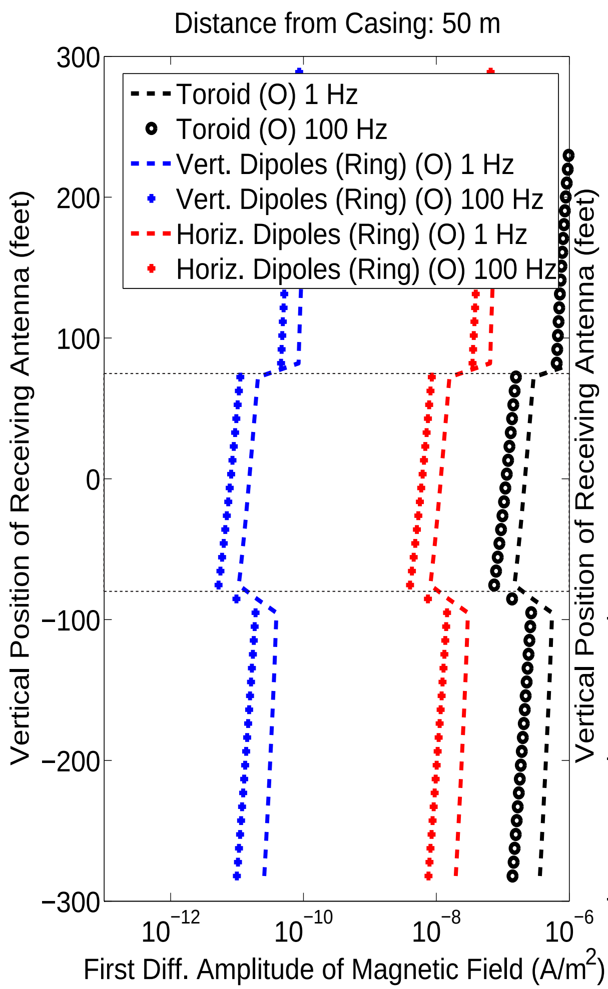

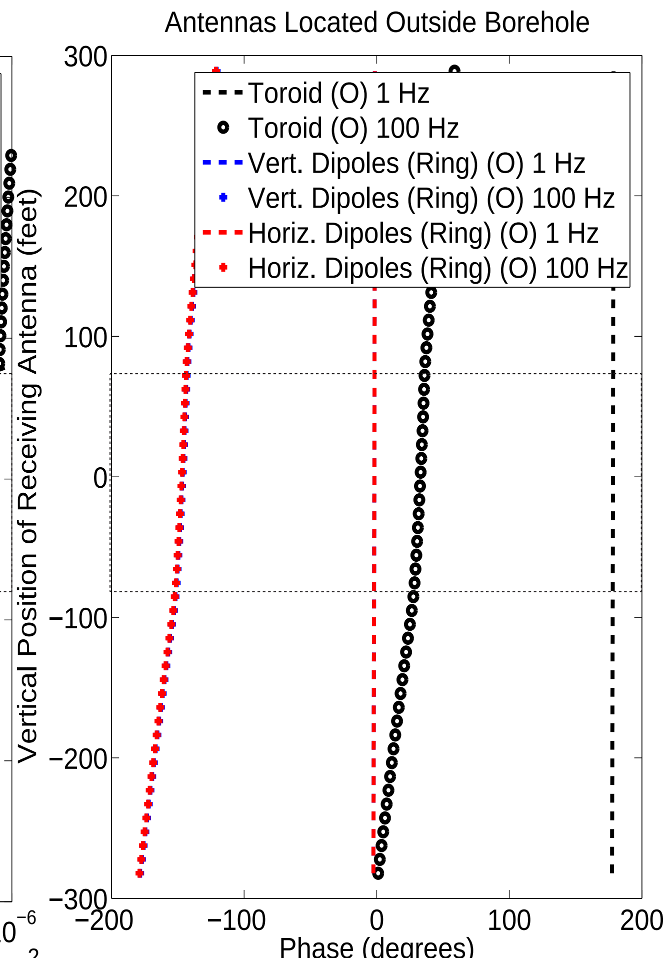

2D hp-FEM: THROUGH CASING CROSS-WELL

A Cross-Well Study: Water Invasion with Toroids (50 m - H_ϕ -)

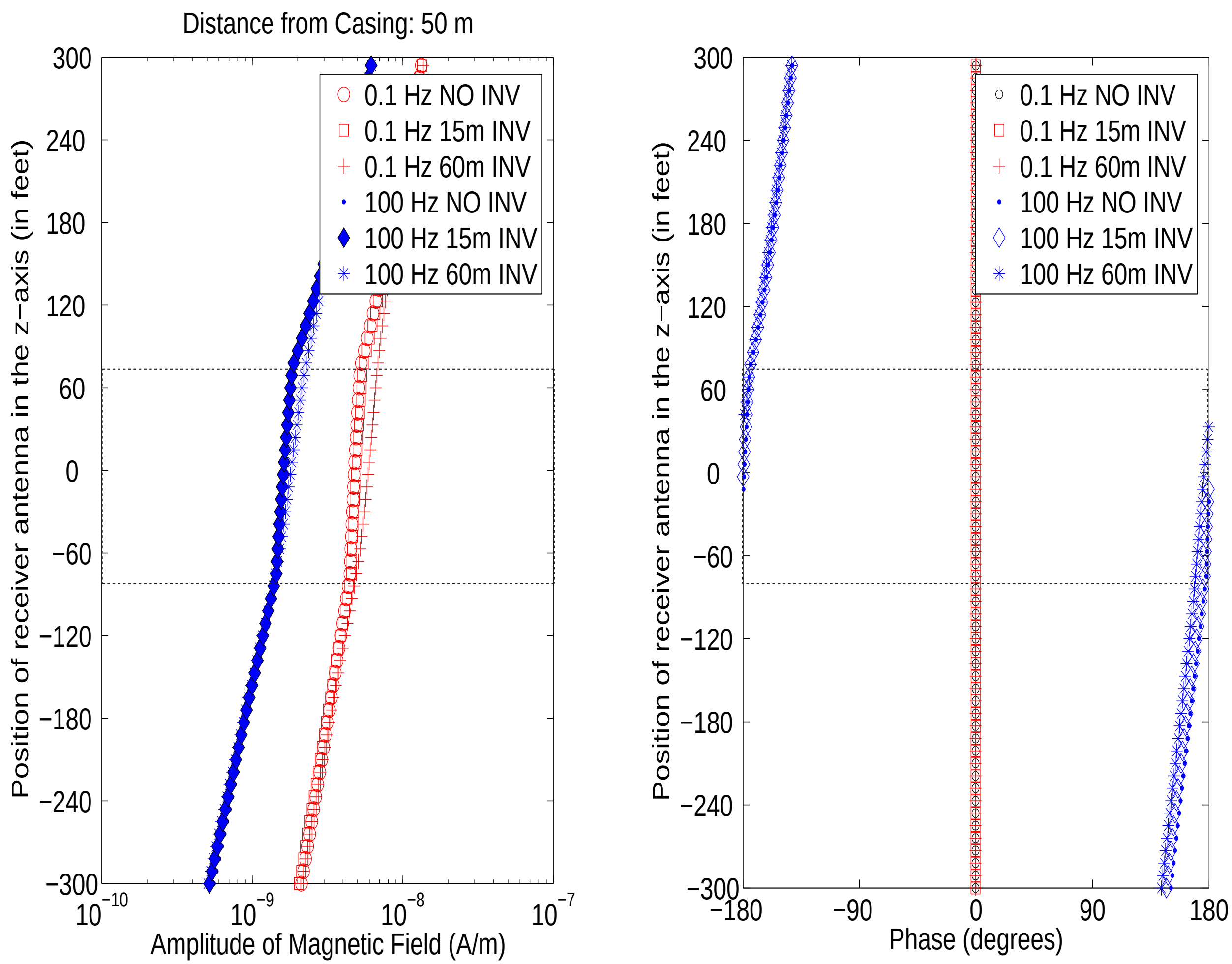

2D hp-FEM: THROUGH CASING CROSS-WELL

A Cross-Well Study: Water Invasion with Toroids (50 m - E_z -)

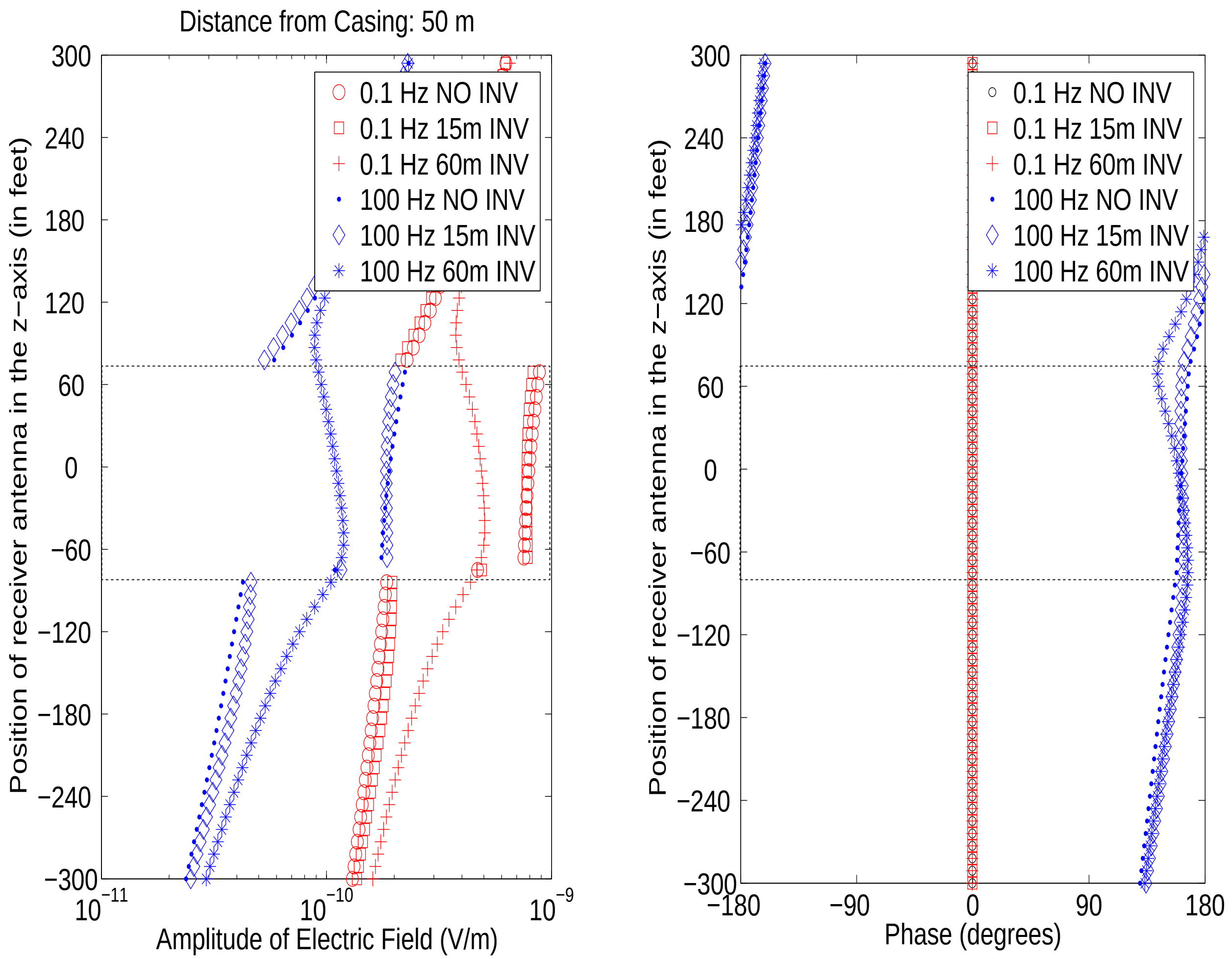

2D hp-FEM: THROUGH CASING CROSS-WELL

A Cross-Well Study: Water Invasion with Toroids (250 m)

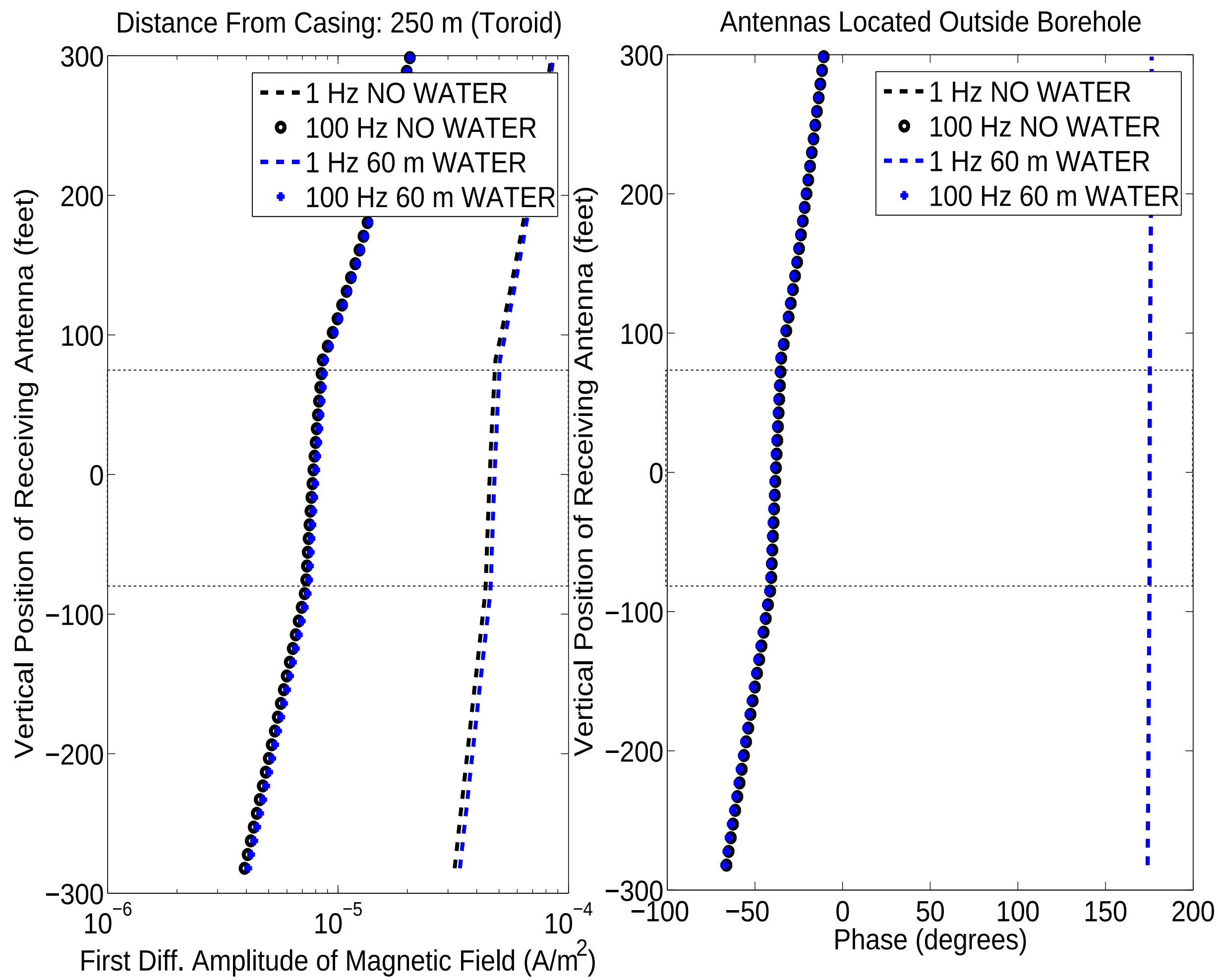

2D hp-FEM: THROUGH CASING CROSS-WELL

A Cross-Well Study: Water Invasion, Vert. Dipoles (250 m)

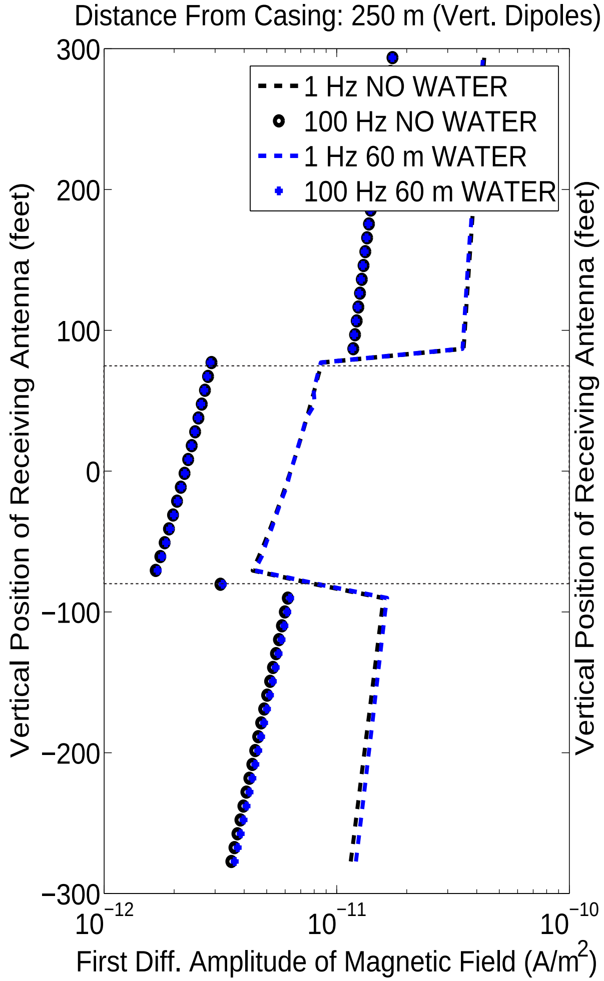

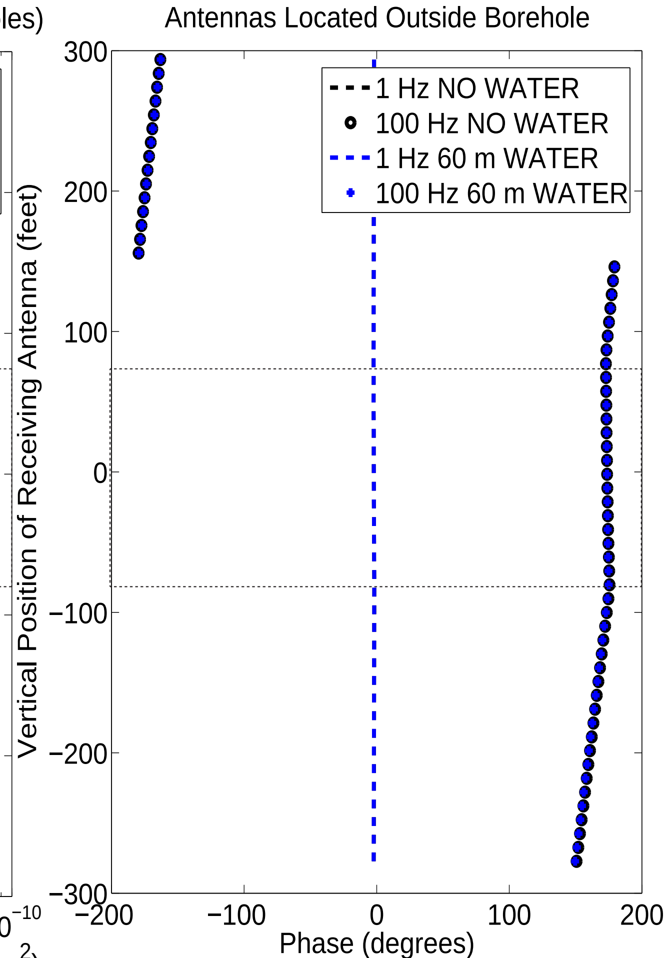

2D hp-FEM: THROUGH CASING CROSS-WELL

A Cross-Well Study: Water Invasion, Horiz. Dipoles (250 m)

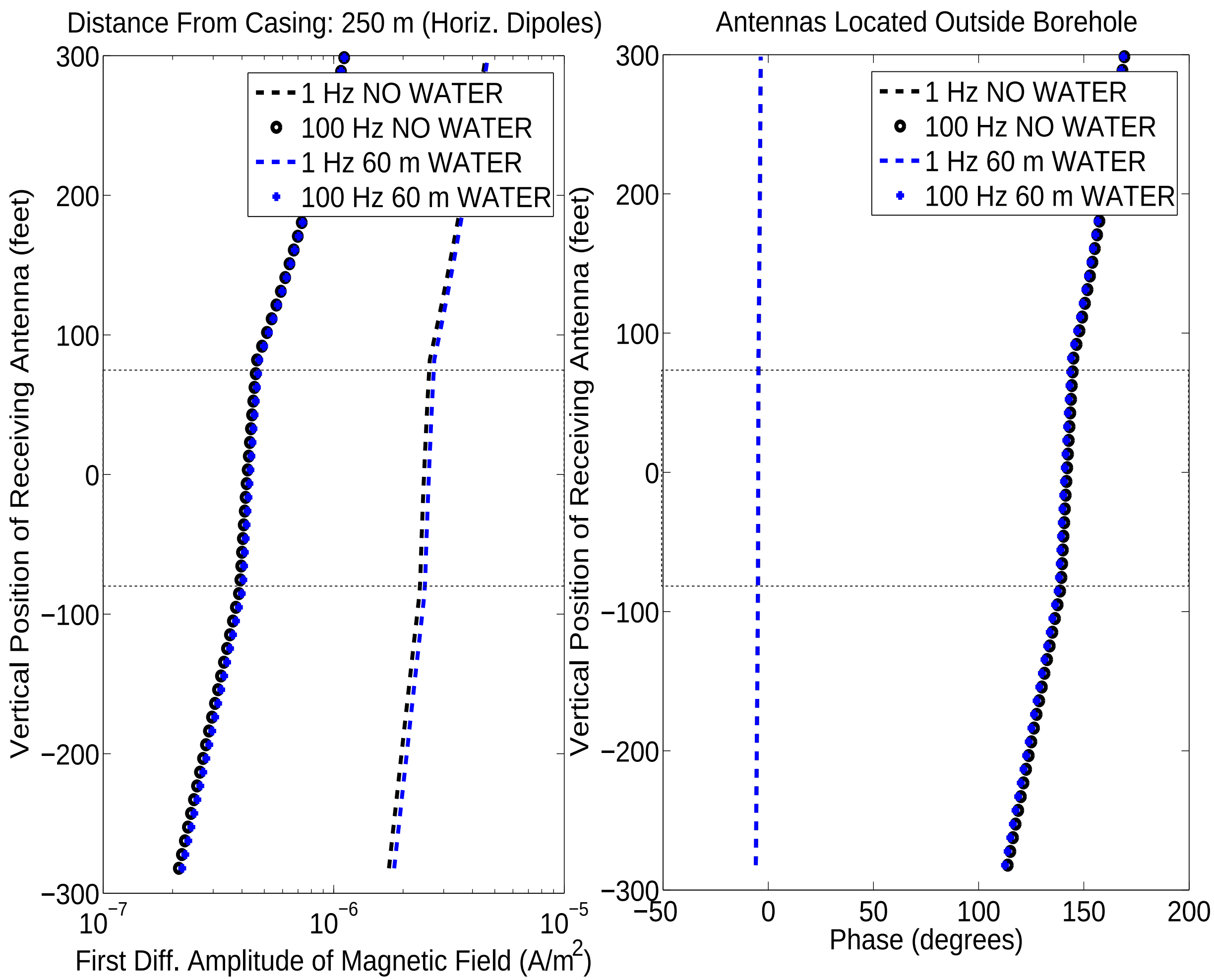

2D hp-FEM: THROUGH CASING CROSS-WELL

A Cross-Well Study: Water Invasion, Toroid (50 m)

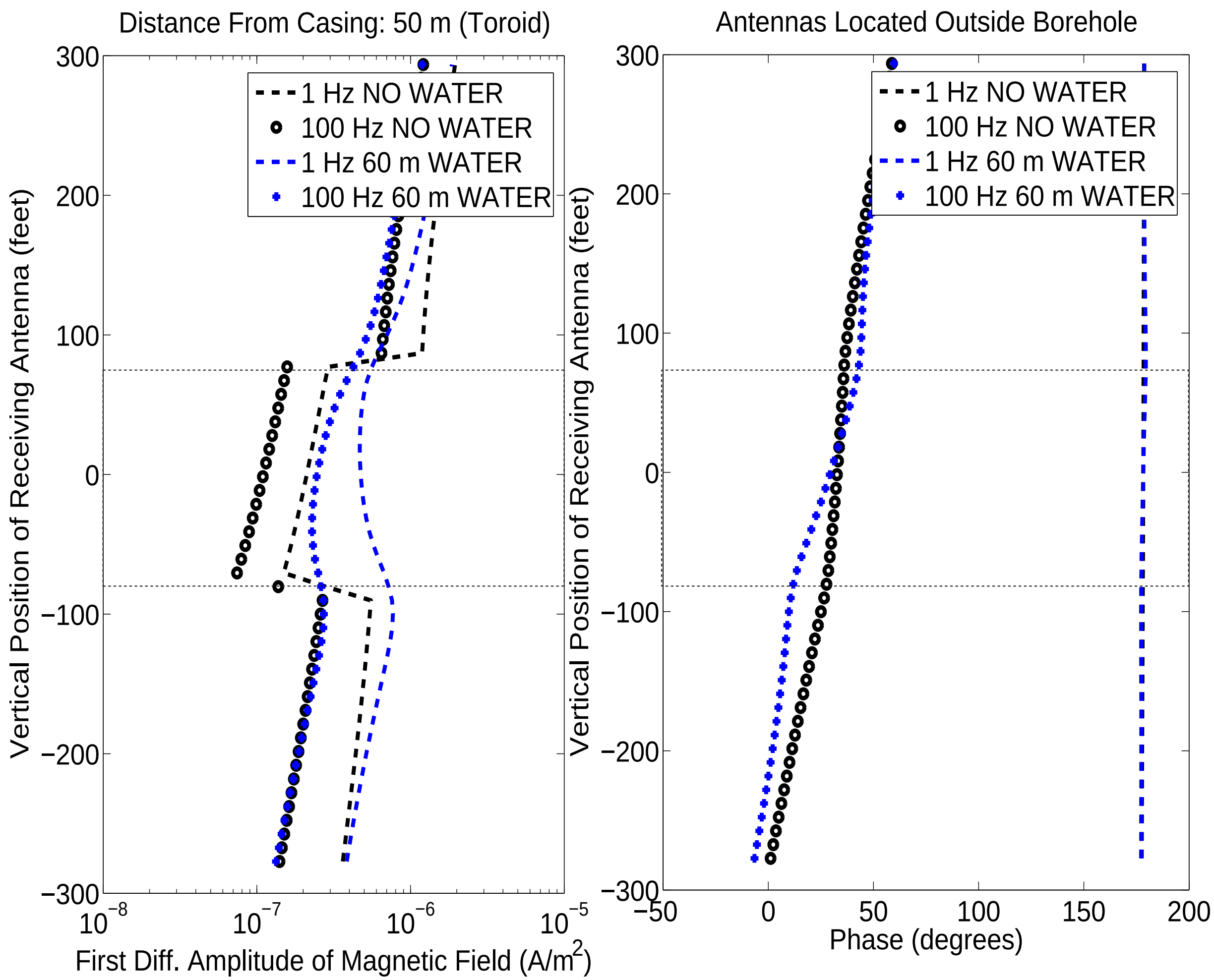

2D hp-FEM: THROUGH CASING CROSS-WELL

A Cross-Well Study: Water Invasion, Vert. Dipoles (50 m)

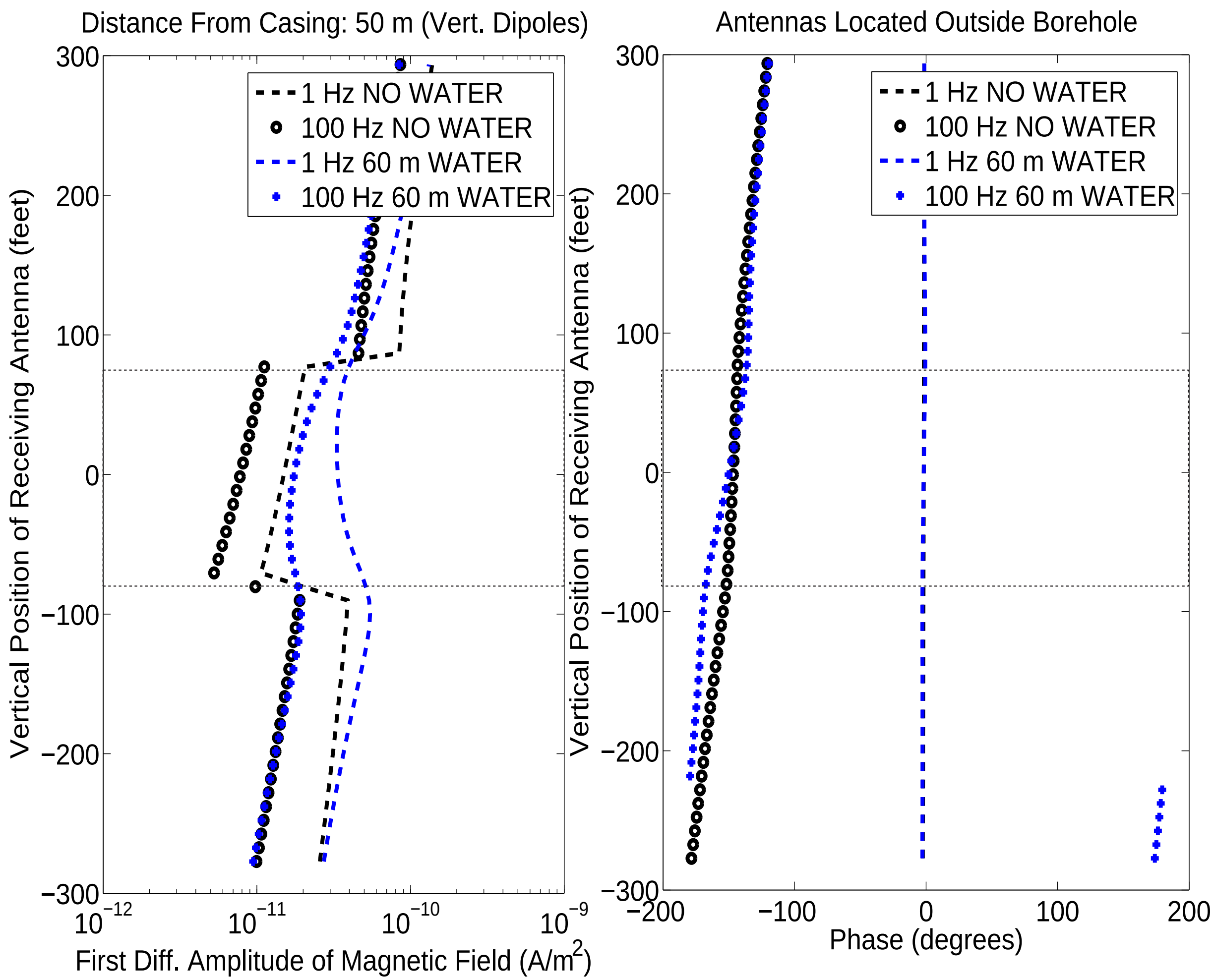

2D hp-FEM: THROUGH CASING CROSS-WELL

A Cross-Well Study: Water Invasion, Horiz. Dipoles (50 m)

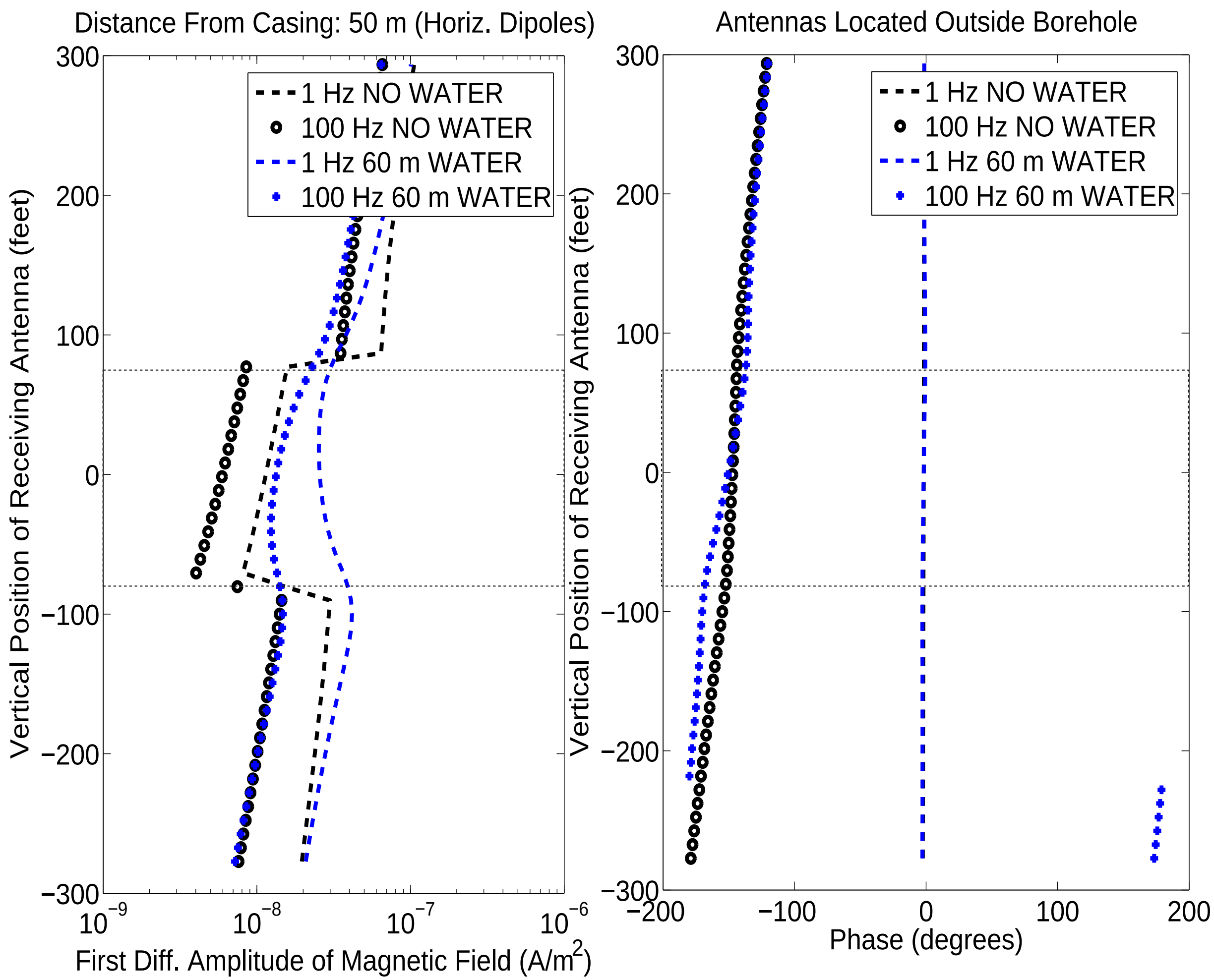

2D hp-FEM: THROUGH CASING CROSS-WELL

A Cross-Well Study: Magnetic Perm., Toroid (250 m)

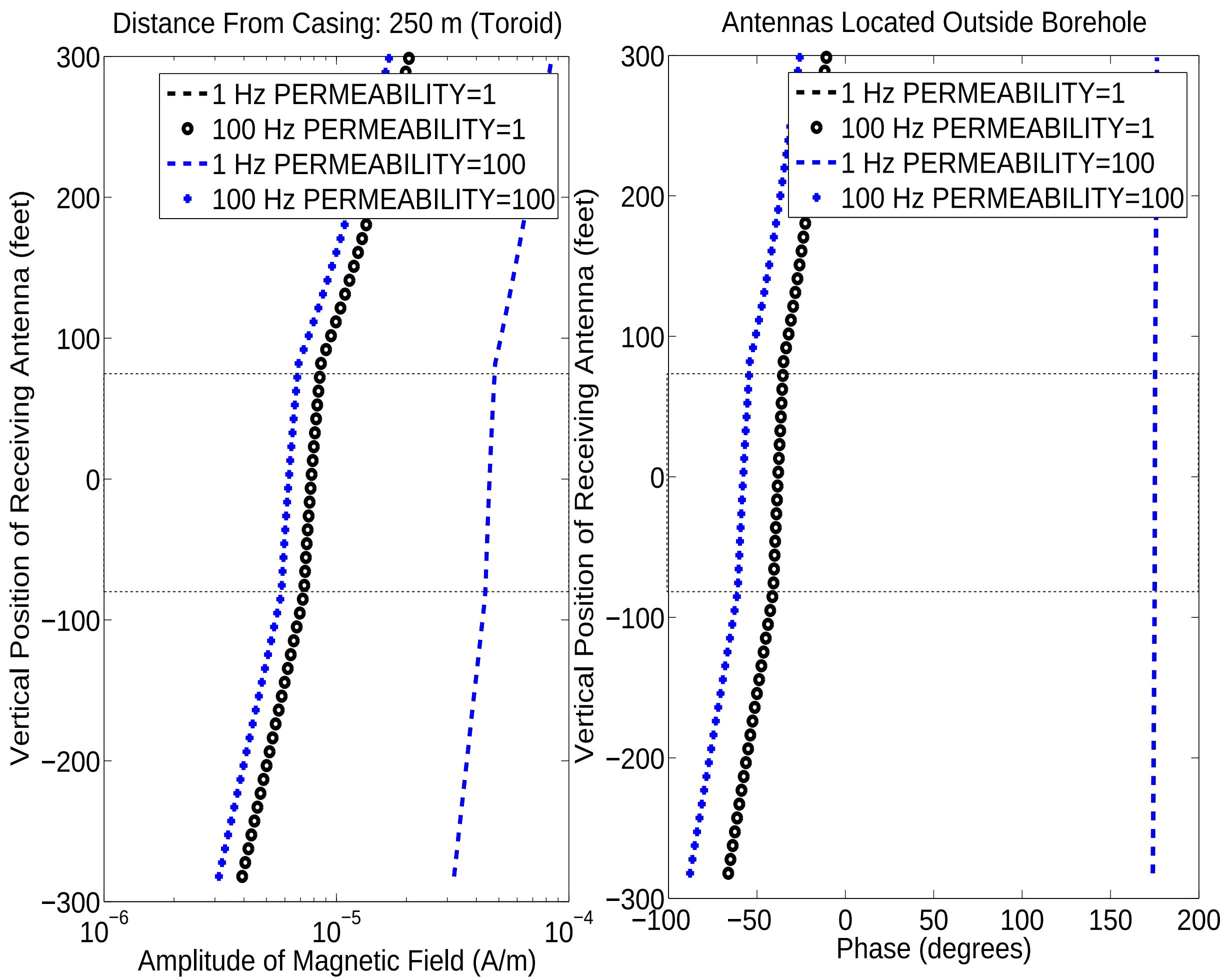

2D hp-FEM: THROUGH CASING CROSS-WELL

A Cross-Well Study: Magnetic Perm., Vert. Dipoles (250 m)

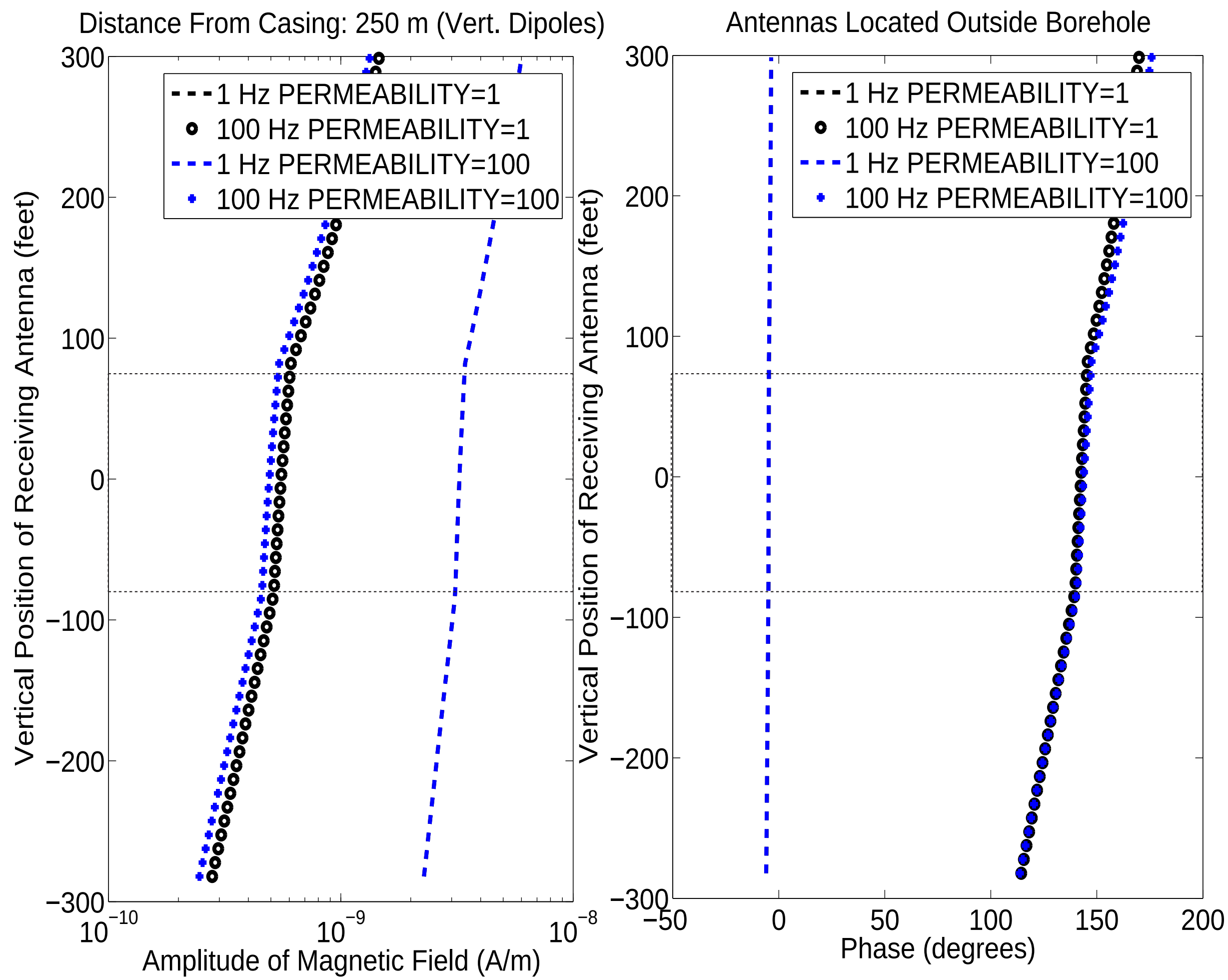

2D hp-FEM: THROUGH CASING CROSS-WELL

A Cross-Well Study: Magnetic Perm., Horiz. Dipoles (250 m)

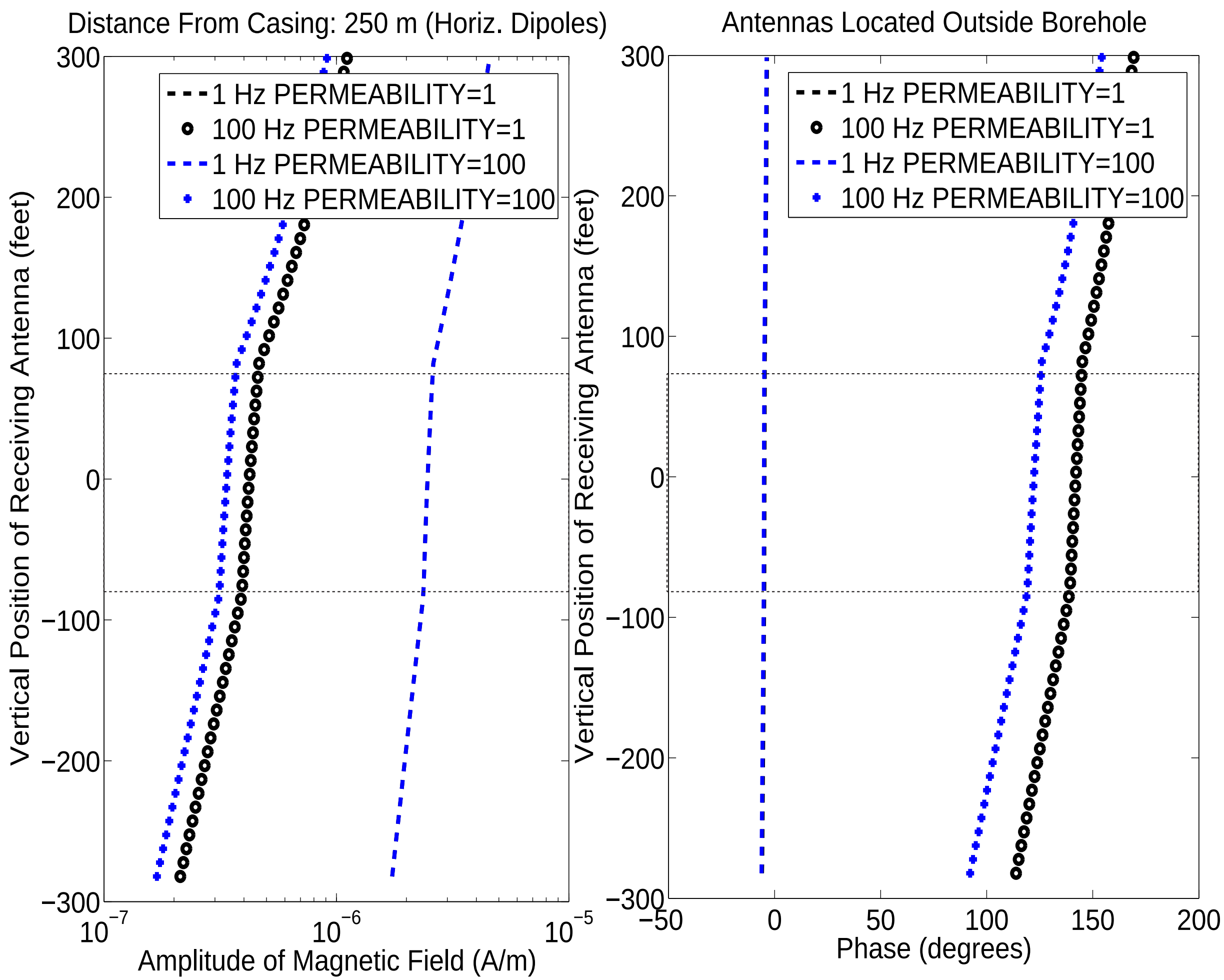

2D hp-FEM: THROUGH CASING CROSS-WELL

A Cross-Well Study: Magnetic Perm., Horiz. Dipoles (250 m)

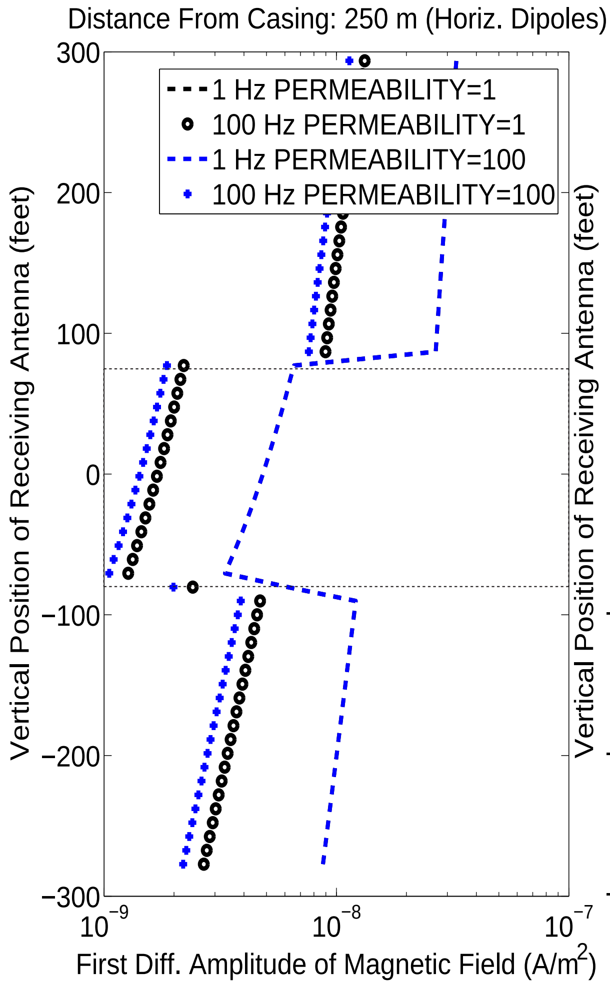

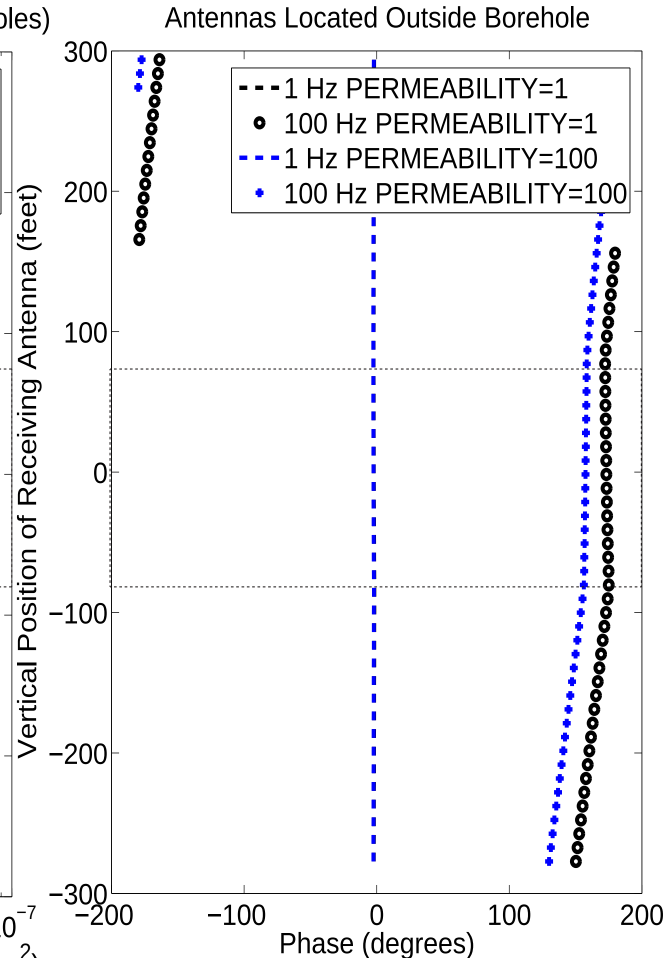

2D hp-FEM: THROUGH CASING CROSS-WELL

A Cross-Well Study: Frequency Dependance at 250 m

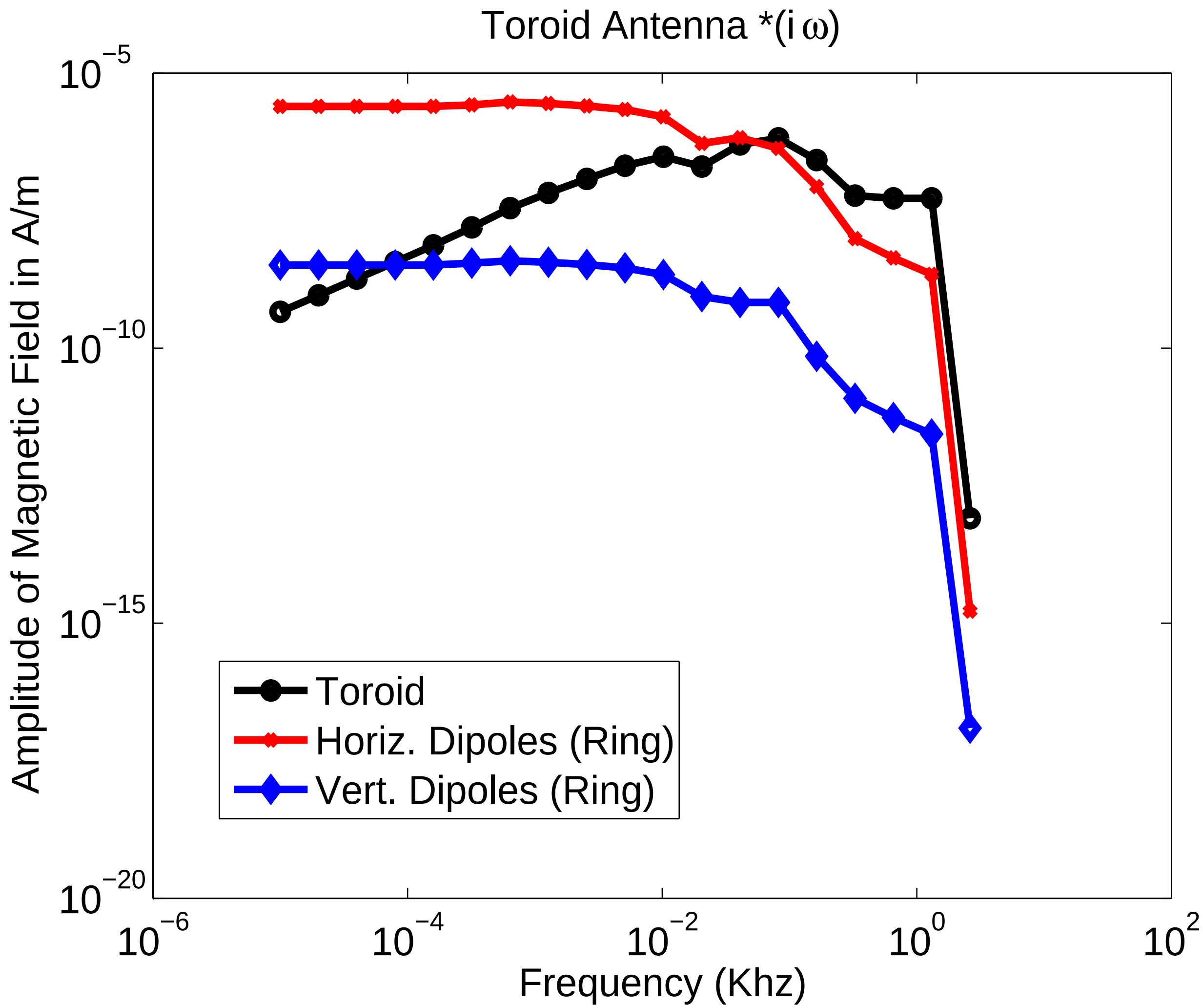

2D hp-FEM: THROUGH CASING CROSS-WELL

A Cross-Well Study: Distance Dependance at 1 Hz

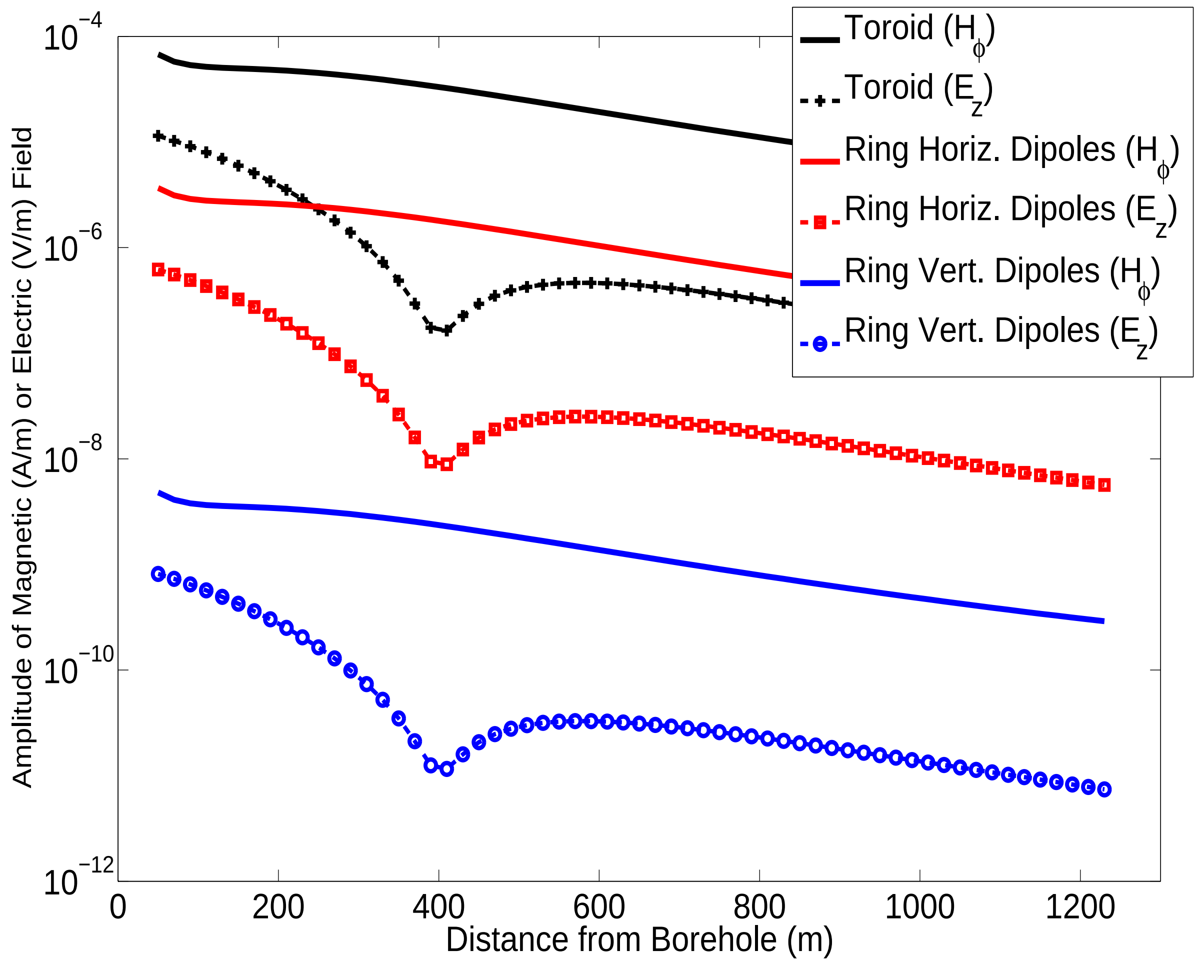

2D hp-FEM: THROUGH CASING CROSS-WELL

A Cross-Well Study with One Cased Well: Vertical Dipoles

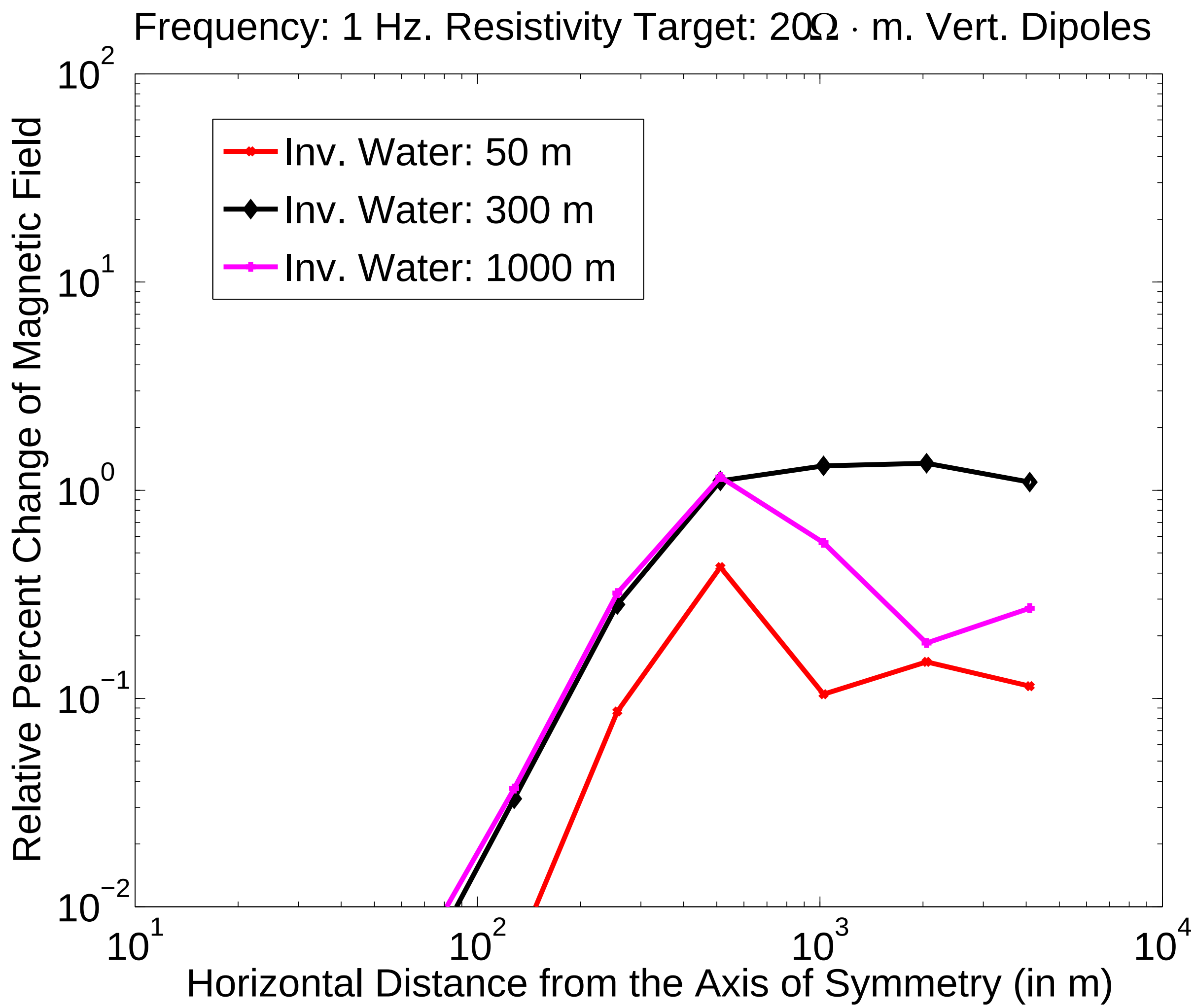

2D hp-FEM: THROUGH CASING CROSS-WELL

A Cross-Well Study with One Cased Well: Vertical Dipoles

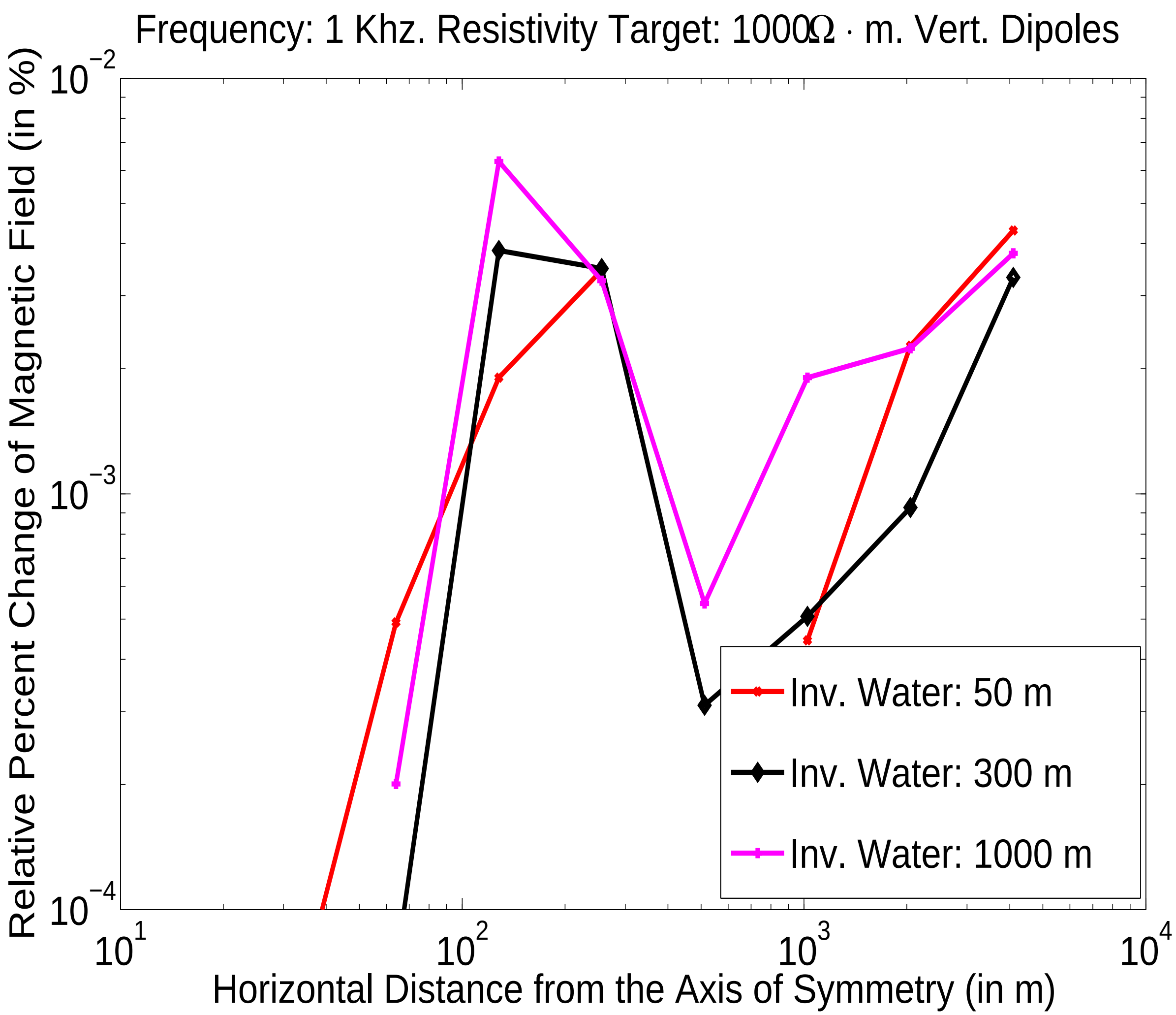

2D hp-FEM: THROUGH CASING CROSS-WELL

A Cross-Well Study with One Cased Well: Vertical Dipoles

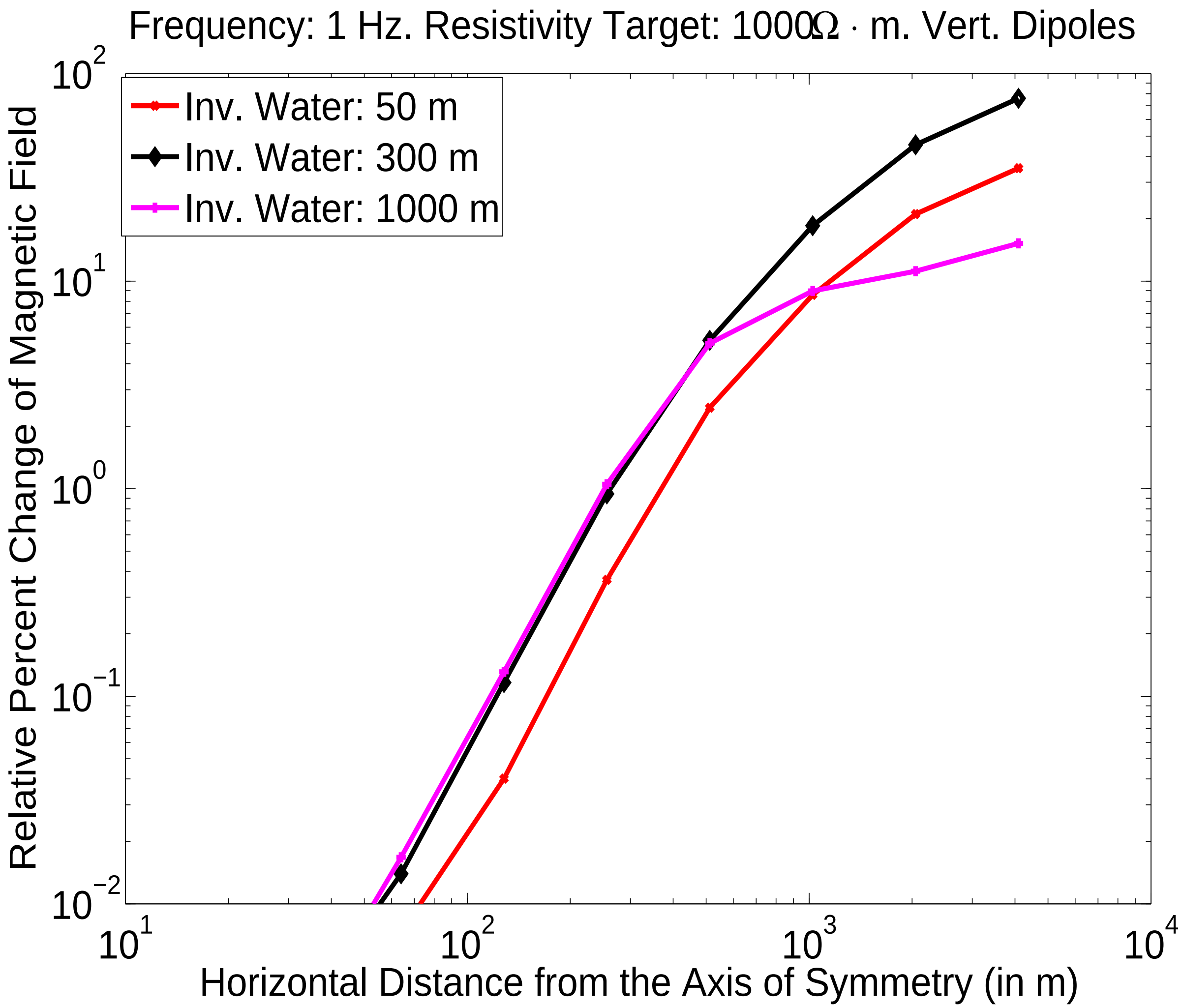

2D hp-FEM: PERFECTLY MATCHED LAYER (PML)

Perfectly Matched Layer (PML) Formulation

The PML is composed of the following anisotropic materials:

$$\begin{cases} \bar{\bar{\sigma}}_{PML} = \bar{\bar{\Lambda}}\bar{\bar{\sigma}} \\ \bar{\bar{\epsilon}}_{PML} = \bar{\bar{\Lambda}}\bar{\bar{\epsilon}} \\ \bar{\bar{\mu}}_{PML} = \bar{\bar{\Lambda}}\bar{\bar{\mu}} \end{cases} \quad ; \quad \bar{\bar{\Lambda}} = \begin{bmatrix} \frac{\tilde{\rho}}{\rho}\frac{s_z}{s_\rho} & 0 & 0 \\ 0 & \frac{\rho}{\tilde{\rho}} s_z s_\rho & 0 \\ 0 & 0 & \frac{\tilde{\rho}}{\rho}\frac{s_\rho}{s_z} \end{bmatrix} \quad ; \quad \tilde{\rho} = \int_0^\rho s_\rho(\rho')d\rho'$$

s_ρ, s_ϕ, **and** s_z **are the stretching coordinate functions. We define:**

$$s_\rho = s_\phi = s_z = 1 + \phi - j\phi$$

We consider three different PML's by defining three different functions $\phi(x)$**:**

$$\phi(x) = \begin{cases} \phi_1(x) = \left[2\left(\frac{x - x_0}{x_1 - x_0}\right)\right]^{17} & \textbf{PML 1,} \\ \phi_2(x) = 20000\left(\frac{x - x_0}{x_1 - x_0}\right) & \textbf{PML 2,} \\ \phi_3(x) = 10000 & \textbf{PML 3.} \end{cases} \qquad x \in (x_0, x_1)$$

Within the PML, both propagating and evanescent waves become arbitrarely fast evanescent waves.

2D hp-FEM: PERFECTLY MATCHED LAYER (PML)

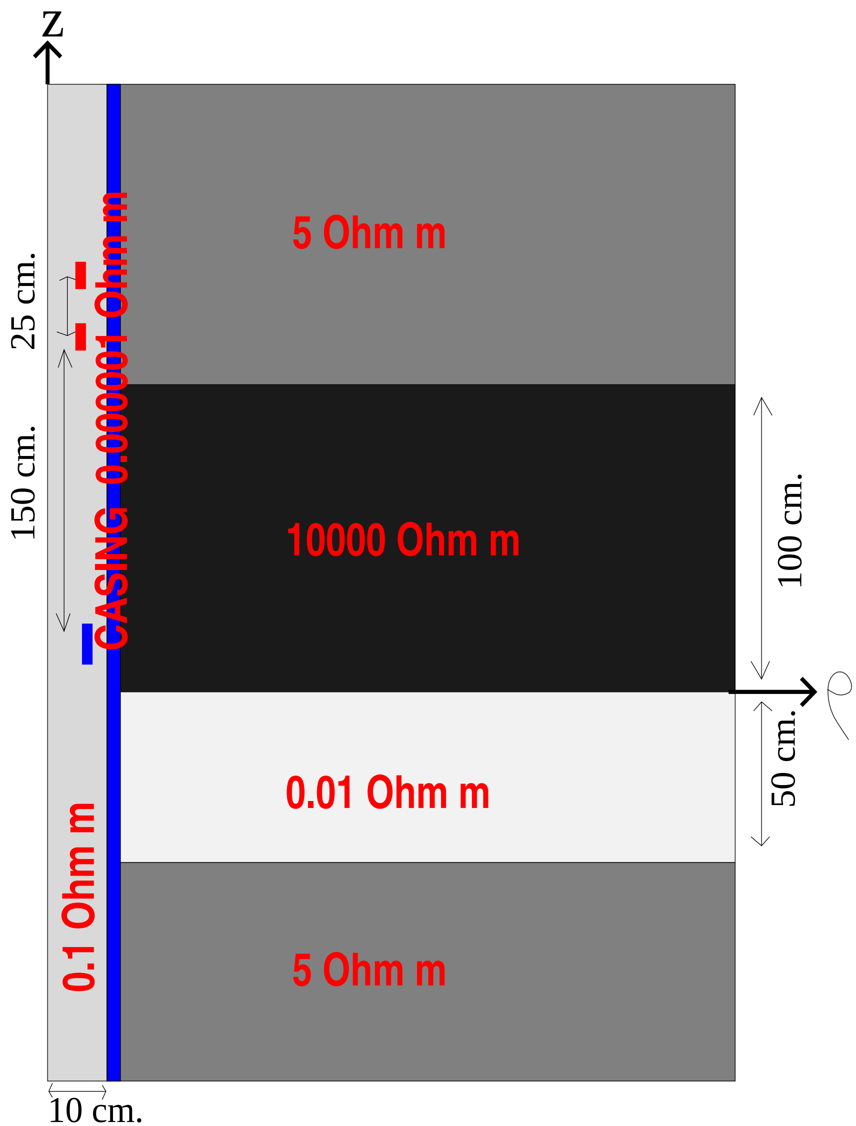

Axisymmetric 3D problem.

Six different materials.

Through casing resistivity instrument.

2D hp-FEM: PERFECTLY MATCHED LAYER (PML)

Final hp-Grid with a 0.5 m Thick PML.

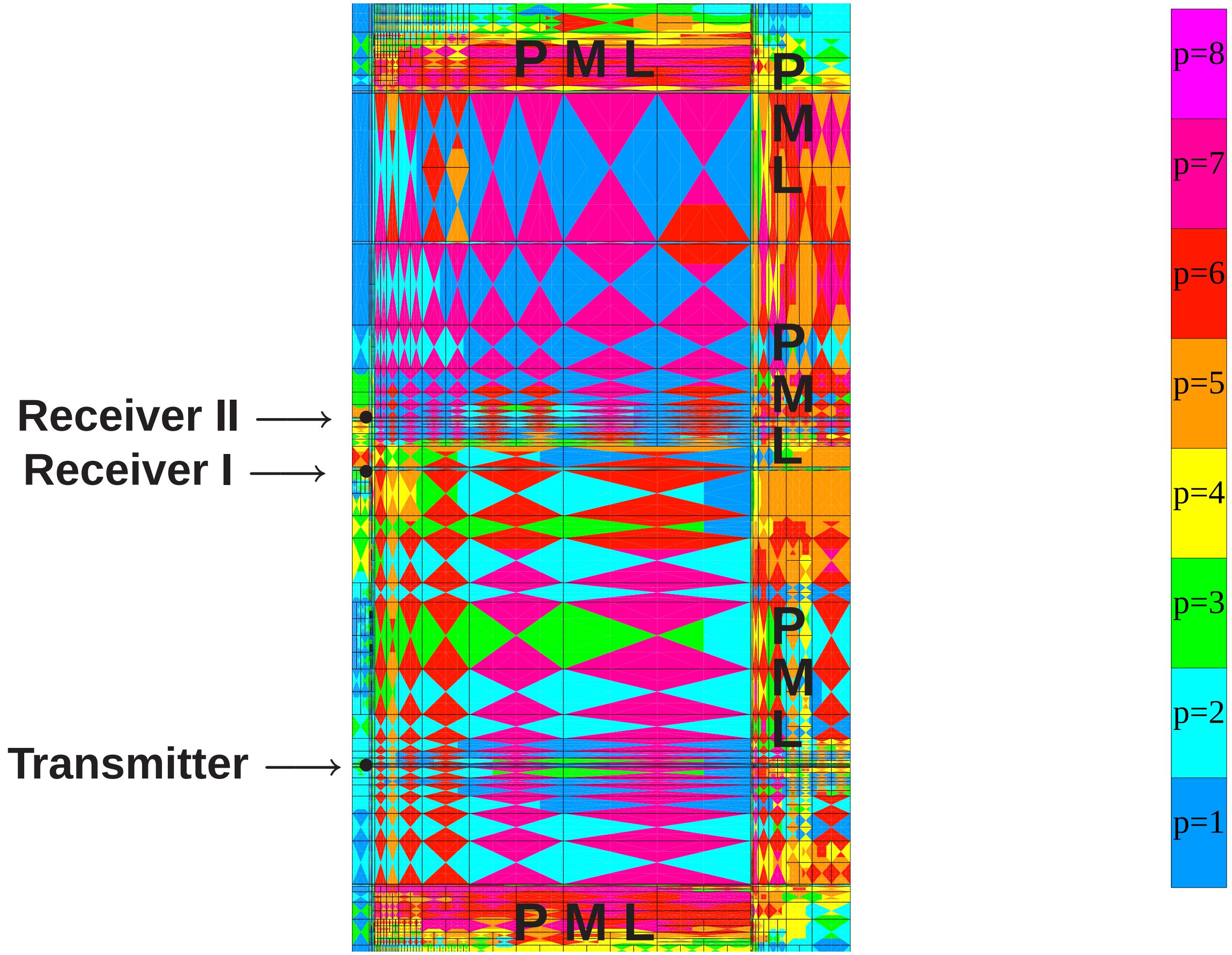

2D hp-FEM: PERFECTLY MATCHED LAYER (PML)

Reference Solution: PML 1 (5 m x 2.5 m)

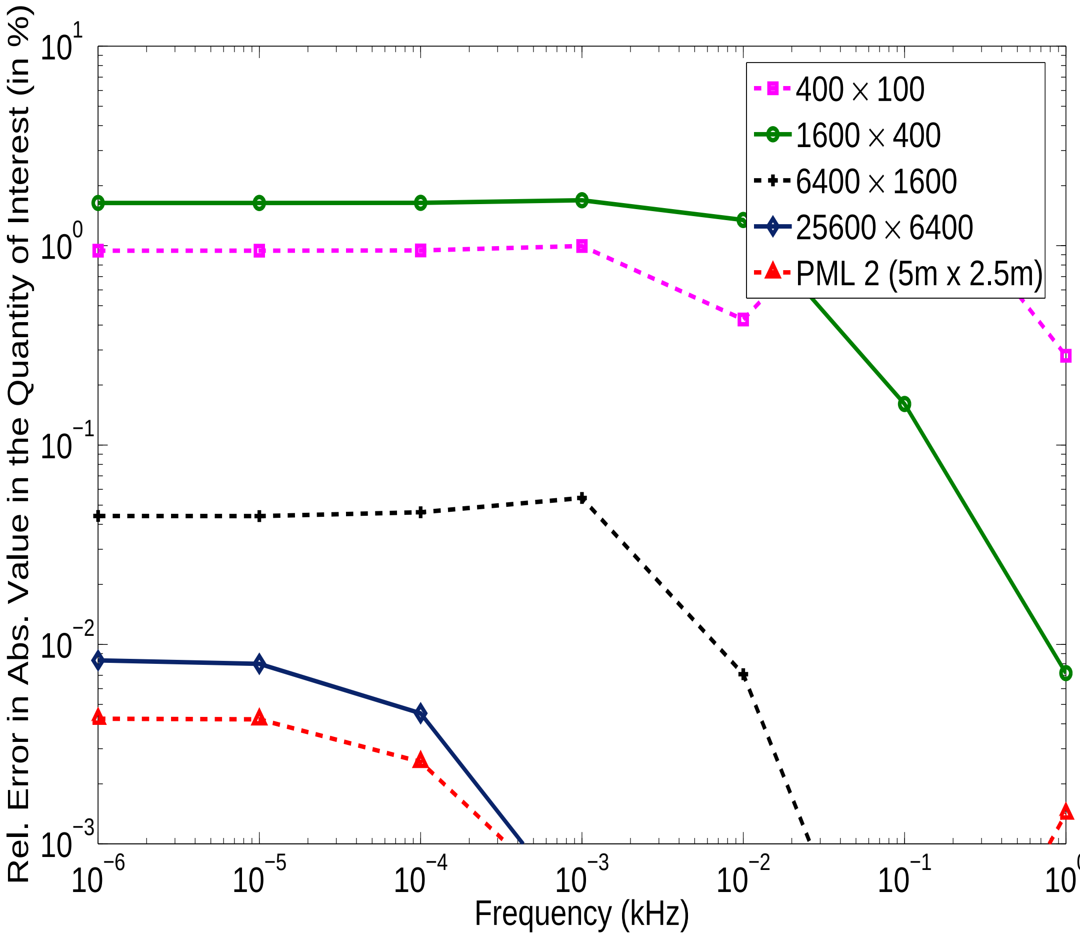

PMLs provide accurate solutions without reflections from the boundary

2D hp-FEM: PERFECTLY MATCHED LAYER (PML)

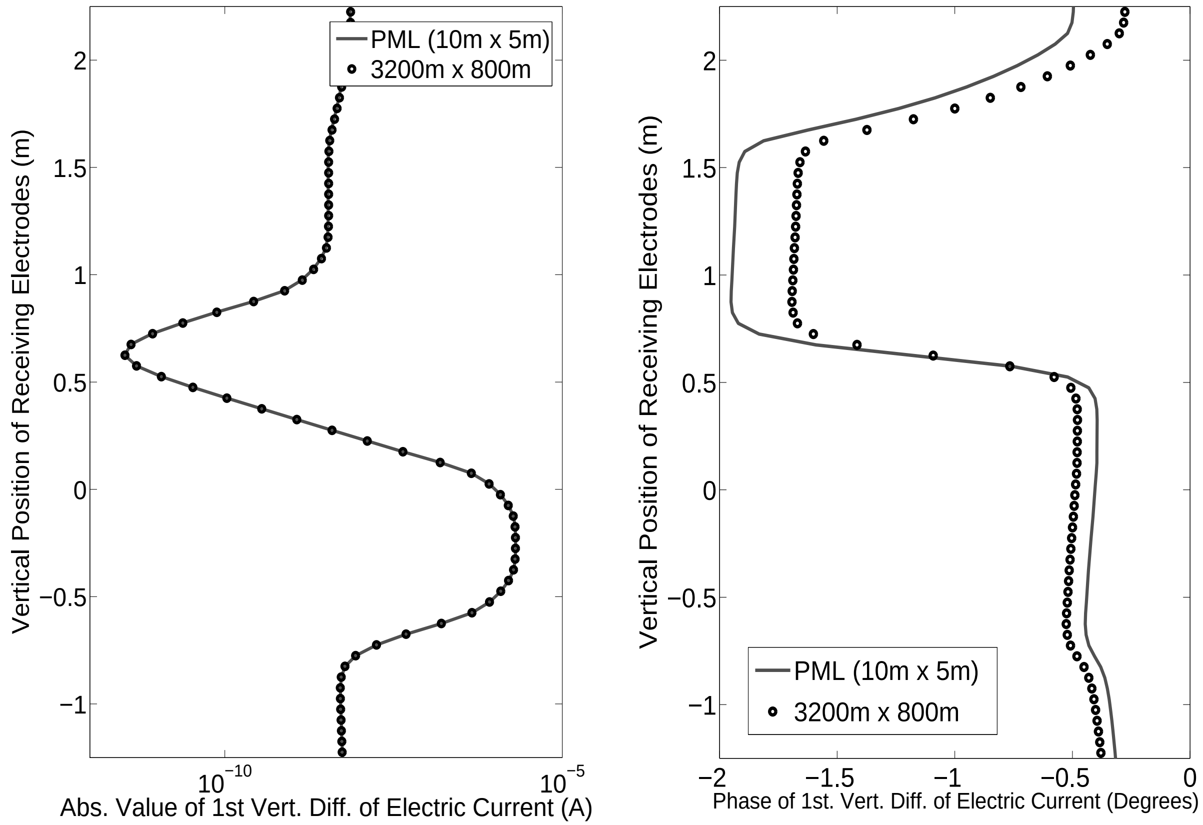

If we compute the phase, a computational domain of 3200 m x 800 m is not large enough.

2D hp-FEM: MULTI-PHYSICS (ACOUSTICS)

Acoustic Scattering From a Cylinder (8 Khz)

(Incoming wave from the right, $V_f = 1200 m/s$)

$$i\omega p + \frac{1}{r}\frac{\partial}{\partial r}(r u_r) + \frac{1}{r}\frac{\partial u_\theta}{\partial \theta} = 0 \quad ; \quad i\omega u_r + \frac{\partial p}{\partial r} = 0 \quad ; \quad i\omega u_\theta + \frac{1}{r}\frac{\partial p}{\partial \theta} = 0$$

Solution ($< 1\%$ error)

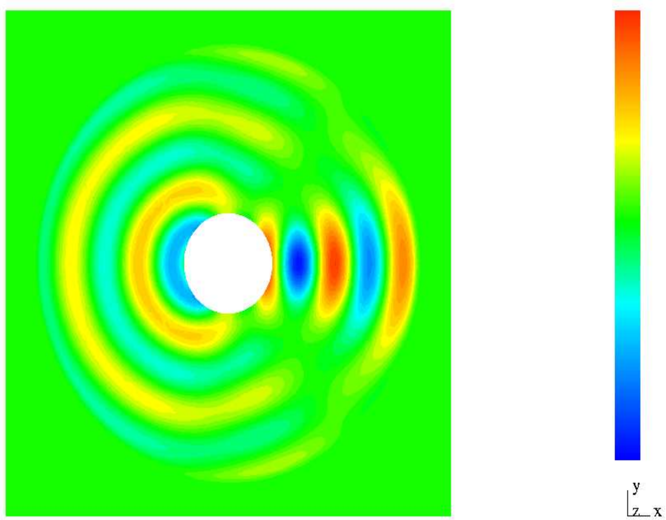

Final hp-grid

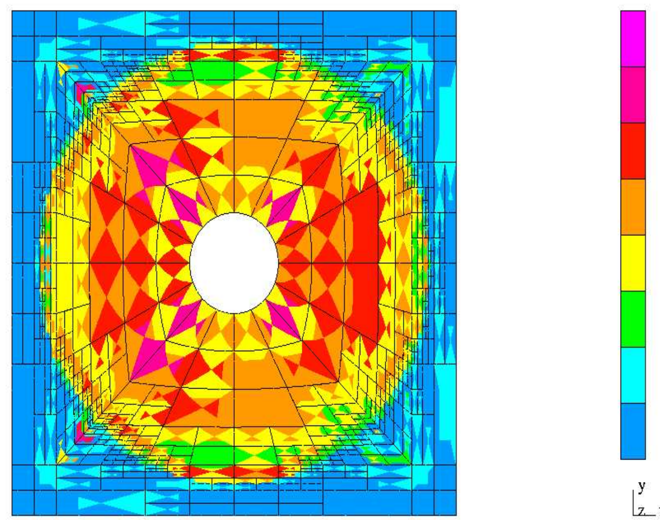

A PML is utilized to truncate the computational domain

2D hp-FEM: MULTI-PHYSICS (ELASTICITY)

Linear Elasticity. Pressure Applied Along the Circumference.

Poisson Ratio=0.3 ; Young Modulus = 4 (top part) and 1 (bottom part) ; Freq.=22.4 Khz

$$\int_{\Omega} \bar{E}_{ijkl} u_{k,l} v_{i,j} \, dx - \omega^2 \int_{\Omega} \bar{\rho} u_i v_i \, dx = \int_{\Gamma_N} g_i v_i \, dS, \quad \forall v \in \bar{V} \; ,$$

Solution (Real Part) **Solution (Imag. Part) ($< 1\%$ error)** **Final hp-grid**

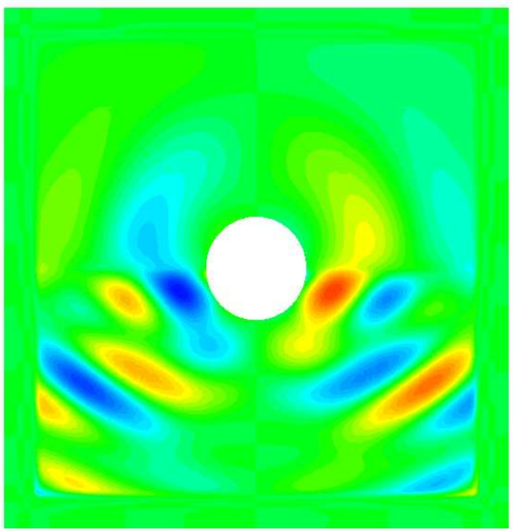

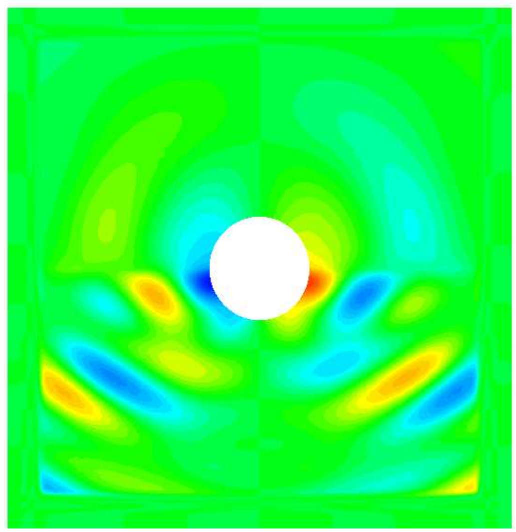

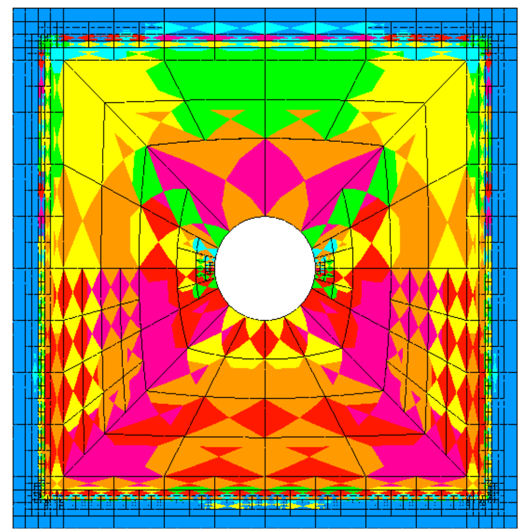

A PML is utilized to truncate the computational domain

3D hp-FEM: NUMERICAL RESULTS

Electrode Problem

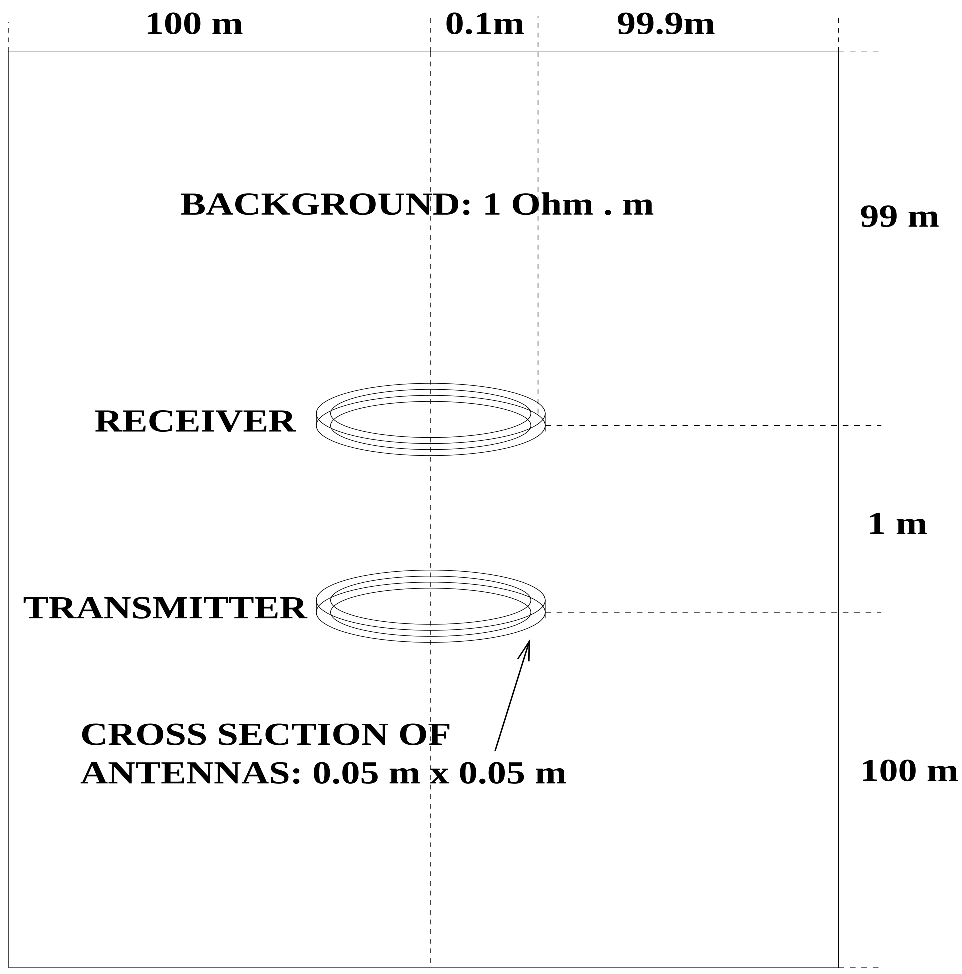

Loop antenna in a homogeneous media at DC.

Computational domain:
100 m x 100 m.

3D hp-FEM: NUMERICAL RESULTS

Electrode Problem

Final hp-grid

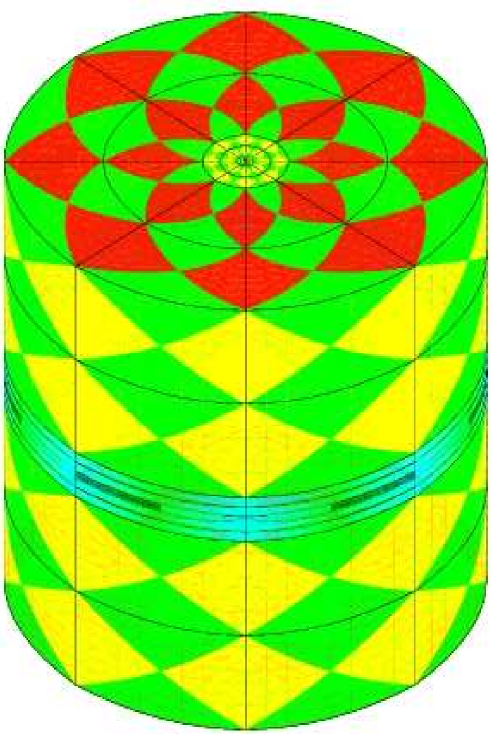

Final solution

2D Solution: 0.078131

3D Solution: 0.078121

3D hp-FEM: NUMERICAL RESULTS

Resources Needed by the Adaptive Algorithm

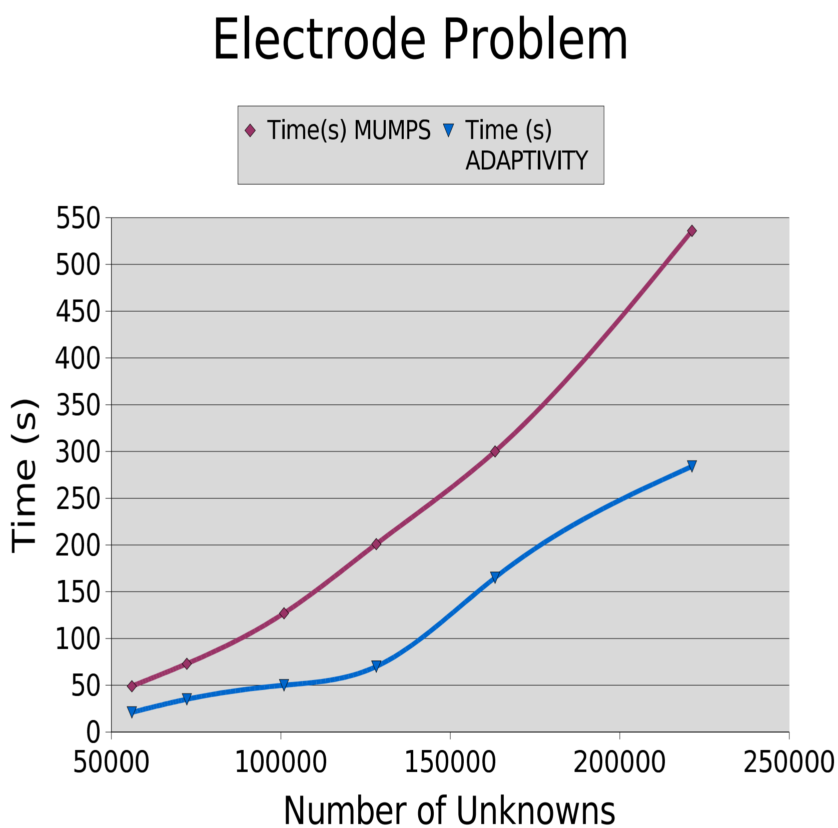

- **The adaptive algorithm utilizes about half of the time used by the solver MUMPS.**
- **The amount of memory used by the adaptive algorithm is negligible, and results are not reported here.**
- **Since the final result is given by the final fine-grid solution, the adaptive algorithm does NOT need to be executed on the last iteration.**
- **For multiple logging instrument positions, the optimal grid may be reutilized without employing the adaptive algorithm.**

Resources needed by the adaptive algorithm are between 4% and 25% of the total resources needed by the 3D code (if MUMPS is used).

3D hp-FEM: NUMERICAL RESULTS

Axisymmetric Model Problem

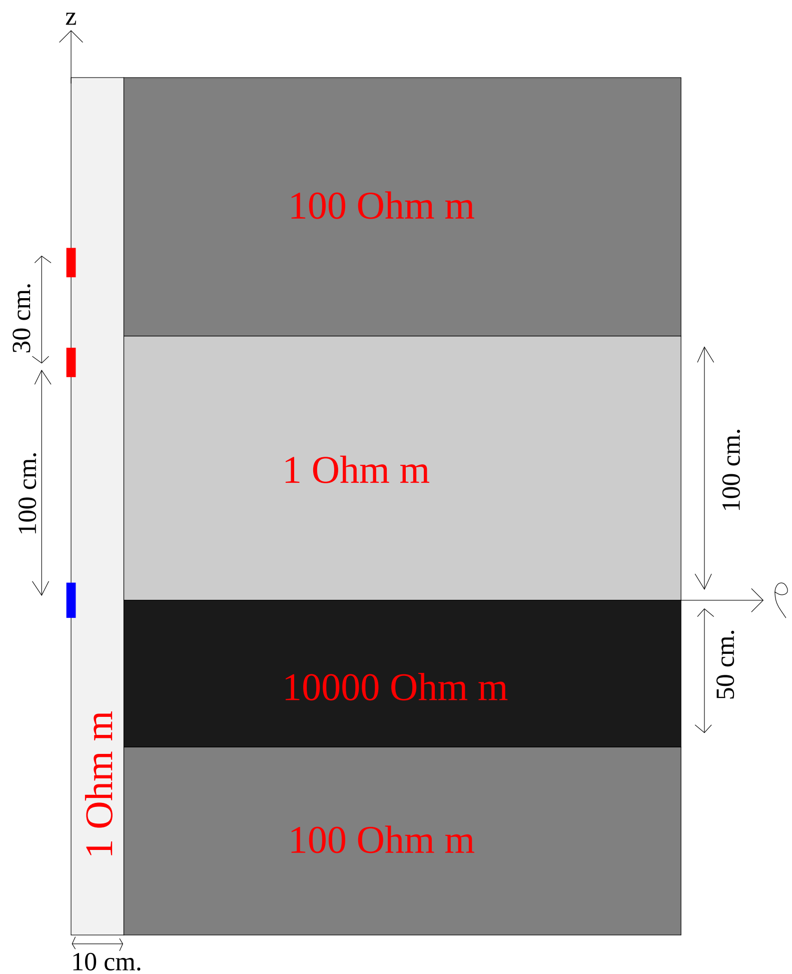

- **Borehole and four materials on the formation.**
- **Size of computational domain: $100m \times 100m$.**
- **Size of electrode: $0.05m \times 0.05m$.**
- **Objective: Compute First Vertical Difference of Potential.**

3D hp-FEM: NUMERICAL RESULTS

Axisymmetric Model Problem

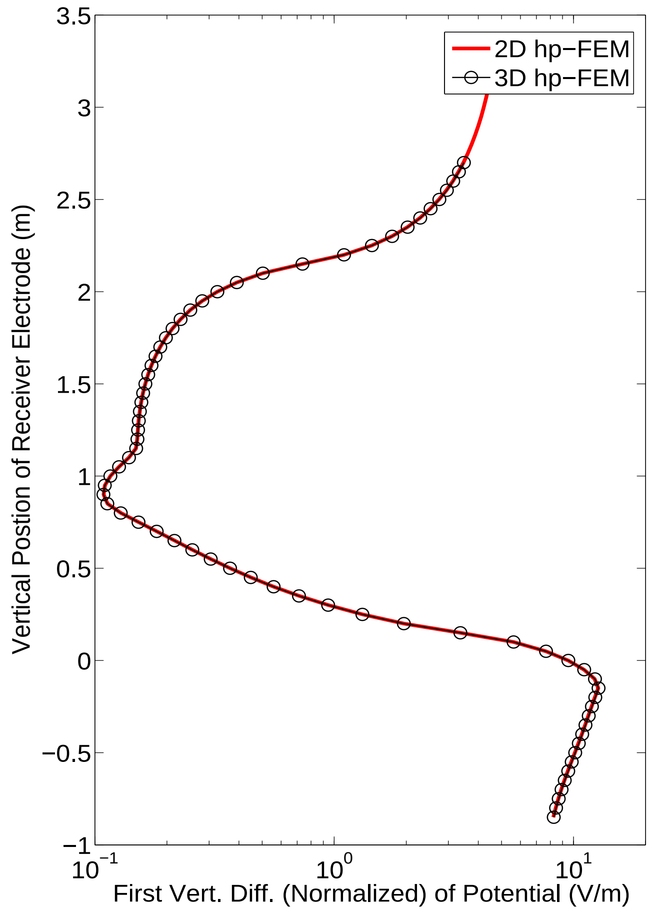

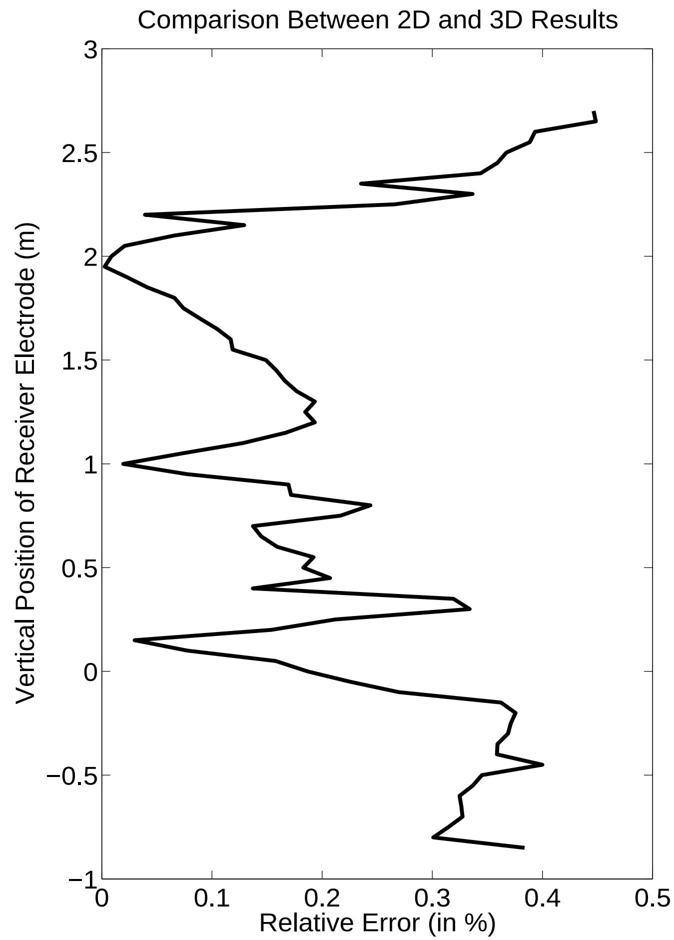

3D hp-FEM: NUMERICAL RESULTS

Fichera problem (unknown exact solution)

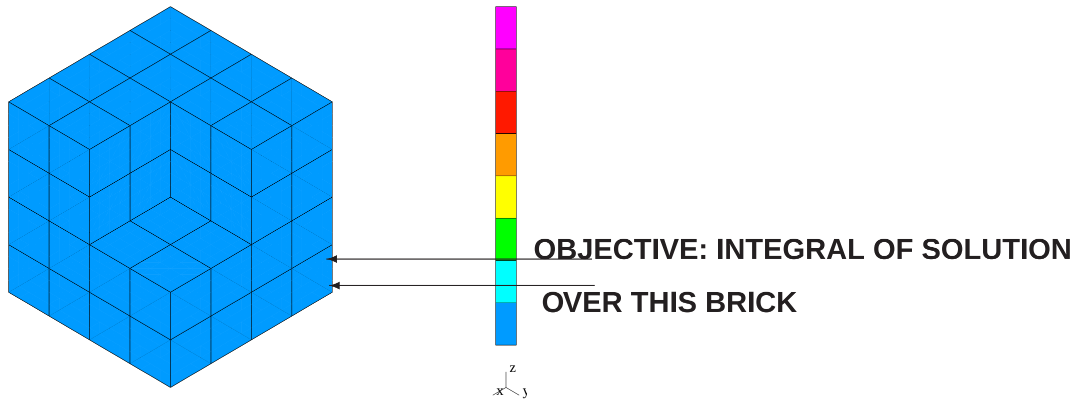

Equation: $-\Delta u = 0$
Boundary Conditions: Neumann, Dirichlet

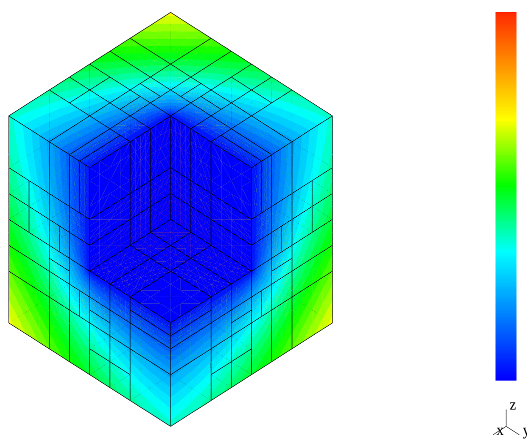

Solution of Direct Problem

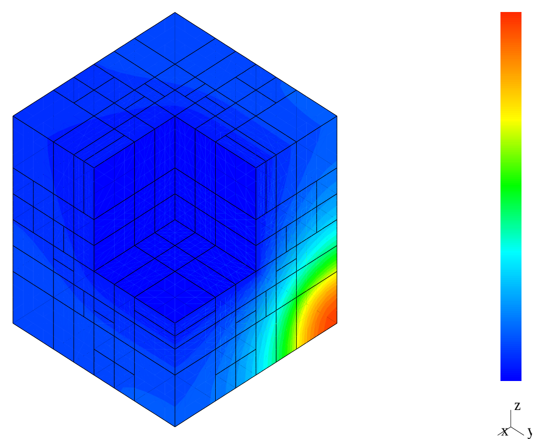

Solution of Dual Problem

3D hp-FEM: NUMERICAL RESULTS

Fichera problem (final hp-grids)

Energy-norm:

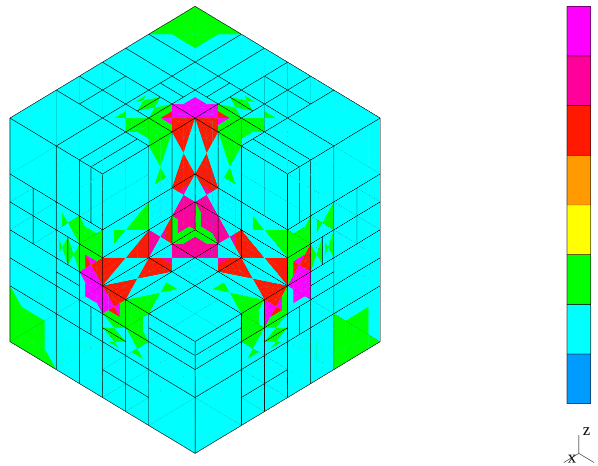

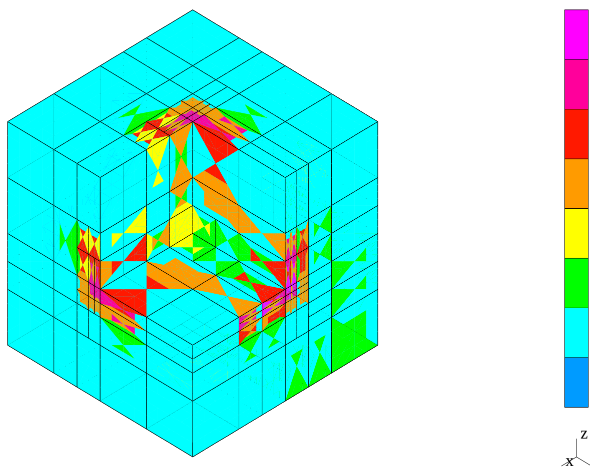

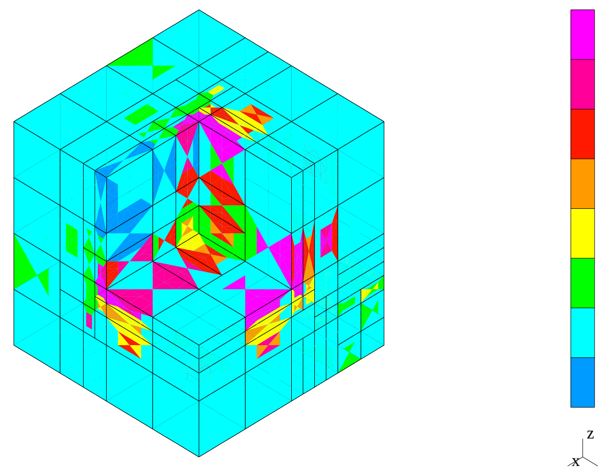

Goal-oriented (algorithm I) **Goal-oriented (algorithm II)**

3D hp-FEM: NUMERICAL RESULTS

Fichera problem (convergence history)

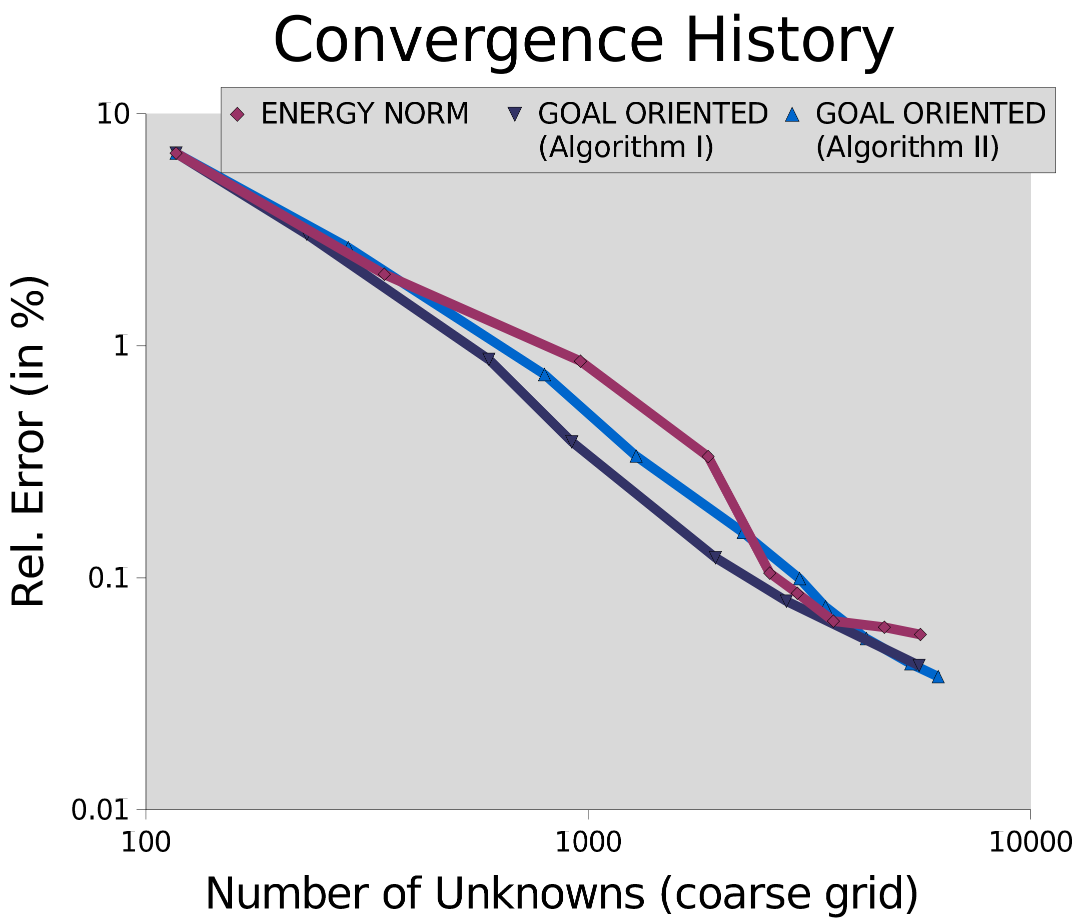

Exponential Convergence in the Quantity of Interest

CONCLUSIONS AND FUTURE WORK

- **The self-adaptive goal-oriented hp-adaptive strategy converges exponentially in terms of a user-prescribed quantity of interest vs. the CPU time.**

- **We obtain fast, reliable and accurate solutions for problems with a large dynamic range and high material constrasts.**

- **We obtain meanigful physical conclusions useful for instrument modeling and for assesment of petrophysical properties.**

Work in Progress

- **To further develop the parallel version of the 3D hp-FE code as well as a multigrid solver.**

- **To apply the self-adaptive goal-oriented hp-FEM for inversion of 2D multi-physic problems.**

ACKNOWLEDGMENTS

ارامكو السعودية
Saudi Aramco

BAKER HUGHES
Baker Atlas

bp

Chevron

ConocoPhillips

Agip
Eni

ExxonMobil

HALLIBURTON®

IMP Innovar
INSTITUTO MEXICANO DEL PETRÓLEO

MARATHON
Marathon Oil Corporation

HYDRO

OXY

BR PETROBRAS

Schlumberger

STATOIL

TOTAL

Weatherford

ES: CHARACTERISTICS 2DHP90 and 3DHP90

2Dhp90, 3Dhp90: main features

- **Isoparametric triangles, squares and hexahedras.**
- H^1 **and** $H(curl)$ **dofs.**
- **Isotropic and anisotropic mesh refinements.**
- **Geometrical Modeling Package (GMP).**
- **New data structure in Fortran 90.**
- **Constrained information reconstructed (not stored).**
- **Two levels of logical operations:**
  1. **operations for nodes - problem independent.**
  2. **operations for nodal dof - problem dependent.**
- **Fully automatic** hp**-adaptive strategy.**

—provides exponential convergence rates—

ES: KAUFMAN's APPROX. FORMULAS

Logging Through Casing (Benchmark Problem)

Rock Formation: Homogeneous Media

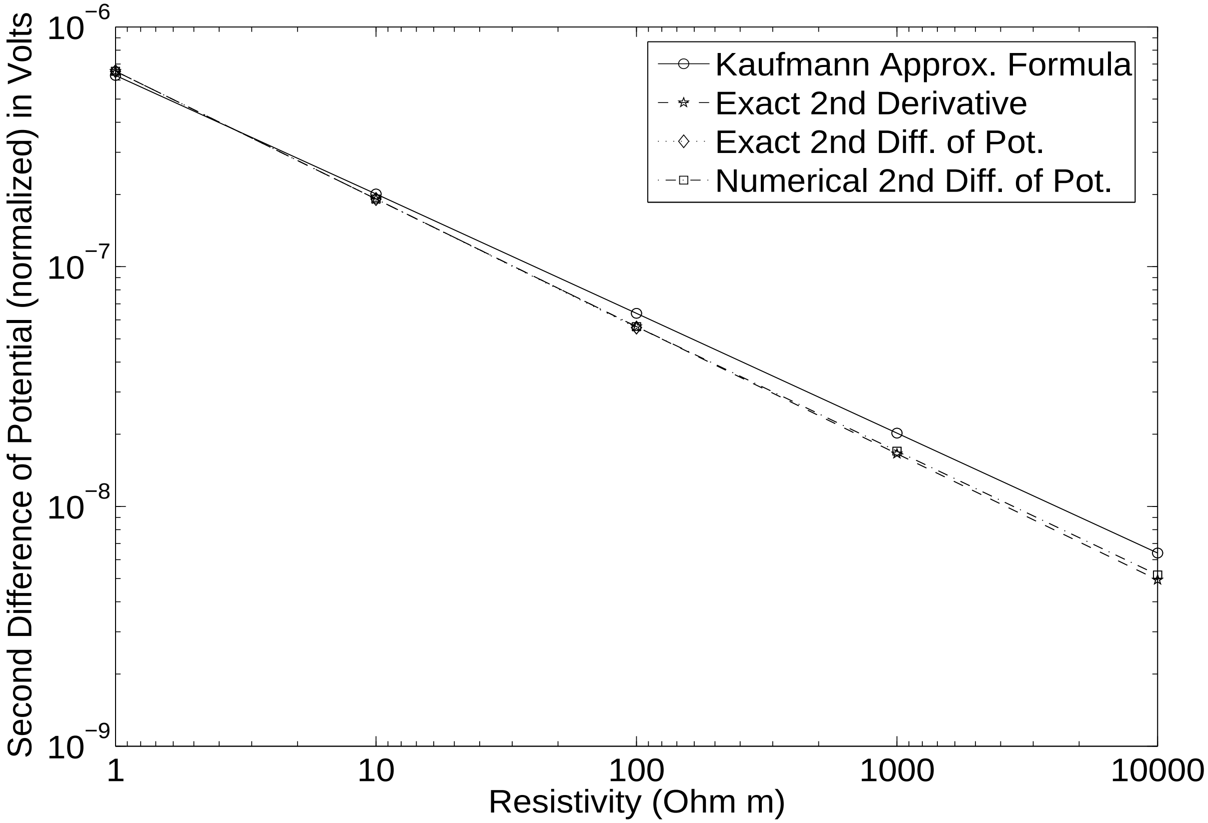

The second vertical difference of the Electric Potential is proportional to the formation conductivity.